

**TO EXPLORE THE CORROSION INHIBITION  
PROPERTIES AND ADSORPTION BEHAVIOUR OF  
SOME PHYTOCHEMICALLY RICH EXTRACT OF  
PLANT WASTE MATERIALS FOR STEEL BEING USED  
IN PETROLEUM INDUSTRY**

A Thesis

Submitted in partial fulfillment of the requirements for the  
Award of the degree of

**DOCTOR OF PHILOSOPHY (Ph.D.)**

In

**CHEMISTRY**

By

**NISHANT BHARDWAJ**

**11720078**

Supervised By

**Dr. VINEET KUMAR**

**ASSISTANT PROFESSOR**



**L** LOVELY  
**P** ROFESSIONAL  
**U** NIVERSITY

*Transforming Education Transforming India*

---

**LOVELY PROFESSIONAL UNIVERSITY**

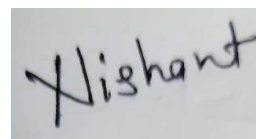
**PUNJAB**

**2021**

## DECLARATION

The research work mentioned in this Ph.D. thesis with the title of “**To explore the corrosion inhibition properties and adsorption behavior of some phytochemically rich extract of plant waste materials for steel being used in petroleum industry**” was carried by me for the fulfillment of **Doctor of Philosophy in Chemistry** under the supervision of **Dr. Vineet Kumar, Assistant Professor, Department of Biotechnology, Lovely Professional University, Punjab, India.**

I declare that the work mentioned in this thesis is original and has done by me and this thesis has not been submitted in any other degree or other course.

A rectangular box containing a handwritten signature in black ink that reads "Nishant".

Date:

Nishant Bhardwaj

Place:

Reg. No. 11720078

## **CERTIFICATE**

This is to certify that the thesis entitled of “**To explore the corrosion inhibition properties and adsorption behavior of some phytochemically rich extract of plant waste materials for steel being used in petroleum industry**” submitted for the award of the degree of **Doctor of Philosophy in Chemistry** to Lovely Professional University Punjab, India is a record of bonafide research work carried out by **Mr. Nishant Bhardwaj** under my guidance. To the best of my knowledge, the thesis has not been previously submitted elsewhere for the award of any other degree, diploma or distinction of any kind anywhere before.



**Dr. Vineet Kumar**

**Research Supervisor**

**Assistant Professor**

**Department of Biotechnology**

**Lovely Professional University**

**Phagwara (INDIA)**

## ABSTRACT

The thesis entitled **“To explore the corrosion inhibition properties and adsorption behaviour of some phytochemically rich extract of plant waste materials for steel being used in petroleum industry”** explain the study of eco-friendly and cost effective plant waste corrosion inhibitor and its effects on stainless steel(SS-410) in 15% HCl solution with the help of various techniques. Corrosion is metal destruction process by interaction between metal and different environmental condition. In general, corrosion is an economic problem closely associated with business loss. Corrosion causes thousands of billion of dollar loss every year worldwide. It should be control by providing most advantages method. The use of natural corrosion inhibitors is the most practical method to prevent the corrosion.

S.S.is one of main steel used in petroleum industry in various applications. The main reason of corrosion in petroleum industry is acid attack on the steel surface. Generally inhibitors are mixed into the acid solution for reducing the aggressiveness of corrosion on the steel surface. The major commercial composition found in corrosion inhibitors are aromatic aldehydes, alkenyl phenones and various products of amine and carbonyl. There are various difficulties come in the using of these inhibitor like they are very expensive and harmful to the environment, which is the main reason for finding ecofriendly and cost effective corrosion inhibitors.

The corrosion inhibition properties of selected plant waste material as corrosion inhibitors for S.S.in 15% HCl were explained depending on the various parameters like temperature, inhibitor concentration and surface roughness of stainless steel. Experiment of weight loss measurement, Potentiodynamic polarization and electrochemical impedance spectroscopy (EIS) were used for calculating the corrosion inhibition efficiency. For explain the surface morphology, scanning electron microscopy (SEM) and atomic force microscopy (AFM) were used. Density function



theory (DFT) was used for theoretical evaluation. There are five chapter mentions in this thesis.

### **Chapter 1: Introduction**

In this chapter, the explanation of corrosion, mechanistic approach to corrosion, factors affecting metallic corrosion, corrosion in petroleum industry, methods of corrosion control and corrosion inhibitors are describes in this chapter.

### **Chapter 2: Review of literature**

In this chapter, corrosion inhibition in hydrochloric acid environment, waste materials from plants as inhibitors of corrosion in hydrochloric acid, plant waste biomass like straw and husk as environmental pollutants, plant based corrosion inhibition used at high concentration, stainless steel 410 in petroleum industry, purpose of present work, scope and intent of present research work, also objectives of the study are mention.

### **Chapter 3: Materials and Methods**

This chapter describes various techniques and experimental procedures applicable in the corrosion test for S.S. 410 in 15 % HCl solution. Weight loss measurements were carried out at the temperature of 298 K. Electrochemical impedance and potentiodynamic study of natural corrosion inhibitor on S.S.in acidic media also have been discuss in this chapter. Comparative study between synthetic paint and selected plant waste extract was discussed. For the identification of functional group present in selected plant waste, Fourier transform infra-red spectroscopy has been discussed. SEM and AFM are used for surface morphological studies of plant waste corrosion inhibitor. Density functional theory were used for calculating quantum chemical parameters like energies of highest occupied molecular orbital, energies of lower unoccupied molecular orbital and the energy gab between highest occupied molecular orbital and lower unoccupied molecular orbital. With the help of these parameters, corrosion inhibition mechanism of selected pant on S.S.-410 surface in acidic media was easy to analyses.

### **Chapter 4: Results and Discussion**

There are nine parts (4.1 to 4.9) are explained in this chapter. All the results and their discussion of selected plants including *Oryza sativa*, *Populus tremula*, *Triticum aestivum*, *Brassica nigra*, *Saccharum officinarum*, *Beta vulgaris* and *Phyllanthus emblica* are mentioned in this chapter.

### **Chapter 5: Summary and Conclusions**

In this chapter, overall characteristics of selected corrosion inhibitors, conclusion, comparisons of the results, summary of the results, future work scope, list of publications and bibliography are mention.

## ACKNOWLEDGEMENT

I am utilizing this great opportunity to expressing my thanks to everyone who supported me directly or indirectly during the time of my research work.

I want to express my gratitude to my supervisor **Dr. Vineet Kumar** for the continuous support of my Ph.D. work for his patience, motivation, and immense knowledge. His advice towards research plays an important role in my research career.

I want to give special thanks to my mother **Mrs. Jaimala Sharma** and father **Mr. Sudesh Pal Sharma** for their love and sacrifices that they have made for me. I also want to express my gratitude to my uncle **Mr. Rajkumar Sharma** for his blessing and unconditional support. I appreciate my younger brother **Mr. Shashank Bhardwaj** for taking all the responsibility on his shoulder in my absence.

I want to give a special thanks to my research mate **Ms. Pooja Sharma** for her advices and supports regarding my research work.

Finally, I am thankful to the God for giving me the good health that was needed to complete this research work.

Nishant Bhardwaj

**“I dedicate this thesis to my parents  
(Mrs. Jaimala Sharma and Mr. Sudesh Pal Sharma)  
For their constant support and unconditional love”**

## Table of Contents

Title	Page Number
<b>Declaration</b>	ii
<b>Certificate</b>	iii
<b>Abstract</b>	iv-vi
<b>Acknowledgement</b>	vii
<b>List of Tables</b>	xii-xiii
<b>List of Figures</b>	xiv-xix
<b>List of Appendices</b>	xx-xxi
<b>Chapter 1: Introduction</b>	
• Corrosion	1-2
• Mechanistic approach to corrosion	2
• Factors affecting metallic corrosion	3
• Corrosion in petroleum industry	3-5
• Methods of corrosion control	5-6
• Corrosion inhibitors	6-8

<b>Chapter 2: Review of Literature</b>	
• Corrosion inhibition in Hydrochloric acid environment	9-16
• Waste materials from plants as inhibitors of corrosion in hydrochloric acid	17-20
• Plant waste biomass like Straw and husk as environmental pollutants	20-21
• Plant based corrosion inhibition used at high concentration	21-22
• S.S.- 410 in petroleum industry	23-24
• Purpose of the present work	24
• Scope and intents of the present research work	24-25
• Objectives of the study	25
<b>Chapter 3: Materials and Methods</b>	
• Chemicals and Reagents	26
• Selected plants for the investigation	26
• Preparation of plant extract	26-27
• Elemental analysis of S.S.- 410	27
• Preparation of working electrodes	27
• FT-IR spectroscopy	27-28
• UV-visible spectroscopy	28
• Weight-loss experiments	29
• Langmuir adsorption isotherm	29-30
• Electrochemical techniques	30-32
• Comparative studies with some existing synthetic paints	33
• Surface investigations	33-34
• Quantum chemical calculations	34
<b>Chapter 4: Results and Discussion</b>	
• Corrosion inhibition properties and adsorption behavior of	35-43

<p><i>Oryza sativa</i></p> <ul style="list-style-type: none"> <li>• Corrosion inhibition properties and adsorption behavior of <i>Oryza sativa</i> 44-52</li> </ul>	44-52
<p><i>Populus tremula</i></p> <ul style="list-style-type: none"> <li>• Corrosion inhibition properties and adsorption behavior of <i>Populus tremula</i> 53-61</li> </ul>	53-61
<p><i>Triticum aestivum</i></p> <ul style="list-style-type: none"> <li>• Corrosion inhibition properties and adsorption behavior of <i>Triticum aestivum</i> 62-70</li> </ul>	62-70
<p><i>Brassica nigra</i></p> <ul style="list-style-type: none"> <li>• Corrosion inhibition properties and adsorption behavior of <i>Brassica nigra</i> 71-79</li> </ul>	71-79
<p><i>Saccharum officinarum</i></p> <ul style="list-style-type: none"> <li>• Corrosion inhibition properties and adsorption behavior of <i>Saccharum officinarum</i> 80-89</li> </ul>	80-89
<p><i>Beta vulgaris</i></p> <ul style="list-style-type: none"> <li>• Corrosion inhibition properties and adsorption behavior of <i>Beta vulgaris</i> 89-93</li> </ul>	89-93
<p><i>Phyllanthus embelica</i></p> <ul style="list-style-type: none"> <li>• Corrosion inhibition properties and adsorption behaviour of <i>Phyllanthus embelica</i></li> </ul>	
<b>Chapter 5: Summary and Conclusion</b>	
<ul style="list-style-type: none"> <li>• Summary 94-97</li> </ul>	94-97
<ul style="list-style-type: none"> <li>• Conclusion 97</li> </ul>	97
<ul style="list-style-type: none"> <li>• Future scope 98</li> </ul>	98
<ul style="list-style-type: none"> <li>• List of publication, conferences and workshop 99-100</li> </ul>	99-100
<ul style="list-style-type: none"> <li>• Bibliography 101-130</li> </ul>	101-130

### List of Tables

<b>Table No</b>	<b>Title</b>	<b>Page number</b>
2.1	Plant based corrosion inhibition used at high concentration	22
4.1.1	Corrosion parameters from weight loss, and electrochemical experiments for S.S.- 410 in 15% HCl with different concentrations of <i>O. sativa</i> extract	40
4.1.2	Calculated quantum chemical parameters of phytochemicals of <i>O. sativa</i>	43
4.2.1	Corrosion parameters from weight loss, and electrochemical experiments for S.S.-410 in 15% HCl with different concentrations of <i>P. tremula</i> extract	49
4.2.2	Calculated quantum chemical parameters of phytochemicals of <i>P. tremula</i>	52
4.3.1	Corrosion parameters from weight loss, and electrochemical experiments for S.S.-410 in 15% HCl with different concentrations of <i>T. aestivum</i> extract	58
4.3.2	Calculated quantum chemical parameters of phytochemicals of <i>T. aestivum</i>	61



4.4.1	Corrosion parameters from weight loss, and electrochemical experiments for S.S.-410 in 15% HCl with different concentrations of <i>B. nigra</i> extract	67
4.4.2	Calculated quantum chemical parameters of phytochemicals of <i>B. nigra</i>	70
4.5.1	Corrosion parameters from weight loss, and electrochemical experiments for S.S.-410 in 15% HCl with different concentrations of <i>S. officinarum</i> extract	76
4.5.2	Calculated quantum chemical parameters of phytochemicals of <i>S. officinarum</i>	79
4.6.1	Corrosion parameters from weight loss, and electrochemical experiments for S.S.-410 in 15% HCl with different concentrations of <i>B. vulgaris</i> extract	85
4.6.2	Calculated quantum chemical parameters of phytochemicals of <i>B. vulgaris</i>	88
4.7.1	Corrosion parameters from weight loss, and electrochemical experiments for S.S.-410 in 15% HCl with different concentrations of <i>P. emblica</i> extract	94
4.7.2	Calculated quantum chemical parameters of phytochemicals of <i>P. emblica</i>	97
4.8.1	Inhibition efficiency and corrosion rate of the paint-coated S.S.-410 without and with selected inhibitors	98

## List of Figures

Figure No	Title	Page number
1.1	Types of corrosive agents generally found in petroleum industry	4
1.2	Types of mechanism of corrosion prevention by inhibitor	7
3.1	S.S.-410 used in (a) weight loss, and (b) Electrochemical studies	27
3.2	FT-IR instrument used for the study.	28
3.3	UV-visible spectrophotometer used for the study.	28
3.4	Langmuir plot of <i>O. sativa</i> as an example	30
3.5	(a) Three electrode cell assembly, and (b) used electrochemical workstation	31
3.6	An example of an experimental potentiodynamic curve	32
3.7	(a) Used SEM, and (b) AFM instruments for the study.	34
4.1.1	(a) Image of <i>O. Sativa</i> plant (b – d) molecular structure of phytochemicals present in <i>O. Sativa</i> extract (OSE)	35
4.1.2	FT-IR spectra of <i>O. sativa</i> extract (OSE)	36
4.1.3	UV-visible absorption spectra of the <i>O. sativa</i> extract (OSE)	37
4.1.4	Langmuir adsorption isotherm for <i>O. sativa</i> extract (OSE) with the help of weight loss measurement	38

4.1.5	(a) Potentiodynamic polarization plot (b) Electrochemical impedance plot (c) Bode plot (d) phase angle plot for different concentration of <i>O. sativa</i> extract (OSE)	39
4.1.6	(a) AFM micrographs of S.S.-410 (b) AFM micrographs of S.S.-410 immersed in 15% HCl solution (c) AFM micrographs of S.S.-410 immersed in 15% HCl solution with <i>O. sativa</i> extract (OSE) (d) SEM micrographs of S.S.-410 (e) SEM micrographs of S.S.-410 immersed in 15% HCl solution (f) SEM micrographs of S.S.-410 immersed in 15% HCl solution with <i>O. sativa</i> extract (OSE)	41
4.1.7	Optimized structures, HOMO and LUMO of phytochemicals present in <i>O. sativa</i> extract (OSE)	42
4.2.1	(a) <i>P. tremula</i> plant (b – d) molecular structure of phytochemicals present in <i>P. tremula</i> extract (PTE)	44
4.2.2	FT-IR spectra of <i>P. tremula</i> extract (PTE)	45
4.2.3	UV-visible absorption spectra of the <i>P. tremula</i> extract (PTE)	46
4.2.4	Langmuir adsorption isotherm for <i>P. tremula</i> extract (PTE) with the help of weight loss measurement	47
4.2.5	(a) Potentiodynamic polarization plot (b) Electrochemical impedance plot (c) Bode plot (d) phase angle plot for different concentration of <i>P. tremula</i> extract (PTE)	48
4.2.6	(a) AFM micrographs of S.S.-410 (b) AFM micrographs of S.S.-410 immersed in 15% HCl solution (c) AFM micrographs of S.S.-410 immersed in 15% HCl solution with <i>P. tremula</i> extract (PTE) (d) SEM micrographs of S.S.-410 (e) SEM micrographs of S.S.-410 immersed in 15% HCl solution (f) SEM micrographs of S.S.-410 immersed in 15% HCl solution with <i>P. tremula</i> extract	50

	(PTE)	
4.2.7	Optimized structures, HOMO and LUMO of phytochemicals present in <i>P. tremula</i>	51
4.3.1	(a) <i>T. aestivum</i> plant (b – d) molecular structure of phytochemicals present in <i>T. aestivum</i> extract (TAE)	53
4.3.2	FT-IR spectra of <i>T. aestivum</i> extract (TAE)	54
4.3.3	UV-visible absorption spectra of the <i>T. aestivum</i> extract (TAE)	55
4.3.4	Langmuir adsorption isotherm for <i>T. aestivum</i> extract (TAE) with the help of weight loss measurement	56
4.3.5	(a) Potentiodynamic polarization plot (b) Electrochemical impedance plot (c) Bode plot (d) phase angle plot for different concentration of <i>T. aestivum</i> extract (TAE)	57
4.3.6	(a) AFM micrographs of S.S.-410 (b) AFM micrographs of S.S.-410 immersed in 15% HCl solution (c) AFM micrographs of S.S.-410 immersed in 15% HCl solution with <i>T. aestivum</i> extract (TAE) (d) SEM micrographs of S.S.-410 (e) SEM micrographs of S.S.-410 immersed in 15% HCl solution (f) SEM micrographs of S.S.-410 immersed in 15% HCl solution with <i>T. aestivum</i> extract (TAE)	59
4.3.7	Optimized structures, HOMO and LUMO of phytochemicals present in <i>T. aestivum</i>	60
4.4.1	(a) <i>B. nigra</i> plant (b – d) molecular structure of phytochemicals present in <i>B. nigra</i> extract (BNE)	62
4.4.2	FT-IR spectra of <i>B. nigra</i> extract (BNE)	63

4.4.3	UV-visible absorption spectra of the <i>B. nigra</i> extract (BNE)	64
4.4.4	Langmuir adsorption isotherm for <i>B. nigra</i> extract (BNE) with the help of weight loss measurement	65
4.4.5	(a) Potentiodynamic polarization plot (b) Electrochemical impedance plot (c) Bode plot (d) phase angle plot for different concentration of <i>B. nigra</i> extract (BNE)	66
4.4.6	(a) AFM micrographs of S.S.-410 (b) AFM micrographs of S.S.-410 immersed in 15% HCl solution (c) AFM micrographs of S.S.-410 immersed in 15% HCl solution with <i>B. nigra</i> extract (BNE) (d) SEM micrographs of S.S.-410 (e) SEM micrographs of S.S.-410 immersed in 15% HCl solution (f) SEM micrographs of S.S.-410 immersed in 15% HCl solution with <i>B. nigra</i> extract (BNE)	68
4.4.7	Optimized structures, HOMO and LUMO of phytochemicals present in <i>B. nigra</i>	69
4.5.1	(a) <i>S. officinarum</i> plant (b – d) molecular structure of phytochemicals present in <i>S. officinarum</i> extract(SOE)	71
4.5.2	FT-IR spectra of <i>S. officinarum</i> extract (SOE)	72
4.5.3	UV-visible absorption spectra of the <i>S. officinarum</i> extract (SOE)	73
4.5.4	Langmuir adsorption isotherm for <i>S. officinarum</i> extract (SOE) with the help of weight loss measurement	74
4.5.5	(a) Potentiodynamic polarization plot (b) Electrochemical impedance plot (c) Bode plot (d) phase angle plot for different concentration of <i>S. officinarum</i> extract (SOE)	75

4.5.6	(a) AFM micrographs of S.S.-410 (b) AFM micrographs of S.S.-410 immersed in 15% HCl solution (c) AFM micrographs of S.S.-410 immersed in 15% HCl solution with <i>S. officinarum</i> extract (SOE) (d) SEM micrographs of S.S.-410 (e) SEM micrographs of S.S.-410 immersed in 15% HCl solution (f) SEM micrographs of S.S.-410 immersed in 15% HCl solution with <i>S. officinarum</i> extract (SOE)	77
4.5.7	Optimized structures, HOMO and LUMO of phytochemicals present in <i>S. officinarum</i>	78
4.6.1	(a) <i>B. vulgaris</i> plant (b – d) molecular structure of phytochemicals present in <i>B. vulgaris</i> extract (BNE)	80
4.6.2	FT-IR spectra of <i>B. vulgaris</i> extract (BNE)	81
4.6.3	UV-visible absorption spectra of the <i>B. vulgaris</i> extract (BNE)	82
4.6.4	Langmuir adsorption isotherm for <i>B. vulgaris</i> extract (BNE) with the help of weight loss measurement	83
4.6.5	(a) Potentiodynamic polarization plot (b) Electrochemical impedance plot (c) Bode plot (d) phase angle plot for different concentration of <i>B. vulgaris</i> extract (BNE)	84
4.6.6	(a) AFM micrographs of S.S.-410 (b) AFM micrographs of S.S.-410 immersed in 15% HCl solution (c) AFM micrographs of S.S.-410 immersed in 15% HCl solution with <i>B. vulgaris</i> extract (BNE) (d) SEM micrographs of S.S.-410 (e) SEM micrographs of S.S.-410 immersed in 15% HCl solution (f) SEM micrographs of S.S.-410 immersed in 15% HCl solution with <i>B. vulgaris</i> extract (BNE)	86

4.6.7	Optimized structures, HOMO and LUMO of phytochemicals present in <i>B. vulgaris</i>	87
4.7.1	(a) <i>P. embelica</i> plant (b – d) molecular structure of phytochemicals present in <i>P. embelica</i> extract (PEE)	89
4.7.2	FT-IR spectra of <i>P. embelica</i> extract (PEE)	90
4.7.3	UV-visible absorption spectra of the <i>P. embelica</i> extract (PEE)	91
4.7.4	Langmuir adsorption isotherm for <i>P. embelica</i> extract (PEE) with the help of weight loss measurement	92
4.7.5	(a) Potentiodynamic polarization plot (b) Electrochemical impedance plot (c) Bode plot (d) phase angle plot for different concentration of <i>P. embelica</i> extract (PEE)	93
4.7.6	(a) AFM micrographs of S.S.-410 (b) AFM micrographs of S.S.-410 immersed in 15% HCl solution (c) AFM micrographs of S.S.-410 immersed in 15% HCl solution with <i>P. embelica</i> extract (PEE) (d) SEM micrographs of S.S.-410 (e) SEM micrographs of S.S.-410 immersed in 15% HCl solution (f) SEM micrographs of S.S.-410 immersed in 15% HCl solution with <i>P. embelica</i> extract (PEE)	95
4.7.7	Optimized structures, HOMO and LUMO of phytochemicals present in <i>P. embelica</i>	96

### List of Abbreviations

S.S.	Stainless steel
MS	Mild steel
K	Kelvin
C	Concentration
IE	Inhibition energy
WE	Working electrode
SEM	Scanning electron microscopy
AFM	Atomic force microscopy
EIS	Electrochemical impedance spectroscopy
PDP	Potentiodynamic polarization
OCP	Open circuit potential
HOMO	Highest Occupied Molecular Orbitals
LUMO	Lowest Unoccupied Molecular Orbitals
$i_{\text{corr}}$	Corrosion current density
$E_{\text{corr}}$	Corrosion potential
$R_{\text{ct}}$	Charge transfer resistance
$C_{\text{R}}$	Corrosion rate
$\theta$	Surface coverage



## CHAPTER 1: INTRODUCTION

### 1. Corrosion

Corrosion has been discussed by the scientific community from last several decades due to its economic and environmental losses. It is recognized as a significant in many industrial processes and domestic structures, causing deterioration, failure, and severe incidents and threats [1, 2]. Corrosion is the oxidation of metals caused by a corrosive agent in their environment, such as chlorine, fluorine, carbon dioxide, oxygen, and so on. It is normally defined as destruction of metals and also a spontaneous process. Maintenance and repair costs, material loss, equipment damage, a reduction in productivity, and the loss of usable or productive life are all examples of economic damages caused by corrosion. Other social consequences of corrosion damage include safety issues (bursts, toxic material release), health issues (pollution due to toxic product contamination), and resource depletion [3]. Corrosion can affect the natural resources same as other phenomena like climate occasions. There are various methods for controlling corrosion rates and reduces their harmful effect on economy and public safety [4].

The most important thing about corrosion is that it is an unwanted phenomenon that destructs the materials and reduces their life time. Corrosion cannot be stop completely by any methods but its rate of reaction can be control. Its prevention is more achievable as compare to its disposal [5]. Corrosion is not always simply restricted to metals; it could likewise occur on distinct materials, for instance, polymers and plastic manufacturing. Amongst many metals, corrosion is experienced firmly in iron and steel. The formation of oxides in the process of oxidation does no longer hold immovably to the surface of metal, as a result it gets off the metal effortlessly [6]. Corrosion consists of an electrochemical procedure which depends on vital environmental factors like pH, temperature, pressure etc. [7]. Corrosion has vast monetarily and ecological impact directly or indirectly on highways, bridges, buildings, petroleum industries, chemical processing and wastewater systems, and all aspects of global infrastructure [8]. In various reports, it is mentioned that the total losses due to corrosion is around 2.5 trillion US dollars, which corresponds to 3.4% of gross domestic product (GDP) in the world (2013). From the national point of view, India lost around USD 70.3 billion, or 4.2%

of the country's GDP due to corrosion (2013) [9]. It causes several damages to materials, risks to community protection, disrupts industrial processes and involves wide restoration of stopped properties. In addition, the substitute of a corroded boiler or condenser in a large plant may additionally require dollar 1,000,000 or more for energy bought from inter linked electric power plants for supply to customers while the boiler is down. In the United States, this types of electric utilities, tens of millions of dollars annual amount are used [10-11].

## 1.2 Mechanistic approach to corrosion

At the initial stage, the process of corrosion was explained by Evans, Wagner and Traud based on local cell model and corrosion potential model [12]. According to electrochemical theory of corrosion, on immersing a metal or alloy in corrosive medium different potential zones are developed because of the destruction of its crystalline lattices by means of corrosion. Because of this potential difference anodic and cathodic areas are formed on the surface of metal where oxidation and reduction take place respectively [13]. Generally, the corrosion of a metal can be explained by considering the local electrochemical cells that are formed over the surface of metal during metal dissolution. Some part of surface acts as anode and other as cathode [14].

Two partial reactions, oxidation and reduction take place at the same time on the surface of metal. The reactions for the corrosion of iron are given below-

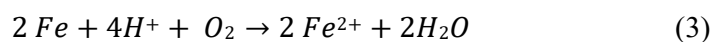
### Anodic reaction



### Cathodic reaction



### Overall reaction



### **1.3 Factors affecting metallic corrosion**

For the most part all metals and alloys show a crystalline structure. The crystals or grains of a metal are comprised of these unit cells repeated in a three dimensional arrangement. The crystalline nature of metals is not promptly clear in light of the fact that the metal surface are generally fits with the shape in which it has been formed [15]. Corrosion cells are made on the surface of metal in contact with an electrolyte as a result of energy differences between the metal and the electrolyte. Diverse regions on the metal surface could likewise have distinct potentials for the electrolytes. These variations are due to metallurgical factors, i.e. differences in their composition of microstructures, manufacture process, field establishment and environmental factors [16]. Corrosion is primarily influenced and relies upon the primary and secondary factors. Generally, the primary factors are specifically connected with the metal or alloy while secondary factors are related with specific environment. Since, corrosion is a natural condition that enables a substance to dissolve when exposed to aggressive conditions [17]. Corrosion is influenced by a number of factors, the most significant of which are the material and the surrounding atmosphere. If the material is involved or adjacent to a nobler component in the galvanic chain, it corrodes, causing the first one to dissolve. Specific climatic factors, such as gases dissolved in air out of which oxygen along with carbon dioxide are generally considered, pH and temperature of the surrounding area also cause the material more prone to corrosion. Depending on the process of corrosion, corrosion can take many different forms, pitting, crevice, uniform, galvanic environmentally-induced cracking, intergranular, and de-alloying are some examples [18- 20].

### **1.4 Corrosion in petroleum industry**

The oil industry's annual corrosion costs are in the billions of dollars. From drill platforms to casing, corrosion affects any aspect of research and development. The petroleum industry is home to a diverse range of corrosive conditions. Some of these are exclusive to the sector [21]. As a result, it is easier to group all of these conditions together. Steel and iron pipe, tubing, pumps, valves, and sucker rods are all used extensively in oil and gas fields. Leaks result in the loss of oil and gas, as well as the

purification of water and silt, causing corrosion damage. In oilfields, saline water and sulphides are common. Corrosion happens within and without the casing in wells [22]. Inorganics like water, hydrochloric acid, sodium chloride, sulfuric acid, carbon dioxide etc. are to blame for the majority of corrosion problems in refineries. The petroleum industry and the chemical industry have a lot in common [23].

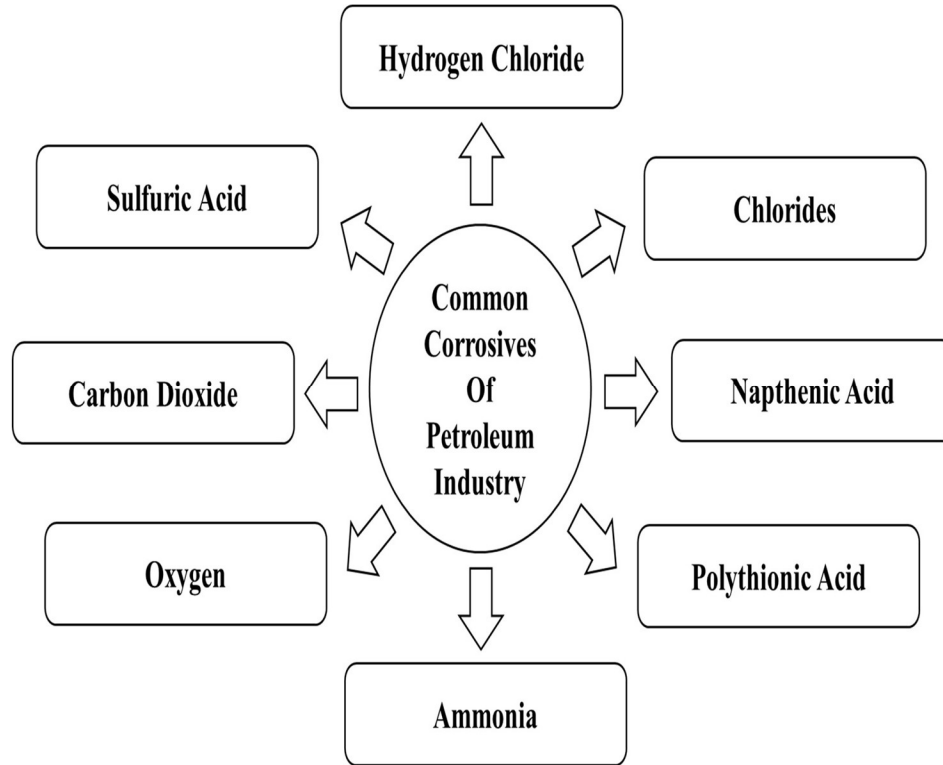


Fig. 1.1 Types of corrosive agents generally found in petroleum industry

Corrosive agents are classified into two parts: those found in raw material or petroleum products, and those associated with the analysis or control. Accordingly, hydrolysis results in the formation of hydrochloric acid. It may also be an unintentional addition to the product stream. Since this is a means of friction acid, it is often found in separation processes as well as in condensed crude oils like use of hydrofluoric acid in alkylation process [24]. Around 98 percent, commonly available carbon steel is the most important alloy, which is used as main alloy in materials used for building processes. In general, steel should be used wherever possible. This can be accomplished by altering the mechanism, such as decreasing the temperature or introducing inhibitors

[25]. Apart from cast iron, steel is the most affordable engineering metal. Because of corrosion by the cooling system, carbon steel is often unsuitable for heat-exchanger tubes. Arsenical Admiralty Metal, brass and red brass, and cupronickels are all popular materials. Austenitic steel structures are costly and prone to cracking in chloride-rich environments [26]. These steels, on the other hand, have been used for still piping and gas-cracking pipes. The film's passive nature protects the steel from corrosion while also allowing it to self-heal [27]. In steel, chromium is the most advantageous alloying element for Sulphur compound resistance. As a result, the chromium content of steel increases with rising Sulphur and temperature, beginning at 1 percent Cr [28]. The extent of corrosion protection is dependent on the percentage proportion of chromium as well as other metallic alloys to maintain their metallurgical properties. For this reason, now-a-days chromium–nickel steel structures become most widely used components for both low and high temperatures in harsh corrosive conditions [29]. Hence, due to their exceptional and diverse mechanical properties, these steels are broadly used throughout the industries which are working in chemical, oil & gas, significantly necessitating corrosion protection for various parts of the industrial instruments and processes which employ steels because steel corrodes, corrosion protection is needed for engineering, automobiles, boiler plates, pipes, reaction vessels, storage tanks, and bridges and construction projects [30].

However, such steels are influenced by the presence of chloride ions exposed due to various acid utilizing industrial procedures which causes localized corrosion more specifically to pitting corrosion. Most of the corrosion which occur in petrochemical sector is pitting corrosion and is mostly responsible for degradation of stainless steels [31]. Martensitic stainless steels consist of the 400 series of stainless steel which are chromium-containing general-purpose steels with excellent corrosion resistance. Due to their wide applicability, duplex and martensitic stainless steel have been studied extensively for corrosion resistance and vulnerability in corrosive conditions [32].

### **1.5 Methods of corrosion control**

The significance of corrosion prevention might be perceived in perspective of vast financial losses endured because of metallic corrosion in all spheres of life and

especially by industries [33]. From the view purpose of country's economy, it is extremely important to receive proper ways and intends to lessen the misfortunes due to corrosion. With increasing development in technology and industries the utilization of metals and alloys is expanded quickly and any progression in the heading of avoiding corrosion would be an incredible help [34]. Corrosion scientific experts and technologists trust that around one third of misfortunes because of corrosion can be spared by applying anticipation technique. The attacks of corrosion can be accomplished by numerous conceivable choices. The most essential among them are- Modification of materials by additionally alloying or de-alloying- where the substrate modification is made such that the oxide layer will either be relatively unreactive or protective coating is formed generally known as passivation for specific harsh environments [35]. Adjustment in the conditions of corrosive environments- addition of some corrosion preventing agents or adjusting of surrounding conditions like corrosive temperature or pH [36]. Utilization of defensive coatings- physical barrier methods like preventive films or coating can be used to reduce the rate of corrosion [37]. Cathodic and anodic protection- the corrosion current is inhibited, forcing it to flow to the metal that needs to be covered. It is accomplished by adding a more active (anodic) substrate to the system to be covered or by using a source of power [38]. Utilization of corrosion inhibitors- its mechanism follows the resistance of corrosion initiation by adsorbing themselves on the steel substrate and by the formation of thin film which act as defensive barrier against corrosion [39]. Prevention of corrosion by applying inhibitors is one of the most convenient way. In the present study corrosion inhibition has been considered by utilizing corrosion inhibitors, in this manner an itemized discussion on corrosion inhibitors and their applications has been done [40].

### **1.6 Corrosion inhibitors**

They are substances that can slow down corrosion reactions when applied to the process. Their inhibition function is not always easy to decipher and analyze. Anodic, cathodic, or mixed inhibition effects are possible [41]. Substances which reduces the rate of reaction without influencing the environment are known as corrosion inhibitors. The inhibitors utilized as a part of corrosive environment basically functions by forming a protective layer on the metal surface [42]. The mixed class comprises majority of

green corrosion inhibitors. By lowering both their electrochemical concentrations, mixed-type inhibitors can protect at both cathodic and anodic ends simultaneously. The adsorption of molecules with functional group or elements comprising free electron couples, such as N, P, S, and O, is often linked to the mechanism of inhibition [43- 44].

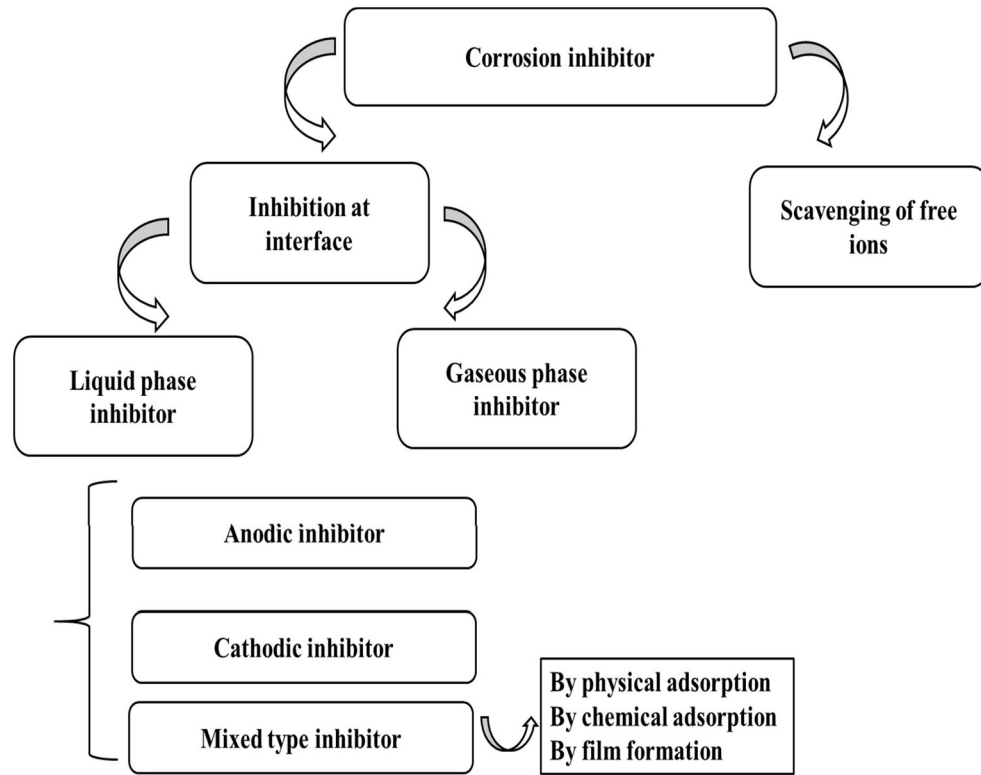


Fig. 1.2 Types of mechanism of corrosion prevention by inhibitor

Metal tubulars, down hole equipment, substrate lines, and other metals are more prone to corrosion. Since, the rate of corrosion increase dramatically in wells having higher temperature ranges. Hence, corrosion control becomes an important problem to be handled with caution [45]. Different compounds are there that are considered in the form of appropriate inhibitors. They ordinarily have N, O and conjugated systems and strong capacity of being adsorbed on the surface [46]. The most imperative disadvantage relative with the greater part of them is their high cost and non-eco-friendly character. Numerous corrosion inhibitors are being used successfully in the industry, including quaternary ammonium products, propargyl alcohol-based compounds, and so on. Due to strict environmental legislation, therefore, attention has

shifted to the production of new environmentally friendly protective coatings. Inorganic materials, especially chromates and their derivatives, are highly regarded for inhibitory properties. Despite this, they have a negative effect [47]. The consequences for human lives and the ecosystem has prompted their abolition. Along these lines the investigation of most recent low harmful inhibitors is essential to discard this disadvantage. The area of metallic materials deterioration, which is typically addressed with harmful substances, has found fertile ground in green chemistry [48]. In reality, when oxidation process needs to be stopped, regulated, or delayed, the use of inhibitors is a well-known technique. Green inhibitors are biodegradable, environmentally friendly, and regenerative. Nowadays inhibitors are being developed by using various parts of plants as they can be accessed easily and they are sustainable [49]. Food-grade chemicals that are called "green" chemicals have a lot of potential in the petroleum industry as corrosion protection. Plant parts extracts are excellent corrosion inhibitors in the acid range of concentrations studied (0.1–2 M), mostly acting as mixed form corrosion inhibitors, though a few studies have shown that they can also act as anodic and cathodic type inhibitors [50]. The presence of different compounds like polyphenols, polysaccharides etc. increases the capability of such inhibitors (plant extract) to restrain the procedure of corrosion. The viability of inhibitors is reliant on different factors like - the relationship between corrosion inhibition and inhibitor concentration has been examined by other researchers [51]. The increase in corrosion resistance with the effect of concentration of inhibitor trend to approach a most extreme effectiveness at a certain concentration past which no critical increment in efficiency is observed. This is known as the optimum concentration and the maximum surface area of metal is covered at this concentration [52-53]. Since, in petroleum industries, pipelines are indeed the secure and most cost-effective way to move oil and gas in both offshore and onshore systems. Corrosion inhibitors appear to play an important role in preventing internal corrosion in pipelines [54]. A variety of corrosion inhibitors have also been developed that have a low impact on the environment while maintaining their inhibitory effectiveness



## CHAPTER 2: REVIEW OF LITERATURE

Metals corrosion is a natural and inevitable process that causes desirable metal properties to deteriorate due to contact with certain elements in the setting. Metals, with the exception of gold, platinum, and a few others, are found in nature in impure forms, mostly as sulphides or oxides, and are stable [56]. In order to combat corrosion, many techniques have been implemented. Development, selection of materials, protection at anode or cathode, composites, and the application of corrosion inhibiting substances are all examples of these. In all of these methods, corrosion inhibitor is perhaps the most cost-effective and straightforward [57]. Corrosion inhibitors are compounds that can slow the rate of metal dissolution in corrosive conditions when present in low concentrations. There has been a lot of research into corrosion inhibition using extracts from different parts of the plant. In reality, bioactive compounds contained in plant extracts have been found to be almost as effective as synthetic inhibitors [58]. Plant extracts are often tested as corrosion inhibitors due to their environmental friendliness and economic value. Numerous phytoconstituents are present in plant extracts which can prove very effective substituent for the harmful inorganic and synthetic inhibitors. The composition of active ingredients determines the mechanism of inhibition for plant based inhibitors [59]. The main components vary from one plant to the next, and also within the same plant. Since the structures of such parts are so likely to be related, the mechanism of corrosion protection for various plants and their parts may or may not differ [60]. This opens up a lot of possibilities for using bio-resources from plant for corrosion inhibition at various levels in an environmentally friendly way [61-62].

### 2.1 Corrosion inhibition in hydrochloric acid environment

Hydrochloric acid is a well-known industrial acid that is used for pickling and acidification of oil wells. Since less pickling time and improved surface quality can be achieved at low temperatures, HCl is preferred over other acids for pickling exercises [63]. Temperatures above 30 °C are not needed for the procedure because this would result in an excessive amount of hydrogen chloride gas being released. Pickling with 5–15 percent HCl acid is recommended, while acidification with higher concentrations up to 32 percent is recommended [64]. Recent studies on plant component extracts as

an anticorrosive agent in an HCl setting suggest that the aim is to prevent metal corrosion during pickling. Plant extracts are effective corrosion inhibitors that primarily serve as mixed form inhibitors [65]. During pickling, plant extract is often used as an anticorrosive agent in an HCl setting. Oil well stimulation, which is typically performed with hot hydrochloric acid solutions, can significantly leads to corrosion of tubes and pipes in production area and also the other equipments exposed to acid [66]. Industries utilizes a number of chemicals like single or mixture of acids are used along with surfactants for well acidizing processes. During such procedures, the tubing and pipeline materials suffers acid attack and to protect them from deterioration, inhibitors are employed [67-68]. The process of inhibition in industries dealing with oil pipelines, distillatory, refineries etc. becomes more complex due to the presence of different forms of aggressive media and their usage in cleaning operations [69-70]. Before deciding on the appropriate materials, each case must be considered in its entirety. For all forms of corrosion, there is no universal anti-corrosive content. Some of the plant extract in which were used as anticorrosive in hydrochloric acid are explained below:

Pandian Bothi raja et al. 2013 studied the anticorrosive properties of *Neolamarckia cadamba* for MS in 1M hydrochloric acid solution. To check the corrosion resistance nature of *Neolamarckia cadamba*, electrochemical analysis was performed. Protective film formation is verified by SEM study on the MS surface. From the studies conducted, it was concluded that the studied plant showed an approximate 80% inhibition efficiency at 5 mg/L concentration. The inhibitors acted as both anodic and cathodic type of inhibitors as shown by PDP. EIS studies revealed that the corrosion inhibition occurred due to increase in the resistance of system against corrosion. Also, the process of corrosion inhibition was adsorption which followed Langmuir adsorption isotherm pattern. From the SEM studies it was concluded that there is a kind of barrier formation which blocks the acid attack, thereby preventing corrosion [71].

*Euphorbia falcata* was studied in 1M HCl solution by Bribri et al. 2013 for carbon steel. Corrosion impedance was analyzed with the use of electrochemical studies which suggested an approximate 93 % inhibition efficiency at a concentration of 3.0 g/L. From the Tafel analysis, mixed type of corrosion inhibition, anodic and cathodic was shown and impedance studies revealed that the mechanism of inhibition of corrosion was due

to the increased system resistance towards acid attack and decrement in  $C_{dl}$  value indicated a layer formation on the steel surface. Since, the process of corrosion inhibition was adsorption, it followed the Langmuir adsorption isotherm pattern. Also SEM studies proved that a protective layer was formed on the steel surface, hence preventing it from the process of corrosion [72].

Hamdy and Gendy 2013 investigated the corrosion inhibition property of *Henna* in 1M HCL solution for low carbon steel. SEM, FTIR, XRD study were done along with electrochemical studies for the carbon steel surface. It was seen that the studied plant showed an approximate 92.72% inhibition efficiency at 3000 mg/L concentration. Mixed type of inhibition was shown by inhibitor as concluded from potentiodynamic polarization. From the SEM studies it was seen that a barrier was formed on the steel surface which resisted the acid attack, hence preventing it from the process of corrosion, when the EDX analysis was done it was seen that there is suppression of Fe, O and Cl peaks in steel surface which was treated with the inhibitor molecules as compared to the steel which was untreated. This resulted in the formation of protective layer on the steel and hence prevents metal from corrosion. SEM studies indicated that the adsorption played a factor in corrosion control and it followed the Langmuir adsorption isotherm pattern. From the analysis of activation energy parameters, it was found that the process of adsorption was spontaneous and also endothermic [73].

In 1M HCl solution, Shalabi et al., 2014 tested the corrosion resistance of *Atropa belladonna* for carbon steel. Gravimetric analysis and electrochemical tests were used to analyze the inhibition efficiency for corrosion of *Atropa belladonna*. According to the electrochemical tests, the investigated plant had a 96.6 % inhibition efficiency at 500 ppm concentration. Also, the inhibitors acted as mixed type of inhibitors but acted as anodic inhibitor at first place and impedance studies revealed that the corrosion inhibition occurred which is shown as increase in the system resistance and double layer capacitance value also decreased which suggested thick layer presence on the steel surface [74].

Soltani et al. 2014 investigated the corrosion resistance of *Silybum marianum* for S.S.-304 in 1M HCl solution. To check the corrosion resistance nature of *Silybum marianum*,

PDP and EIS were done at different temperature. From the electrochemical studies, it was observed that the studied plant showed an approximate 96% inhibition efficiency at 1.0 g/L concentration. The inhibitors acted as mixed type of inhibitors as shown by potentiodynamic polarization. The adsorption played a factor in corrosion control and it followed the Langmuir adsorption isotherm pattern. From the analysis of activation energy parameters, it was found that the process of adsorption was spontaneous and also endothermic suggesting adsorption by chemical process. Also, molecular dynamic studies were performed which showed inhibitor molecules are well adsorbed on the substrate [75].

*Eleusine aegyptiaca* was investigated by Rajeswari et al. 2014 for corrosion protection of cast iron in 1M HCl solution. From the electrochemical studies, it was seen that the studied plant showed an approximate 91.5% inhibition efficiency for *Eleusine aegyptiaca* and 94.6 % inhibition efficiency for *croton rotleri* at 2400 ppm concentration. From the XRD analysis, it was seen that there is suppression of peaks in steel surface which was treated with the inhibitor molecules as compared to the steel which was untreated. This was attributed to the formation of barrier on the surface of steel towards acid attack and hence prevents metal from corrosion. SEM studies indicated that the adsorption played a factor in corrosion control and it followed the Langmuir adsorption isotherm pattern. From the analysis of activation energy parameters, it was found that the process of adsorption was spontaneous and also endothermic. It was also concluded that inhibition of corrosion was due to adsorption which followed physical mechanism of adsorption [76].

C38 steel was used by Faustin et al. 2015 to analyze the anticorrosive properties of *Geissospermum martianum* in 1M HCl solution. To characterize the active molecule functioning as corrosion inhibitor from this plant was identified by NMR and Geissospermene was found to be the most active molecule from the plant *Geissospermum martianum*. From the electrochemical studies, it was seen that the studied plant showed an approximate 92 % efficiency of inhibition at a concentration 100 mg/L. The inhibitors acted as anodic type of inhibitor more prominently. SEM and EDX studies indicated the role of adsorption which played a key factor in corrosion control and it followed the Langmuir adsorption isotherm pattern [77].

Anupama et al. 2015 analyzed the anticorrosive properties of leaf extract *Pimenta dioica* for MS in 0.5 M and 1M HCl solution. Along with electrochemical studies, SEM and AFM study was done to check the inhibitors effect on the MS surface. It was seen that the leaf extracts of studied plant showed a good inhibition efficiency of more than 90 % at different concentrations and with different type of leaf extracts. The inhibitors acted as anodic type of inhibitor more prominently according to potentiodynamic polarization. SEM and AFM studies suggested that the inhibitor formed a protective barrier on the steel surface, hence preventing it from the process of corrosion. SEM studies indicated that the adsorption played a factor in corrosion control and it followed the Langmuir adsorption isotherm pattern [78].

Prabakaran et al. 2016 studied the corrosion resistance of *Ligularia fischeri* for MS in 1M HCl solution. Protective film formation is verified by SEM, AFM and WAXD study on the mild steel surface. Plant showed an approximate 92% inhibition efficiency at 500 ppm concentration as shown by electrochemical studies. When the EDX analysis was done it was seen that there is increase in the concentration of iron and oxygen on the steel surface which was treated with the inhibitor molecules as compared to the steel which was untreated. This was attributed to the protective barrier formation on the surface of steel and hence prevents metal from corrosion. SEM studies indicated that the adsorption played a factor in corrosion control and it followed the Langmuir adsorption isotherm pattern. From the analysis of activation energy parameters, it was found that the process of adsorption was spontaneous and also endothermic [79].

Anupama et al. 2016 studied the corrosion resistance of extract of *Phyllanthus amarus* for MS in 1M HCl solution. To check the corrosion resistance nature of *Phyllanthus amarus*, gravimetric analysis, PDP and EIS were used. From the electrochemical studies, it was seen that the extract of studied plant showed a good inhibition efficiency of more than 90 % at different times of immersion of steel surface in corrosive media. Mixed type of inhibition was explained with the help of PDP. EIS claimed that the corrosion inhibition occurred due to increased system resistance towards corrosion and decrease in double layer capacitance value indicated the thick layer formation by inhibitor. The adsorption played a factor in corrosion control and which was supported

by Langmuir adsorption isotherm pattern. QCC were also performed to get the details of electronic structures of the main component from the plant which is phyllanthin [80].

Rose et al. 2016 studied of *Tabernaemontan adivaricata* for MS in 1M HCl solution. From the electrochemical studies, it was suggested that the studied plant showed an approximate 95% efficiency for corrosion inhibition at inhibitor concentration 500 ppm. PDP showed that the inhibitors acted as mixed type of inhibitors. Also, the process of corrosion inhibition was adsorption which followed Langmuir adsorption isotherm pattern. A protective layer was formed due to adsorption of molecules from the inhibitors on the steel surface [81].

Anupama et al. 2017 studied the anticorrosive property of *Plectranthus bamboinicus* for MS in 1M HCl solution. From the electrochemical studies, it was seen that the extract of studied plant showed a good inhibition efficiency of more than 90 % at different inhibitor concentration as shown by gravimetric and electrochemical studies. Synergism and theoretical studies were also performed using Gaussian 03 and from the study the combination of the active constituents-thymol and cineole showed good inhibition properties [82].

*Gum arabica* extract was studied as anticorrosive agent for MS in 1M HCl acid solution by Azzaoui et al. 2017 investigated the corrosion resistance of for. AFM and XPS study were used to analyze surface changes on the mild steel surface due to the presence of inhibitor. From the electrochemical studies, it was seen that the studied plant showed an approximate 92% inhibition efficiency at 1.0 g/L concentration. The inhibitors acted as both anodic and cathodic type of inhibitor. From the surface studies it was concluded that the inhibitor a barrier on steel surface which helped in corrosion protection, when the XPS analysis was done it was analyzed from the studied parameters that there is less dissolution of iron from steel surface when it was treated with the inhibitor molecules as compared to the steel which was untreated, hence prevents metal from corrosion [83].

Allbakhshi et al. 2018 analyzed the corrosion resistance of *Glycyrrhiza glaba* for MS in 1M HCl solution, the corrosion current density decreased significantly as observed in the presence of inhibitor which results an increment in the corrosion inhibition

efficiency. Also, different modelling studies like molecular dynamics, quantum mechanics and Monte Carlo were done to find out the presence of inhibitors molecules from the plant. It was found that organic molecules like Glycyrrhizin, Glabridin, 18  $\beta$ -Glycyrrhetic acid, Licochalcone E, Liquiritigenin and Licochalcone participated in adsorption process thus by blocking the initiation of corrosion process [84].

Corrosion resistance of *Coconut* for MS in 1M HCl solution was studied by Umoren et al. 2014 investigated. To check the corrosion resistance nature of *Coconut*, gravimetric analysis and hydrogen evolution were used with methanol and water extracts of the coconut coir. From the gravimetric analysis, it was suggested that the studied plant showed an approximate 80.0% inhibition efficiency at 500 g/L inhibitor concentration. PDP showed that the inhibitors acted as mixed type of inhibitors. The adsorption played a factor in corrosion control and it followed the Langmuir adsorption isotherm pattern [85].

Liao et al. 2017 investigated *Longan* as anticorrosive agent for MS in 1M HCl solution. Protective film formation is verified by SEM study on the MS surface. From the analysis, it was suggested that the studied plant showed an approximate 92.35 % inhibition efficiency at 600 mg/ L concentration of inhibitor. PDP showed that the inhibitors acted as mixed type of inhibitors. Also, the process of corrosion inhibition was adsorption which followed Langmuir adsorption isotherm pattern A protective barrier was formed due to adsorption of molecules from the inhibitors on the steel surface as depicted by SEM analysis [86].

*Plantago* extract was used to investigate its anticorrosive properties for MS in 1M HCl solution by Mobin and Rizvi 2017. Various methods like PDP, EIS and weight loss were used to analyze the anticorrosive nature of the *Plantago* extract. From the electrochemical studies, it was suggested that the studied plant showed an approximate 93.54 % inhibition efficiency at 1000 ppm inhibitor concentration. PDP showed that the inhibitors acted as mixed type of inhibitors. Also, the process of corrosion inhibition was adsorption which followed Langmuir adsorption isotherm pattern A protective barrier was formed due to adsorption of molecules from the inhibitors on the steel surface as depicted by SEM and AFM studies [87].

*Pisum sativum* was investigated as anticorrosive for MS in 1M HCl solution by Srivastava et al. 2018. From the electrochemical studies, it was suggested that the studied plant at an inhibitor concentration of 400 mg/L showed an approximate inhibition efficiency of 90%. Also, the process of corrosion prevention was adsorption which followed Langmuir adsorption isotherm pattern. SEM and AFM studies were done to identify the presence of protective barrier on the steel surface. The process of barrier formation was adsorption which happened as a result of bonding at the interface of inhibitor- steel surface, hence preventing it from the process of corrosion [88].

Hassannejad and Nouri 2018 investigated the anticorrosive nature of Sunflower for MS in 1M HCl solution. From the electrochemical studies, it was seen that the studied plant showed at 400 ppm inhibitor concentration an approximate 98% inhibition efficiency. PDP showed that mixed type of inhibition was shown by the studied plant and impedance studies revealed that the inhibition of corrosion occurred due to increase in the resistance of system against corrosion. Also the activation energy studies suggested that the physical adsorption takes place and the process was exothermic which meant that there is no increment in the inhibitory potential when temperature is increased [89].

*Xanthan gum* was studied by Biswas et al. 2014 in 1M HCl acid solution for corrosion resistance of MS. It was suggested that the studied plant showed an approximate more than 90% inhibition efficiency at an inhibitor concentration of 0.5 g/L. Mixed type of inhibition i.e. both anodic and cathodic type was shown by the inhibitor. Also, the process of corrosion inhibition was adsorption which followed Langmuir adsorption isotherm pattern. From the SEM studies it was concluded that the inhibitor formed a protective barrier on the steel, hence preventing it from the process of corrosion [90].

## **2.2 Waste materials from plants as inhibitors of corrosion in hydrochloric acid**

Green chemistry has sparked a lot of interest in the last decade by developing chemical processes and consumer products with the goal of avoiding toxins and reducing waste. Waste generation and the use of harmful and dangerous chemicals are causing increasing concern. Environmental problems and strategies have risen to the top of the global agenda [91]. Green chemistry has shown over time that how basic methodologies developed by scientific approach can help in safeguarding the health and well-being



and also the environment while still being beneficial with respect to economic value. Many industrial applications utilize sustainable raw materials and biomass as green chemistry and sustainability approach [92]. The metallic surface protection has become an important area wherein the green chemistry methods including the products derived from biomass are providing development in order to decrease environmental effects and wastes. The use of harmful to the environment organic materials has been a common cause of metal degradation processes [93]. To remove scales which are deposited on the surfaces of metallic structures in process industries, acidic and destructive solutions are commonly used at various levels of industrial operating procedures. When metal corrosion needs to be managed, stopped, to be delayed, the use of preventive measures as inhibitors is a considerable technique [94]. Some of the waste products of plants which were studied for their anticorrosive properties are given below:

Odewunmi et al. 2015 investigated the anticorrosive properties of Water melon waste product for MS in 1M HCl solution. To check the corrosion resistance nature of Water melon, electrochemical tests, weight loss immersion tests were performed. Protective film formation is verified by SEM study on the MS surface. From the findings, it was suggested that the studied plant showed an approximate 86.08 % inhibition efficiency at 2 g/L inhibitor concentration. Also, the process of corrosion inhibition was adsorption which followed Langmuir adsorption isotherm pattern. From the SEM studies it was concluded that the inhibitor formed a protective barrier on the steel, hence preventing it from the process of corrosion [95].

Carbon steel was used by Ismail et al. 2011 to investigate the corrosion resistance of waste from fresh banana leaves in 1M HCl solution. Protective film formation is verified by SEM study on the carbon steel surface. From the electrochemical studies, it was suggested that the studied plant showed an approximate 69.60 % inhibition efficiency at 10 % v/v inhibitor concentration. Also, the process of corrosion inhibition was adsorption which followed Langmuir adsorption isotherm pattern. From the SEM studies it was concluded that the inhibitor formed a protective barrier on the steel, hence preventing it from the process of corrosion [96].

*Punica granatum Linne* Husk was studied in 1M HCl solution by Chen et al. 2013 to investigate anticorrosive properties for mild steel in oil fields. To check the corrosion resistance nature of *Punica granatum Linne* Husk, gravimetric measurements, PDP and EIS were used. From the electrochemical studies, it was suggested that the studied plant at 1.0 g/L inhibitor concentration showed an approximate 95% inhibition efficiency. PDP showed that the inhibitors acted as mixed type of inhibitors. Also, the process of corrosion inhibition was adsorption and it was concluded that the inhibitor formed a protective barrier on the steel, hence preventing it from the process of corrosion [97].

The corrosion resistance of *Musa paradisiaca* (Banana) Peel for carbon steel was studied by Tiwari et al., 2018 investigated in 1M HCl solution. From the electrochemical studies, it was suggested that the studied plant showed an approximate inhibition efficiency of 80% at an inhibitor concentration 400 mg/L. To better understand the process of inhibition, quantum chemical calculations by DFT were done. PDP showed that the inhibitors acted as mixed type of inhibitors. From the SEM and AFM studies it was concluded that the inhibitor formed a protective barrier on the steel, hence preventing it from the process of corrosion [98]

*Argemone mexicana* root was studied by Gopal et al. 2017 in 1M HCl solution at different temperatures for the corrosion resistance of carbon steel. Different methods like gravimetric analysis, tafel polarization and EIS studies, SEM, AFM were used to study the anticorrosive nature of *Argemone mexicana* root. Protective film formation is verified by SEM study on the carbon steel surface. From the gravimetric analysis, inhibition efficiency of 94 % at an inhibitor concentration of 400 mg/L was seen. PDP showed that mixed type of inhibition was shown by the studied plant. SEM and AFM studies were done to identify the formation of protective barrier on the steel surface. The process of barrier formation was adsorption which happened due to the bonding of inhibitor molecules with the surface of carbon steel, hence preventing it from the process of corrosion [99].

Krishnan and Shibli, 2018 investigated the corrosion resistance of *Sesbania grandiflora* Leaf for mild steel in 1M HCl solution. From the electrochemical studies, it was suggested that the studied plant showed an approximate 98.01 % inhibition efficiency

at 10,000 ppm inhibitor concentration. Tafel polarization showed that anodic type of inhibition was shown by the studied plant. The process of barrier formation was adsorption which was facilitated by the bonding of molecules from inhibitor to the surface of the mild steel, hence preventing it from the process of corrosion [100].

Carbon steel was used by Al- Senani, 2016 to investigate the corrosion resistance of *Cucumis sativus* (cucumber) Peel in 1M HCl solution. It was suggested from the studies, that the studied plant showed an approximate 79.7% inhibition efficiency at 1.0 g/L inhibitor concentration. PDP showed that mixed type of inhibition was shown by the studied plant. The process of barrier formation was adsorption which prevented it from the process of corrosion. The thermodynamic parameters suggested that the process of adsorption was endothermic and spontaneous and the inhibitor followed physicochemical type of adsorption [101].

Rocha et al. 2014 investigated the corrosion resistance of mango peel for carbon steel in 1M HCl solution. From the electrochemical studies, it was suggested that the studied plant showed an approximate inhibition efficiency of 97% at an inhibitor concentration of 0.4 g/L. PDP showed that mixed type of inhibition was shown by the studied plant. SEM and AFM studies were done to identify the presence of protective barrier on the steel surface. The process of barrier formation was adsorption which happened due to the bonding between the inhibitor molecules and steel surface, hence preventing it from the process of corrosion [102].

Umoren et al. 2013 investigated the corrosion resistance of *Date palm (Phoenix dactylifera)* Seed for mild steel in 1M HCl solution. From the electrochemical studies, it was suggested that the studied plant showed an approximate 86.8 % inhibition efficiency at 2.5 g/L inhibitor concentration. PDP showed that mixed type of inhibition was shown by the studied plant. SEM and AFM studies were done to identify the presence of protective barrier on the steel surface. The process of barrier formation was adsorption which happened due to the bonding between the inhibitor molecules and steel surface, hence preventing it from the process of corrosion [103].

Ferreira et al. 2018 investigated the corrosion resistance of Brown onion Peel for carbon steel in 1M HCl solution. Protective film formation is verified by SEM study on the

carbon steel surface. It was suggested from the electrochemical studies, that the studied plant showed an approximate inhibition efficiency 94 % at an inhibitor concentration 300 mg/L. PDP showed that mixed type of inhibition was shown by the studied plant. SEM and AFM studies were done to identify the presence of protective barrier on the steel surface. The process of barrier formation was adsorption which happened due to the bonding between the inhibitor molecules and steel surface, hence preventing it from the process of corrosion [104].

### **2.3 Plant waste biomass like Straw and husk as environmental pollutants**

Agricultural straw residues from crops like rice, barley, and wheat are often burned by farmers. After harvest, wheat, rice, maize, and cotton burning is a common occurrence. Countries which depend largely on agricultural products, faces such environmental pollution due to seasonal burning of agricultural waste [105]. Straw is a by-product of agriculture, consisting of the dry stalks of cereal plants that have been stripped of their grain and chaff. Scientific community has explored various harmful effects of pollution caused by burning of straw. [106]. Particulate matter is one of the pollutants released by straw burning along with carbon dioxide (CO<sub>2</sub>), some volatile organic compounds (VOCs), and other substances considered as poisonous. When straw is burned, it produces a PM levels are high, with submicron and fine particles predominating [107]. Straw burning produces very little SO<sub>2</sub> and NO<sub>x</sub>, two general pollutants from alternative energy sources. Agricultural/waste burning is the regulated burning of vegetative waste from agricultural operations [108]. Land burning of vast areas of crop residue after harvest, pasture restoration fires, and open waste burning are all examples of this. Similarly, converting the land to cropland or pastureland is the most viable and cost-effective alternative [109].

Burning agricultural waste, such as stalks, grasses, leaves, and husks, is still the simplest and least costly way to reduce or eliminate the amount of flammable materials produced during agrarian activity in many countries. Biomass burning is a major cause of emissions in the atmosphere on both a regional and global scale [110]. The combustion of biomass releases a variety of gases and aerosols into the atmosphere, which have an effect on regional air pollutants, global atmospheric

chemistry, visibility, biogeochemical cycles, the earth's radiative budget, and environmental degradation [111].

Biomass burning also produces smoke, which is a popular and noticeable substance. Smoke is also made up of gaseous and aerosol contaminants like brown carbon and mineral dust, both of which have been linked to poor air quality and global warming [112].

#### **2.4 Plant based corrosion inhibition used at high concentration**

Some plant waste materials which have been used as green corrosion inhibitors in past show good inhibition efficiency at higher concentrations. This research work aims at evaluating the corrosion inhibition efficiency of some selected plants at lower concentrations. Some of the plant based waste materials which showed good inhibition efficiency at higher concentrations are given in Table 2.1

#### **2.5 S.S. - 410 in petroleum industry**

The refining of petroleum and its products has become a sophisticated process in the past years. The petrochemical industry has become very complex and the advances in engineering technologies have made the improvement in plant operations and successful increase in product yield [126]. Main emphasis is laid on the materials which can withstand the harsh environments of the petrochemical processes. Such materials include steels which are resistant to corrosion, metal alloys complexes etc. which provide high strength, load taking, good fabrication properties and low maintenance cost [127]. Stainless steels are corrosion-resistant ferrous metals due to the presence of protective thin film on their surface formed due to the mixtures of chromium and iron molecules. The film's passive nature protects the steel from corrosion while also allowing it to self-heal. Chromium is added to the microstructure of steel to enhance its corrosion resistance [128]. The American Iron and Steel Institute has recognized 57 distinct steel compositions as standard and 18 of these 57 have been characterized to be used in petroleum processes. The 400 series of stainless steels come under Martensitic group. These steels are magnetic and heat treatment can harden them. They are resistant to corrosion in some mild corrosive environments [129].

Table 2.1: Plant based corrosion inhibition used at high concentration

Plant name	Concentration (g/L)	Corrosive media	Inhibition efficiency (%)	Reference
<i>Marrubium vulgare L.</i>	8.0	1 M HCl	86.51	113
<i>Tender arecanut</i>	4.5	0.5 M HCl	95.50	114
Polyaspartic acid	10	5 M H <sub>2</sub> SO <sub>4</sub>	80.33	115
<i>Pectin</i>	8	2 M HCl	94.40	116
<i>Matricaria recutita</i>	7.2	1 M HCl	93.28	117
<i>Opuntia ficus indica</i>	5.0	1 M HCl	91.76	118
<i>Malus domestica</i>	5.0	0.5 M HCl	87.9	119
<i>Ocimum basilicum L.</i>	5.7	0.5 M HCl	90.10	120
<i>Citrus sinensis</i>	4.0	5 M HCl	93.38	121
<i>Barley agriculture waste</i>	5.0	1 M HCl	97.10	122
<i>Phyllanthus muellerianus</i>	6.67	3.5% NaCl	97.58	123
<i>Verbena</i>	6.0	1 M HCl	81.10	124
<i>Thymus vulgaris</i>	10.0	5 M H <sub>2</sub> SO <sub>4</sub>	88.60	125
<i>Xylopi aethiopica</i>	10.0	5 M H <sub>2</sub> SO <sub>4</sub>	47.80	125
<i>Zingiber officinale</i>	10.0	5 M H <sub>2</sub> SO <sub>4</sub>	79.60	125

SS- 410 type contains 12% of chromium in its composition which makes it corrosion resistant up to some extent and most widely used S.S.-410 in petroleum used. Corrosion is a major issue in the petrochemical industry, which is intensified by its difficult

manufacturing processes [130]. Most parts/components are destroyed by corrosion, which happens due to the deterioration of the metallic materials and their properties, at any point of the manufacturing process. In the petrochemical industry, the main type of corrosion found is generally pitting corrosion which leads to the loss of characteristics of stainless steels [131]. The corrosive environment which is present in petrochemical and refining industries arises due to the presence of chlorides- generally from the salts of magnesium and calcium which originates from crude oil, cooling water, catalysts etc. and from hydrogen chloride- which forms due to the hydrolysis of calcium and magnesium chloride salts and occurs in overhead vapour streams from the refining processes and upon condensation, highly aggressive and harsh hydrochloric acid is formed [132-133]. From a corrosive aspect, HCl is the most difficult acid to handle. It necessitates extreme caution when used and when selecting products to contain the acid [134-135]. Most common metals and alloys are extremely corrosive to it. The condensing water which is used in the industrial applications readily absorb hydrochloric acid from the condensing systems in the crude unit overhead [136]. In the ambient fractionating column above, hydrogen chloride condenses and forms extremely corrosive hydrochloric acid in the heat exchanger [137]. Many other acids can also lead to corrosion apart from hydrochloric acid if present in higher amounts in the process area due to the breakdown of the protect barrier of iron hydroxide or iron sulphide [138].

### **3.1 Purpose of present research work**

The presented research work in this thesis explore so me novel, better, environmental friendly, green inhibitors for corrosion to protect the S.-410 from corrosion due to acidic media since, natural organic molecule inhibits corrosion in a variety of ways. This thesis is concentrated with the extraction of selected plants and methods for analyzing their prospects in corrosion inhibition of stainless steel. The corrosion inhibition studies of these plant extract on S.S.-410 in 15 % HCl have not been yet reported elsewhere. Gravimetric and electrochemical methods are used to calculate the inhibition efficiency studies of selected plants extract towards S.S.-410 in 15% hydrochloric acid. For supplementing the outcomes other techniques like surface adsorption, morphological characterization and theoretical studies were also performed.

### **3.2 Scope and intents of the present research work**

In this research work some plants extract have been used as eco-friendly, sustainable, non-hazardous, economical natural corrosion inhibitors and investigated by different techniques like; Electrochemical methods EIS and PDP followed by weight loss investigates. Surface characterization methods atomic force microscopy (AFM) supported by scanning electron microscopy (SEM). Other supplementary techniques such as; computational studies (quantum chemical calculations), ultraviolet visible spectroscopic techniques have been carried out for prepared corrosion inhibitors.

Electrochemical methods are prevailing and multipurpose analytical techniques that provide high sensitivity, accuracy, and precision. Green and natural corrosion inhibitors are eco-friendly, effective, sustainable and non-hazardous for the nature as well as the human beings. There inhibitors contain electronegative hetero atoms like N, O, and unsaturation bonds. In this present research work, a new class of natural corrosion inhibitors has been analyzed. These inhibitors are eco-friendly, non-hazardous, non-toxic, economical, sustainable, and natural corrosion inhibitors to restrain corrosion for SS in acidic corrosive media. The greatest advantage of natural inhibitors is that they can be easily and conveniently extracted from the plants with very low/cheap production coast. Because of the existence of various functional groups containing electronegative atoms in the plant inhibitor extract, these inhibitors have been documented as effective inhibitors against corrosion of stainless steel by aggressive media. The formation of bonds between molecules present in the inhibitors with the exposed ions on the surface of the metal and make complexes which covers the surface of the steel substrate thus forming a protective barrier and helps in resisting corrosion by blocking acid attack. The present research work is a compilation of study of selected plants extract as natural corrosion inhibitor for S.S.-410 in the corrosive media.



### **3 Objectives of the study**

- The proposed research work aims at filling the research gap in unexplored area of plant waste material as efficient corrosion inhibitors by using weight loss measurements, EIS and Tafel studies.
- To analyze the extract of plant's waste for their higher corrosion inhibition efficiency at lower concentration.
- To study the mechanism of adsorption of inhibitors on steel surface by using UV, IR, SEM, AFM and Quantum chemistry method.
- To conduct comparative study between selected corrosion inhibitors with existing materials.
- To resolve the environmental pollution by selecting plant waste materials like husk and straw to be used as effective corrosion inhibitors.

## CHAPTER 03: MATERIAL AND METHODS

Analysis was performed to contemplate the corrosion inhibitive capacities of selected plants towards corrosion of S.S.-410 in 15 % HCl solution at various inhibitor concentration at 298K. The gravimetric estimations, PDP and EIS procedures were utilized to explain the corrosion inhibition of the selected inhibitors. Scanning Electron Microscopy and Atomic Force Microscopy were used for Surface morphology of S.S.-410 was examined using Scanning Electron Microscopy (SEM) and Atomic Force Microscopy (AFM). Spectroscopic techniques such as Fourier- Transform Infrared (FT-IR) spectroscopy and Ultraviolet-Visible (UV- Vis) spectroscopy were used to explore the mechanism of adsorption of plant inhibitors. Density Functional Theory (DFT) was utilized for theoretical calculations. The exploratory techniques utilized for the above investigations of corrosion inhibitors are given in this section.

### 3.1 Chemicals and Reagents

All solvents used were of analytical grades and provided by Sigma-Aldrich. For extraction to be performed under dry conditions, solvents were dried by the usual reported laboratory procedures. For weight loss studies, the volume of 15 % HCl was kept 500 mL and for electrochemical estimations 250 mL of 15 % HCl was utilized.

### 3.2 Selected plants for the investigation

The present investigation aims to explore the corrosion inhibition abilities of some plant extracts on S.S.- 410 in 15 % HCl. On the basis of literature survey, some plants were selected for the present study and the selected plants includes *Oryza sativa*, *Populus tremula*, *Triticum aestivum*, *Brassica nigra*, *Saccharum officinarum*, *Beta vulgaris* and *Phyllanthus emblica*.

### 3.3 Preparation of plant extract

All the plants were collected from agricultural field and local market Phagwara, Punjab. The plant samples were verified by Botanical Survey of India (BSI), Dehradun. The powdered sample, 100 g was extracted with 450 mL of solvent at 75 °C for 72 h. The solvent used for extraction of *Oryza sativa* is methanol [139], *Populus tremula* is methanol [140], *Triticum aestivum* is ethanol [141], *Brassica nigra* is ethanol [142], *Saccharum officinarum* is methanol [143], *Beta vulgaris* is methanol [144] and

*Phyllanthus emblica* is [145]. The filtered liquid was evaporated with the help of rotavaporator and allowed to dry completely in a vacuum desiccator.

### 3.4 Elemental analysis of S.S.- 410

S.S.- 410 is used to make a broad assortment of equipment and metallic structures involved in petroleum industry. The S.S.- 410 sheet was purchased from Nihal Chand Harbans Lal, Steel traders, Saharanpur, Utter Pradesh. The elemental analysis of S.S.- 410 sample was done from Central Institute of Hand Tool (CIHT), Jalandhar. The composition of the S.S.- 410 was observed as (weight %) C 0.134 %; P 0.028 %; Cr 11.147 %; Mn 0.822 %; Si 0.662%; S 0.005 % and Fe balance.

### 3.5 Preparation of working electrodes

The S.S.- 410 sheets were manually cut into 5.0 cm × 5.0 cm × 0.03 cm coupons. Silicon carbide papers (100-2000 grade) were utilized to scrape and polish all exposed surface of S.S.- 410 coupons for weight loss process. For electrochemical study, S.S.-410 of 3 mm diameter was used for making the working electrodes. Figure 3.1 shows S.S.- 410 used for weight loss and electrochemical experiment

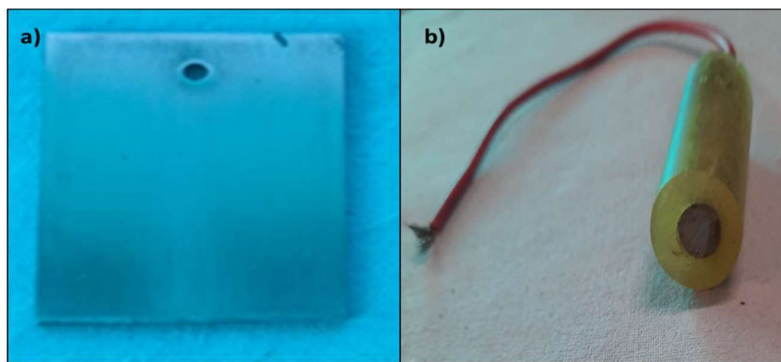


Figure 3.1: S.S.- 410 used in (a) weight loss, and (b) Electrochemical studies.

### 3.6 FT-IR spectroscopy

In the study FT-IR analysis was performed to identify the functional group present in the extract, utilizing Shimadzu FTIR 8400S. The FTIR spectra was recorded in the wavelength range of 450-4000  $\text{cm}^{-1}$ . Figure 3.2 shows the FT-IR spectrometer used for the study.

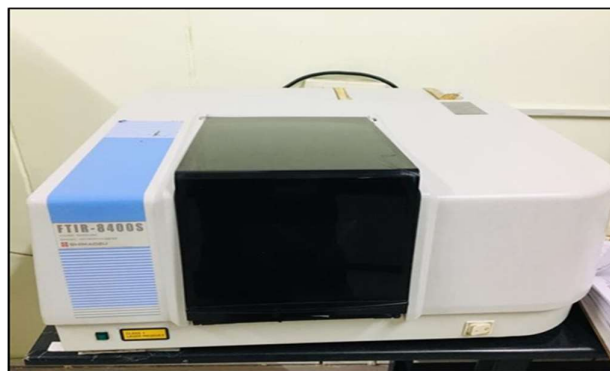


Figure 3.2: FTIR spectrometer used for the study.

### 3.7 UV-visible spectroscopy

UV-visible spectroscopic analysis was conducted using Shimadzu UV-1800 UV-visible absorption spectrophotometer. The UV-visible spectra of selected plant extracts in 15 % HCl was recorded before and after the corrosion tests for 24 h at 298 K. Figure 3.3 shows the UV-visible spectrophotometer used for the analysis.

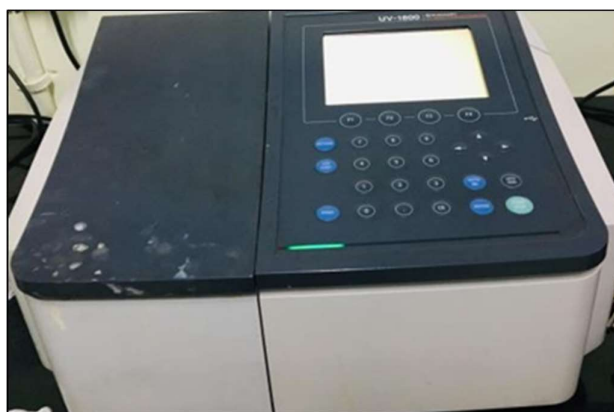


Figure 3.3: Image showing UV-visible spectrophotometer

### 3.8 Weight-loss experiments

S.S.-410 abraded with different grades of silicon carbide papers were weighted and immersed in 500 mL of 15 % HCl without and with various concentrations of inhibitors for 24 h [146-149]. After 24h of immersion, the S.S.-410 were rinsed with acetone, dried under nitrogen flow afterward weighted using Shimadzu BL-220H/D455006313 electronic balance. The corrosion rate (CR) was calculated by following equations [150-151]:

$$C_R = \frac{K \times W}{A \times t \times \rho} \quad (3.1)$$

Where, W represents the weight loss of the S.S.-410 (g), CR represents the corrosion rate (mmy<sup>-1</sup>), t is immersion time (h), K is corrosion constant equals to 8.76 × 10<sup>4</sup>, ρ represents the density in g cm<sup>-3</sup> which is 7.86 g cm<sup>-3</sup> for the S.S.-410 according to ASTM G 31-72, and A represents the surface area (cm<sup>2</sup>) of the stainless steel. The corrosion inhibition efficiency (IE %) of plant extracts were calculated with the help of following formula [152]

$$IE = \frac{C_R^0 - C_R^i}{C_R^0} \times 100 \quad (3.2)$$

Where,  $C_R^0$  and  $C_R^i$  are the corrosion rate of S.S.- 410 in the absence and presence inhibitor respectively

$$\theta = \frac{IE}{100} \quad (3.3)$$

Where, θ is the surface coverage, from weight loss estimations an increment in inhibition efficiency happens on expanding the inhibitor concentration. This increase in inhibition efficiency is due the development of a defensive layer that decreases the corrosion procedure. Keeping in mind the end goal to examine the impact of inhibitors on the inhibition efficiencies, weight loss estimations were completed at a temperature of 298 K in the absence and presence of various concentrations of inhibitor.

### 3.9 Langmuir adsorption isotherm

With the help of adsorption isotherm, essential information regarding interaction between corrosion inhibitor and steel surface have been explained [153]. It also explain the relationship between adsorbed species coverage and their concentration changes [154-155]. The Langmuir adsorption isotherm can be describe in the following equation-

$$\frac{C}{\theta} = \frac{1}{K_{ads}} + C \quad (3.4)$$

Where, C represents the inhibitor concentration and  $K_{ads}$  is the adsorption constant. If the correlation coefficient of straight line obtained by plotting C/θ against C comes near unity, then it is considered that the inhibitors obey the Langmuir adsorption isotherm. A typical graph of C/θ vs. C for Langmuir adsorption isotherm graph is presented in Figure 3.4.

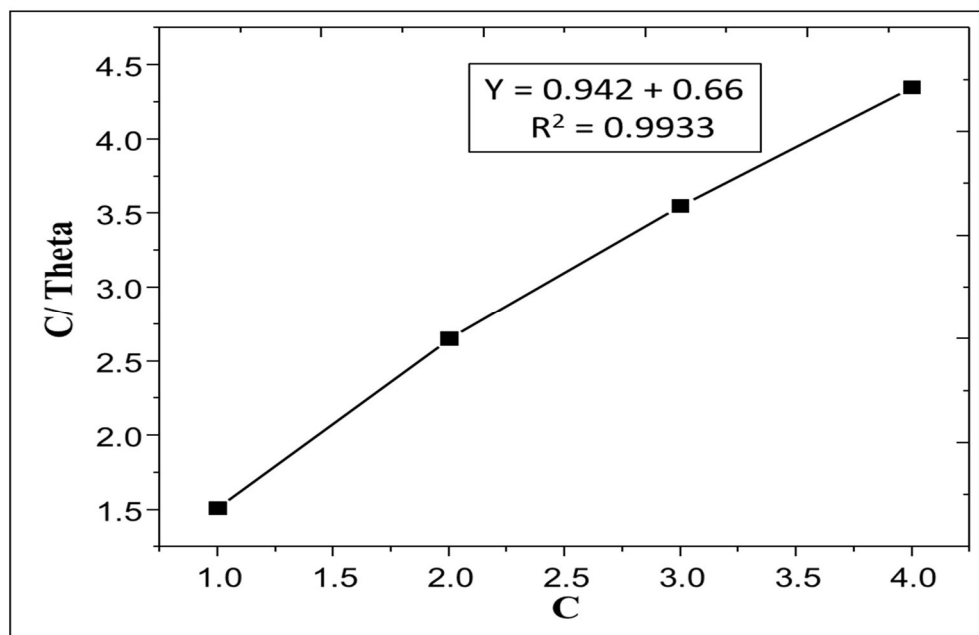


Figure 3.4: Langmuir plot of *Oryza sativa*

### 3.10 Electrochemical techniques

Electrochemical techniques are related to the interrelation of electrical and the chemical effects. A square formed S.S.-410 rod was joined to the copper cable on one side and sealed with epoxy gum to give a two-dimensional surface (1 cm<sup>2</sup>) exposed to the electrolyte. A three-electrode electrochemical system was utilized in all electrochemical experiments. Figure 3.5 shows a three-electrode cell assembly and electrochemical instrument used in this study. Platinum electrode was used as a counter electrode. The working electrode was prepared from S.S.- 410 rod as already discussed. The reference electrode was a saturated calomel electrode (SCE), which was fixed into bent luggin capillary tube and filled with the test solution to avoid any contamination of solution by Cl<sup>-</sup> ions [156-157]. All potentials in this work refer to the SCE. The surface groundwork of the working electrode was conducted by mechanically abrading the specimen with different grads of emery papers (100 to 2000). Luggin kept at a fixed distance of about 1-2 mm between the tip of the capillary and the surface of the working electrode was retained throughout the electrochemical experiments to avoid and ohmic loss. The experiments were carried out in aerated non-stirred 15 % HCl without and with the various inhibitor concentrations of all the

selected inhibitors at 298 K. Every scan was conducted in aerated immobile solution at 298 K, was maintained using water thermostat [158-159]. An electrochemical workstation system Metrohm: Multi-channel Autolab was used to measure the potential and current of oxidation and reduction reactions.

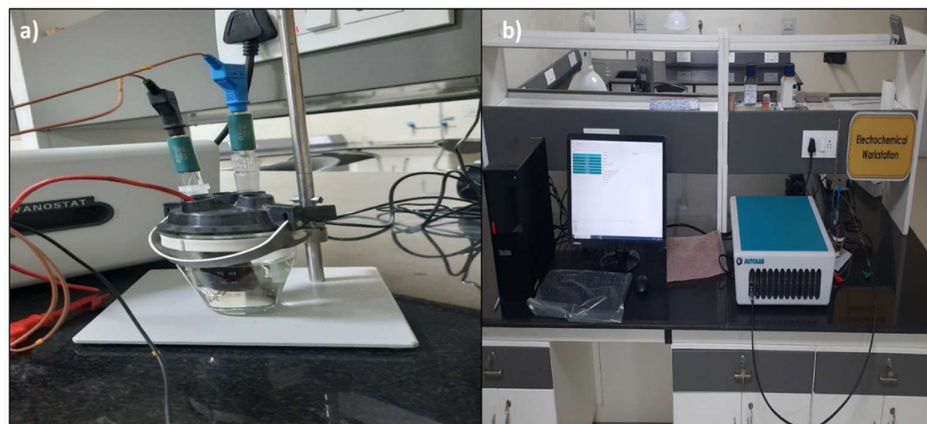


Figure 3.5: Images of (a) Three electrode cell assembly, and (b) Electrochemical workstation

### 3.10.1 Potentiodynamic polarization studies

It is a technique for electrochemical analysis of the kinetics and mechanism of the reactions occurring on the electrodes. It is based on the control of the current flowing through the system. The technique is based on the polarization of the working electrode around OCP. First step is to immersing the working electrode in the test solution for reaching the steady state potential. The scan rate of 1 mV/s with the potential range of -250 mV to +250 mV were used. Figure 3.6 shows an example of PDP curve used to determine the type of inhibition which is followed by the prepared inhibitors. [160-162]. The point of intersection of cathodic and anodic slopes yields the corrosion potential ( $E_{corr}$ ). It has been reported that if the displacement in corrosion potential values of inhibitor is  $>85$  mV with respect to (corrosion potential) of blank, the inhibitor can be regarded as anodic or/and cathodic kind and if the offset is  $<85$  mV, the inhibitor can be considered mixed [163-167].

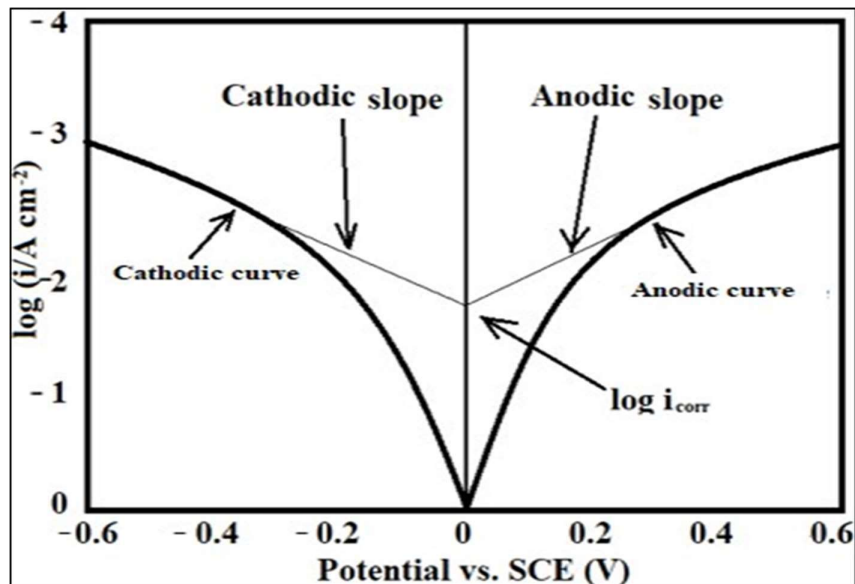


Figure 3.6: An example of an experimental PDP curve

The value of corrosion inhibition efficiency was calculated with the help of following equation [168].

$$I.E. = \frac{I_{corr}^0 - I_{corr}^i}{I_{corr}^0} \times 100 \quad (3.5)$$

Where  $I_{corr}^0$  and  $I_{corr}^i$  were used for corrosion current density of 15% HCl solution and plant extract inhibitor solution.

### 3.10.2 Electrochemical impedance spectroscopic study

EIS is a predominant technique that is used to analyze corrosion mechanism and also several elementary parameters related to electrochemical reactions. In this method, impedance and the phase angle of electrochemical system was investigated along with the variations in the frequency [169-170]. A small 5 mV amplitude AC signal is applied to the sample at OCP. In the Bode's plot the impedance is generally measured as a function of frequency in the range 100 kHz to 0.01 Hz. Figure 3.7 shows a typical Nyquist, Tafel, and Bode's plots for 15% HCl solution [171]. Charge transfer resistance ( $R_{ct}$ ) are related to the maximum of the semi-circular Nyquist plot where  $R_{ct}$  and  $R^0$  represent charge transfer resistance in the presence and absence of inhibitor, respectively [172-173]. Corrosion inhibition efficiency was calculated with the help of



given equation [174].

$$I.E. = \frac{R_{ct} - R_{ct}^0}{R_{ct}} \times 100 \quad (3.6)$$

Where,  $R_{ct}$  and  $R_{ct}^0$  designates charge transfer resistance of different plant extract concentrations and 15% HCl solution, respectively

### 3.11 Comparative studies with some existing synthetic paints

In our investigation, we have checked and analyze the comparative studies between some existing synthetic paints and selected natural extracts. Here, we took two synthetic paint samples (Paint sample 1 and Paint sample 2) and the plants extract. Both the paint samples come in two separate containers (Paint powder and solvent). We took the equal concentration for all the samples, which is 4 g/L. The equal concentration of different samples was coated on the S.S.- 410 surfaces. Pre-coated metal surfaces were been used in the study. To check the inhibition efficiency by using weight loss measurements were carried out in 15 % HCl solution at 298 K for 24 h. The main goal of this investigation is to replace existing synthetic paints by natural inhibitors, and the use of the natural waste material as a green corrosion inhibitor makes it more novel and effective.

### 3.12 Surface investigations

The surface morphology of the steel surface has been explained by the various researchers to get the idea of surface got absorb in the presence of inhibitors [175-181]. The S.S.- 410 coupons of size 1.0 cm × 1.0 cm × 0.03 cm were polished with different grades of emery papers (100-2000) and then rinsed with acetone followed by distilled water. After immersion in 15 % HCl solution in the absence and presence of inhibitors (optimum conc.) for 24 h at 298 K, the specimens were cleaned through distilled water, then dried and afterward the SEM and AFM images have been recorded utilizing LEO435BP and NT-MDT- INTEGRA software, respectively. Figure 3.8 shows the SEM and AFM instruments used for the study.

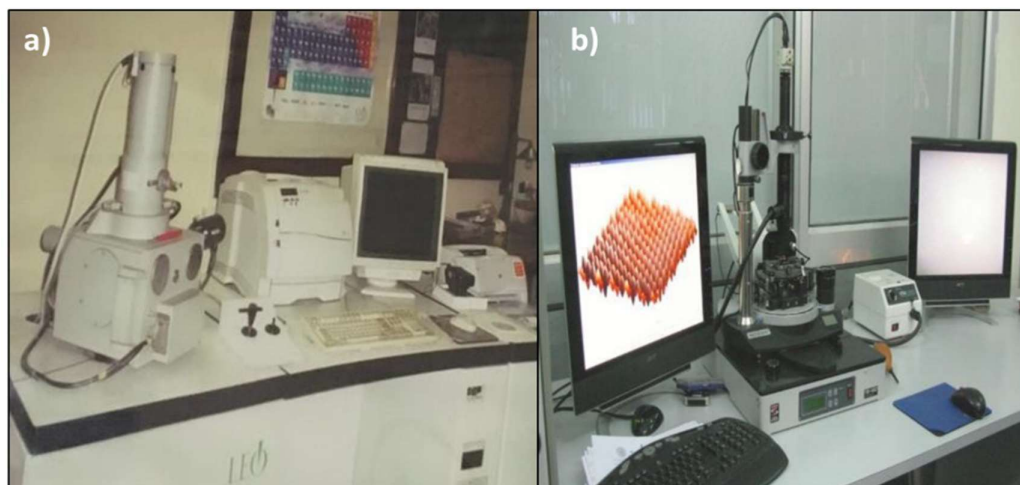


Figure 3.7: Images showing (a) SEM, and (b) AFM.

### 3.13 Quantum chemical calculations

Computational chemistry is a useful tool for theoretical study of adsorption [182-185]. Density functional theory (DFT) method is a useful method to conduct the quantum chemical calculations. Key parameters were obtained from the optimized structures. According to Frontier sub-atomic orbital (FMO) hypothesis of compound reactivity, the establishment of a transition state is because of collaboration among LUMO and HOMO of responding classes. The energy gap ( $\Delta E$ ) amongst LUMO and HOMO, stronger will be the interaction between two responding molecules [186-190]. The key parameters obtained by the quantum chemical studies, for example,  $E_{\text{HOMO}}$ ,  $E_{\text{LUMO}}$  and  $\Delta E$  (energy gap) have been figured utilizing following comparisons [191-192]:

$$\Delta E = E_{\text{LUMO}} - E_{\text{HOMO}} \quad (3.7)$$

As  $E_{\text{HOMO}}$  is frequently connected with electron donating capacity of the compound, high values of  $E_{\text{HOMO}}$  are probably going to demonstrate an inclination of compound to give electrons to fitting acceptor compounds with low energy and empty molecular orbital. Similarly, the low values of energy gap  $\Delta E$  will render great inhibition efficiencies since the energy to remove an electron from last occupied orbital will be minimized. It has been described that good inhibitors indicate higher value of  $E_{\text{HOMO}}$  and lower value of  $E_{\text{LUMO}}$  and  $\Delta E$  [193-195].

## CHAPTER 04: RESULTS AND DISCUSSIONS

### 4.1 *Oryza sativa*

*O. sativa* is a grass diverse genus and belongs to Poaceae family [196]. *O. sativa* is commonly known as Chawal in India. The *O. sativa* residues contain various types of phytochemicals as shown in Figure 4.1.1 [197]. After harvesting seeds, most of the vegetative residues are unutilized and pile up as waste. Most of the residues are burned in India due to lack of strategies to utilize it completely and thus accounts for environmental pollution. This study aims at analyzing the anticorrosive behaviour of *O. sativa* waste.

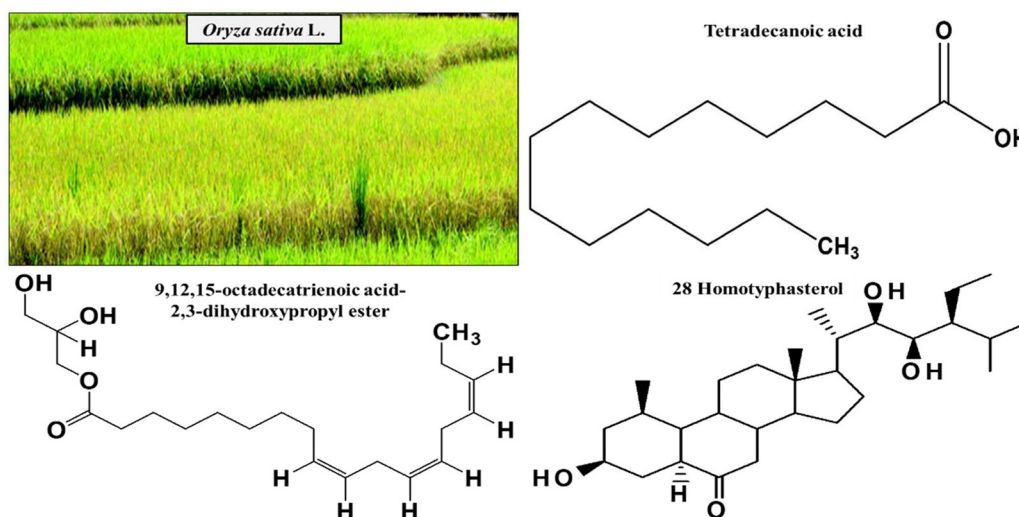


Figure 4.1.1: Image of *O. sativa* plant and molecular structure of phytochemicals present in *O. sativa* extract (OSE).

#### 4.1.1 FTIR analysis of *O. sativa*

FTIR spectrum was used to identify the possible phytochemicals present in *O. sativa* extract and is shown in Fig. 4.1.2. The peaks were seen at 3561, 3334, 2940, 1663, 1429, 1346, 1237, 987, 909, 680, and 549  $\text{cm}^{-1}$ . The peak observed at 3561 and 3334  $\text{cm}^{-1}$  are due to stretching of OH group from alcohol and phenol (hydrogen bonded), the characteristic peak observed at 2940  $\text{cm}^{-1}$  is attributed to stretching of C-H of alkanes, the peak observed at 1663, 1429 and 1346 are assigned to the stretching of

C=O of carbonyl group. The peaks observed at 1237  $\text{cm}^{-1}$  is assigned to the C-O bonding (alcohols, esters, carboxylic acids). The peak observed at 987, 909, 680, and 549  $\text{cm}^{-1}$  are attributed to the presence of bending of C-H group of alkanes. These phytochemicals present in the peel extract of *O. sativa* extract contains heteroatoms which are adsorbed on the S.S.-410 surface and forms bonds with the  $\text{Fe}^{2+}$  ions present on the steel surface and act as potent corrosion inhibitors [199-201].

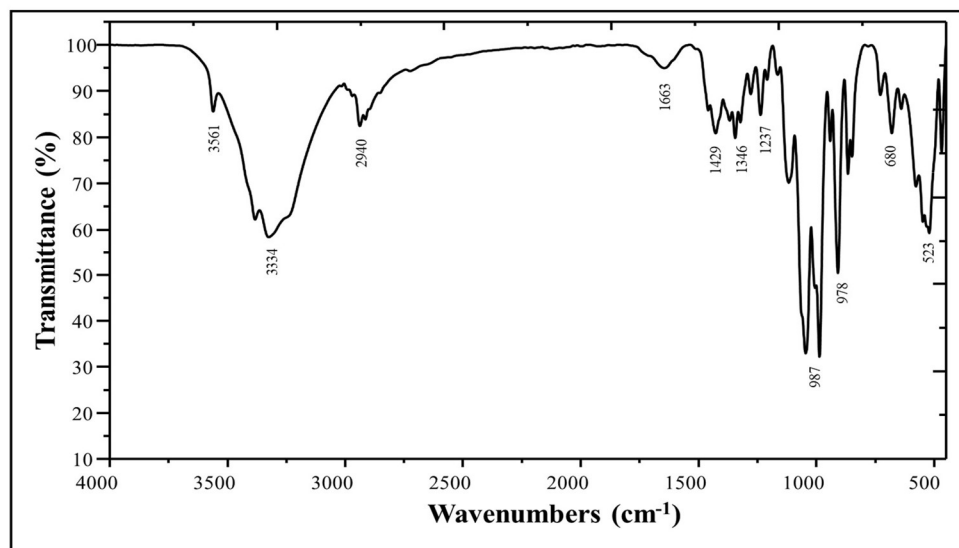


Figure 4.1.2: FTIR spectra of *O. sativa* extract (OSE).

#### 4.1.2 UV visible spectroscopic study

The UV- visible spectra of *O. sativa* extract dissolved in 15% HCl before and after immersion of SS-410 specimen is shown in Fig. 4.1.3. The presence of adsorption peaks at 214 and 360 nm were due to  $\pi - \pi^*$  and  $n - \pi^*$  transition. The solution in which SS-410 samples were not immersed show higher peak absorbance with respect to the solution in which steel samples were immersed and further there was shift in the value of adsorption maxima in latter samples. The phytochemicals from the plant extract leads to the shift in absorption wavelength and lower adsorption peak intensity of S.S.-410 sample exposed acidic solution indicating the adsorption on the surface of S.S.-410 and the formation of bonds between the  $\text{Fe}^{2+}$  particles of steel and plant extract molecules. So, when S.S.-410 specimen is immersed in the 15% HCl solution containing plant extract, the molecules get absorb on the surface of S.S.-410 and make complexes with

the surface atoms of substrate surface thus slow down the corrosion process and act as good corrosion inhibitors [202-204].

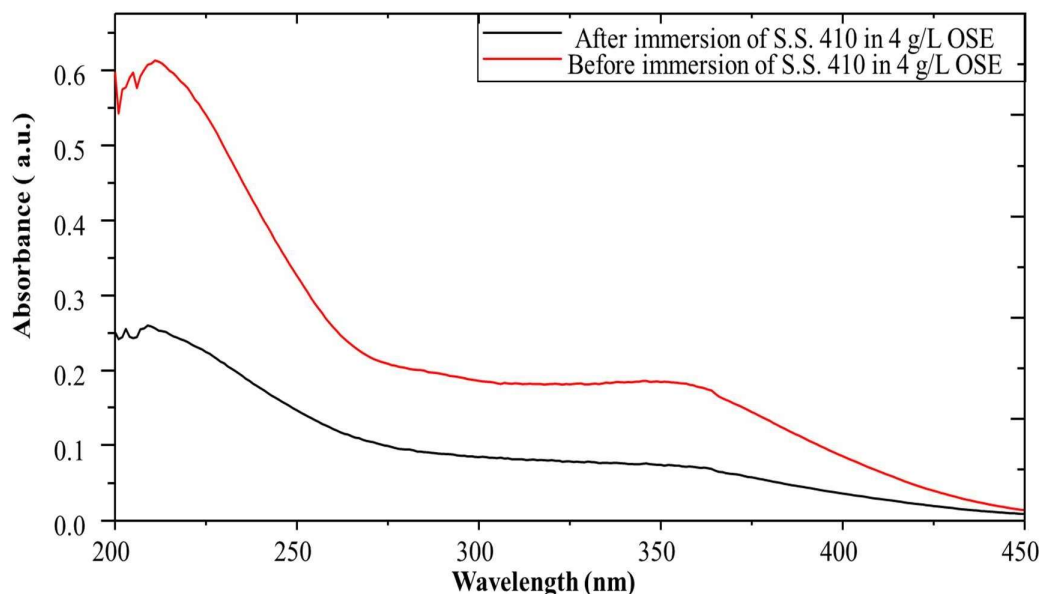


Figure 4.1.3: UV-visible spectra of *O. sativa* extract (OSE).

#### 4.1.3 Weight loss and Electrochemical Study

The corrosion inhibition efficiency of *O. sativa* extract for S.S.-410 in 15% HCl solution were obtained with the help of weight loss, and electrochemical measurements at various concentrations (1-4 g/L) at 298K. All the key parameters have been mentioned in table 4.1.1. As the concentration of *O. Sativa* extract increases, there is also subsequent decrease in corrosion rate in weight loss measurement, thus leading to increase in corrosion inhibition efficiency. Corrosion rate is decreases due to adsorption of *O. sativa* extract phytochemicals on the surface of S.S.-410.

Maximum 91.92 % corrosion inhibition efficiency was obtained using 4 g/L *O. sativa* extract. The linear correlation coefficients 0.9933 was near to 1, which confirms the adsorption of *O. sativa* extract obeys Langmuir adsorption isotherm (Figure 4.1.4) [205].

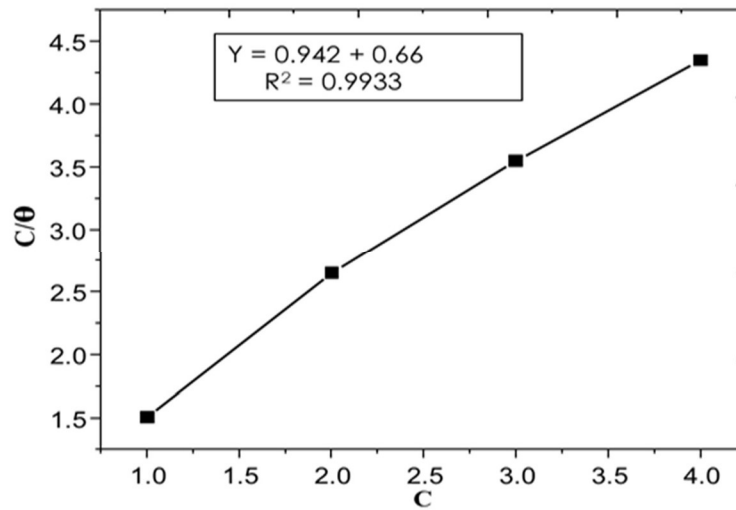


Figure 4.1.4: Langmuir adsorption isotherm for *O. sativa* extract with the help of weight loss measurement.

As the concentration of *O. sativa* extract increases in the corrosive media, the value of corrosion current density decreases, that designate the increase in corrosion inhibition efficiency. The shift of 85 mV value in corrosion potential ( $E_{\text{corr}}$ ) from blank to optimum concentration shows that inhibitor behaves as mixed (anodic or cathodic inhibition) type [206-207]. So, extract has mixed type of inhibition behavior. From the potentiodynamic polarization, it was recorded that at concentration of 4 g/L *O. sativa* extract in 15% HCl solution, a maximum of 76.64 % corrosion inhibition efficiency was attained (Figure 4.1.5(a)) [208].

A maximum 73.00 % corrosion inhibition efficiency was as shown in electrochemical impedance plot (Figure 4.1.5(b)). A layer formation was proven from the  $R_{\text{ct}}$  value that increases with increases the *O. sativa* extract concentration [209]. The Bode plot has been shown in (Figure 4.1.5(c)) the *O. sativa* get adsorbed on the surface of S.S.-410 by involving  $\pi$  electrons of its aromatic ring or the hetero atoms from the plant extract with the free electrons of vacant d-orbital of iron from steel. This process leads to efficient anti-corrosive property of *O. sativa*. The Bode plot support iron *O. sativa* get adsorbed on the surface of SS-410. This process leads to efficient anticorrosive property of *O. sativa* [210-211].

The presence of inhibitors shows the process of charge transfer resistance which started on the interface between electrode and electrolyte as clear from phase angles graph is

shown in Figure (4.1.5(d)). The increment in the values of phase angle with the presence of increasing concentration of *O. sativa* leading to a decrease in the capacitance at the surface of steel, making the steel surface less prone to dissolution in the presence of corrosive media [212].

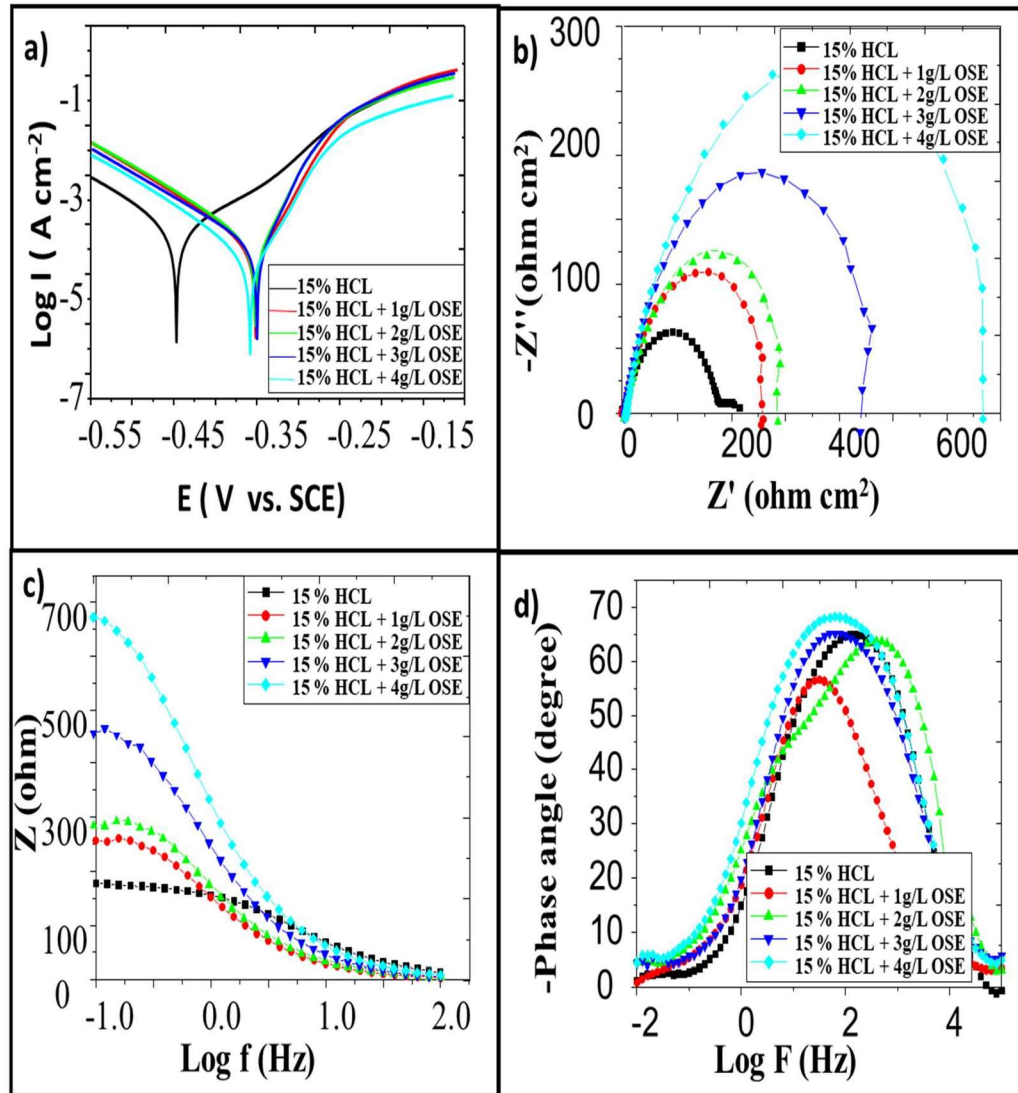


Figure 4.1.5: (a) Potentiodynamic polarization plot (b) EIS plot (c) Bode plot (d) phase angle plot for different concentration of *O. sativa* extract (OSE).

Table 4.1.1: Corrosion parameters from weight loss, and electrochemical experiments for S.S.-410 in 15% HCl with different concentrations of *O. sativa* extract (OSE).

Weight loss			PDP		EIS		
C (g/L)	C <sub>R</sub> (mmy <sup>-1</sup> )	I.E. (%)	E <sub>corr</sub> (mV vs. SCE)	I <sub>corr</sub> (A cm <sup>-2</sup> )	I.E. (%)	R <sub>ct</sub> (Ω cm <sup>2</sup> )	I.E. (%)
15% HCl	39.01		-474.1	0.000054003		180.21	
15% HCl + 1 g/L OSE	13.181	66.21	-352.0	0.000035064	35.07	258.73	30.34
15% HCl + 2 g/L OSE	9.630	75.31	-352.6	0.000032634	39.57	285.78	36.94
15% HCl + 3 g/L OSE	6.120	84.31	-350.0	0.000019284	64.29	439.48	58.99
15% HCl + 4 g/L OSE	3.152	91.92	-358.4	0.000012615	76.64	667.57	73.00

#### 4.1.4 SEM and AFM analysis

The SEM and AFM micrographs of the S.S.-410, S.S.-410 immersed in 15% HCl and S.S.-410 immersed in 15% HCl solution in the presence of *O. sativa* extract are shown in Figure 4.1.6. SEM of S.S.-410 coupons after 24 h immersion in 15 % HCl solution at 298 K shows a severely harmed surface. From AFM studies, the average surface roughness for abraded S.S.- 410 is 26.83 nm and for S.S.- 410 immersed in 15 % HCl,



AFM micrographs of the average surface roughness is 939.14 nm. The surface of steel sample which is immersed in acid solution with the presence of *O. sativa* extract show very less roughness as comparative smooth surface with respect to S.S.-410 immersed in only 15% HCl solution. The surface of S.S.-410 sample exposed to acid solution in the presence of *O. sativa* extract show average surface roughness value of 311.67 nm through AFM, which is very less as compared to roughness value of steel immersed in only 15% HCl solution. This change in surface morphology is attributed to the adsorption of some molecules from the *O. sativa* extract on the steel surface which act as corrosion inhibitor by forming a protective layer on the steel surface and thus prevents corrosion. The mentioned SEM and AFM micrograph have been compared with SEM and AFM micrograph of S.S.-410 immersed in 15% HCl solution [213-217].

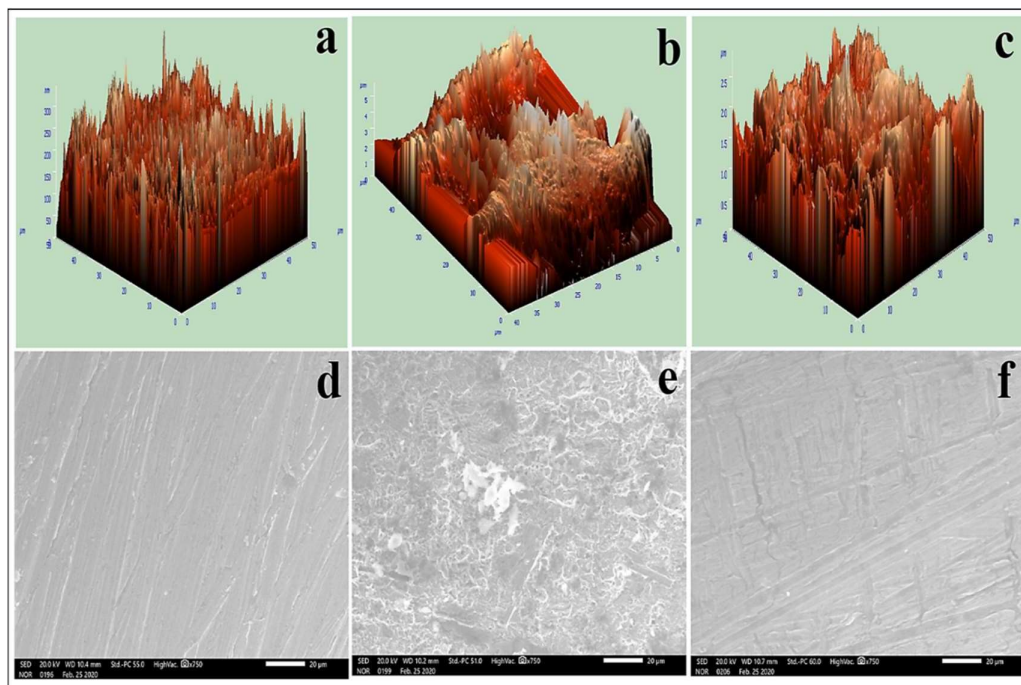


Fig. 4.1.6 (a) AFM micrographs of S.S.-410 (b) AFM micrographs of S.S.-410 immersed in 15% HCl solution (c) AFM micrographs of S.S.-410 immersed in 15% HCl solution with *O. sativa* extract (d) SEM micrographs of S.S.-410 (e) SEM micrographs of S.S.-410 immersed in 15% HCl solution (f) SEM micrographs of S.S.-410 immersed in 15% HCl solution with *O. sativa* extract.

#### 4.1.5 Quantum Chemical Calculations

The frontier molecular orbital density distributions (LUMO and HOMO) with optimum structures of phytochemicals presents in *O. sativa* is shown in Fig. 4.1.7.  $E_{\text{HOMO}}$  and  $E_{\text{LUMO}}$  and  $(\Delta E)$  are the key parameters of theoretical study and have been shown in table 4.1.2 [218-222]. The order which is followed by the energy gap of molecular orbital is: 9,12,15-octadecatrienoic acid-2,3-dihydroxypropyl ester < Tetradecanoic acid < 28 Homotyphasterol. Hence, the inhibition effect follows the order 9,12,15-octadecatrienoic acid-2,3-dihydroxypropyl ester > Tetradecanoic acid > 28 Homotyphasterol. So, 9,12,15-octadecatrienoic acid-2,3-dihydroxypropyl ester, was assumed to be the most essential phytochemical in the corrosion inhibition behaviour of the *O. sativa*.

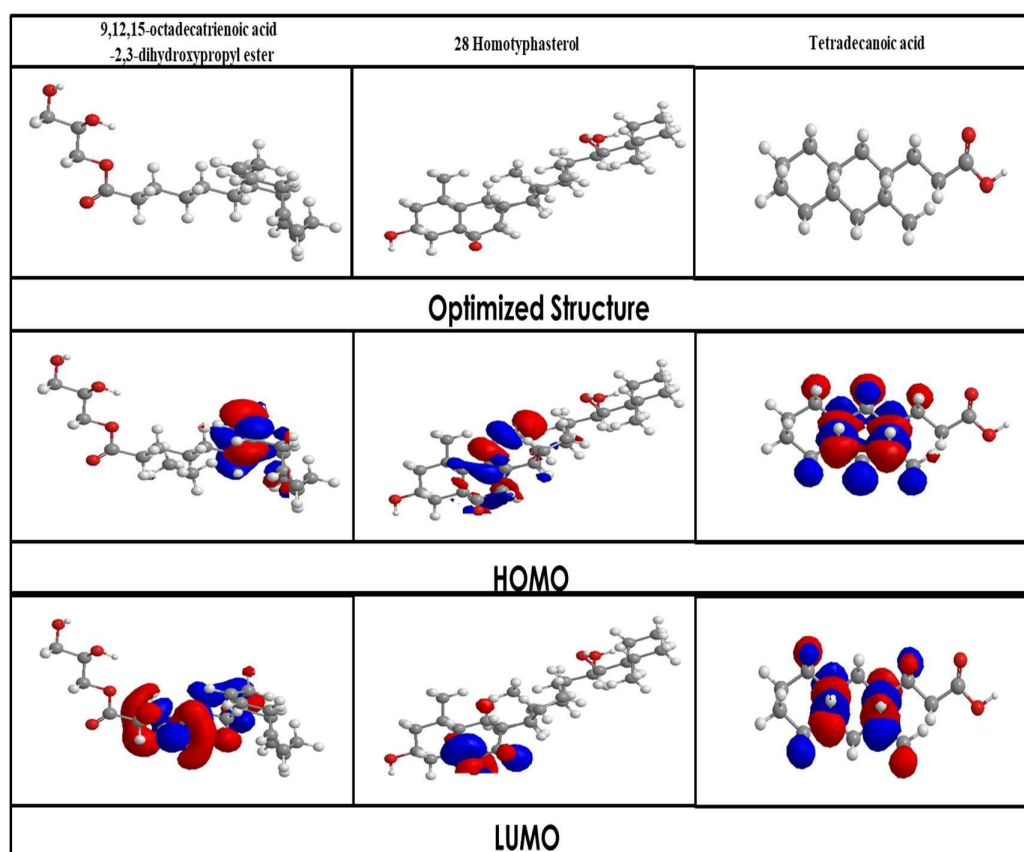


Figure 4.1.7: Optimized structures, HOMO and LUMO of phytochemicals present in *O. sativa* extract.

Table 4.1.2: Calculated quantum chemical parameters of phytochemicals of *O. sativa* extract

S. No	Phytochemicals	E <sub>HOMO</sub> (eV)	E <sub>LUMO</sub> (eV)	ΔE (eV)
1	Tetradecanoic acid	18.960	20.629	1.669
2	9,12,15-octadecatrienoic acid-2,3-dihydroxypropyl ester	1.226	2.719	1.493
3	28 Homotyphasterol	-6.487	-1.234	5.253

#### 4.2 *Populus tremula*

*P. tremula* is a genetically diverse genus with 25–30 species of deciduous flowering plants in the family Salicaceae [223]. *P. tremula* is commonly known as Poplar in India. The *P. tremula* residues contain various types of phytochemicals namely, lignins, flavonoids, anthocyanins, salicylate-like phenolic glycosides (PGs), and tannins [224]. Leave of *P. tremula* plant in spring seasons destroy the surrounding herbs. The main aim of this study is to investigate the use of *P. tremula* leaves as corrosion inhibitor. Leave of *P. tremula* plant in spring seasons destroy the surrounding herbs. Main focus is on exploring the adsorptive and anticorrosion properties of PTLE. The main phytochemicals as mentioned in figure 4.2.1 [225].

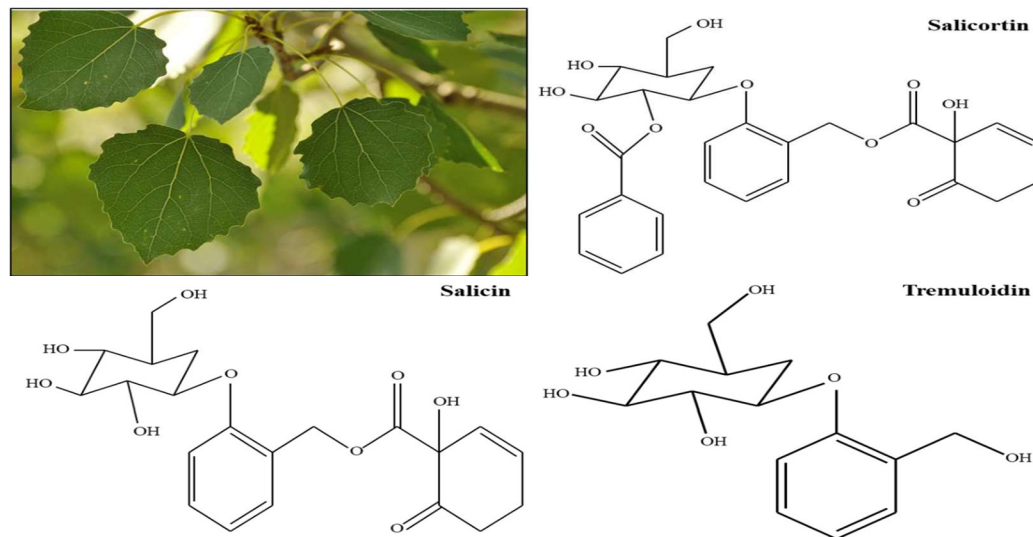


Figure 4.2.1: *P. tremula* plant and molecular structure of phytochemicals present in *P. tremula* extract.

#### 4.2.1 FTIR analysis of *P. tremula*

FTIR spectrum was used to identify the possible phytochemicals present in *P. tremula* extract and is shown in Fig. 4.2.2. The peaks were seen at 3361, 3332, 3000, 2120, 1641, 1457, 1243, 1075, and 608  $\text{cm}^{-1}$ . The peak observed at 3361 and 3332  $\text{cm}^{-1}$  are due to stretching of OH group from alcohol and phenol (hydrogen bonded), the characteristic peak observed at 3000  $\text{cm}^{-1}$  are attributed to stretching of C-H of alkanes, the peak observed at 1641 and 1457 are assigned to the stretching of C=O of carbonyl group. The peaks observed at 1243 and 1075  $\text{cm}^{-1}$  are assigned to the C-O bonding (Alcohols, Esters, carboxylic acids). The peak observed at 608  $\text{cm}^{-1}$  is attributed to the presence of bending of C-H group of alkanes. These phytochemicals present in the peel extract of *P. tremula* extract contains heteroatoms which are adsorbed on the steel surface and forms bonds with the  $\text{Fe}^{2+}$  ions present on the steel surface and act as potent corrosion inhibitors [226-228].

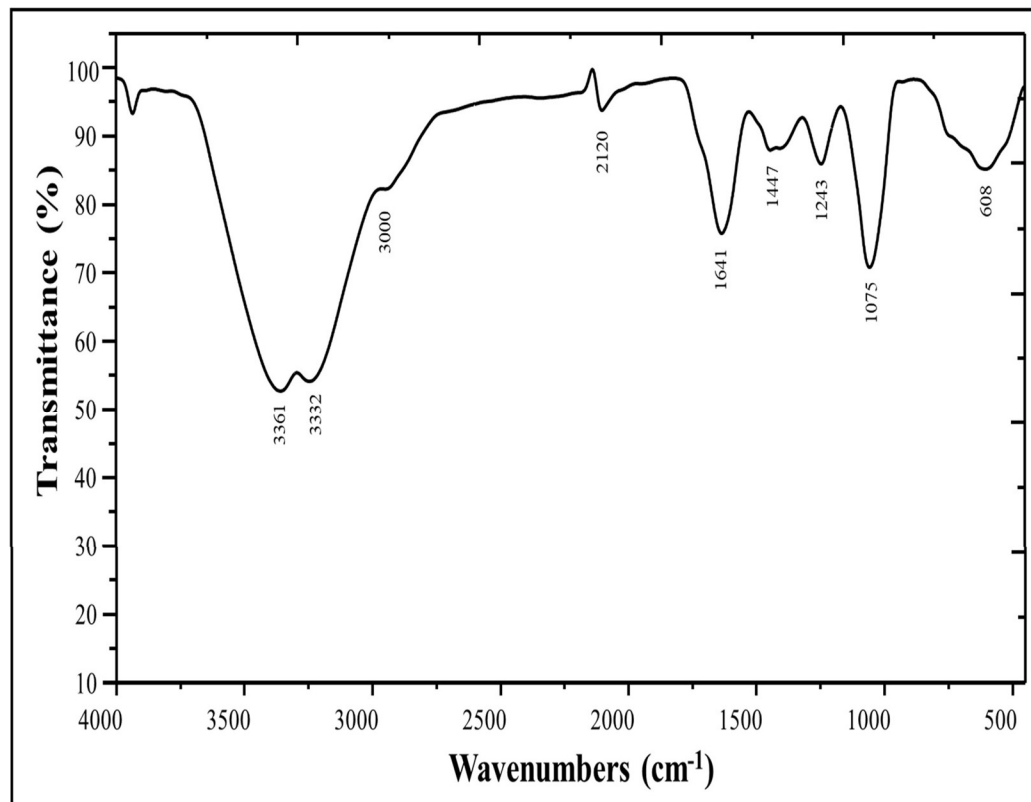


Figure 4.2.2: FT-IR spectra of *P. tremula* extract.

#### 4.2.2 UV visible spectroscopic study

The UV- visible spectra of *P. tremula* extract dissolved in 15% HCl before and after immersion of SS-410 specimen is shown in Fig. 4.2.3. The presence of adsorption peaks at 215 and 284 nm were due to  $\pi - \pi^*$  and  $n - \pi^*$  transition. The solution in which SS-410 samples were not immersed show higher peak absorbance with respect to the solution in which steel samples were immersed and further there was shift in the value of adsorption maxima in latter samples. The phytochemicals from the plant extract leads to the shift in absorption wavelength and lower adsorption peak intensity of steel sample exposed acidic solution indicating the adsorption on the surface of S.S.-410 and the formation of bonds between the  $Fe^{2+}$  particles of steel and plant extract molecules. So, when S.S.-410 specimen is immersed in the 15% HCl solution containing plant extract, the molecules get absorb on the surface of S.S.-410 and make complexes with the surface atoms of substrate surface thus slow down the corrosion process and act as good corrosion inhibitors [202-204].

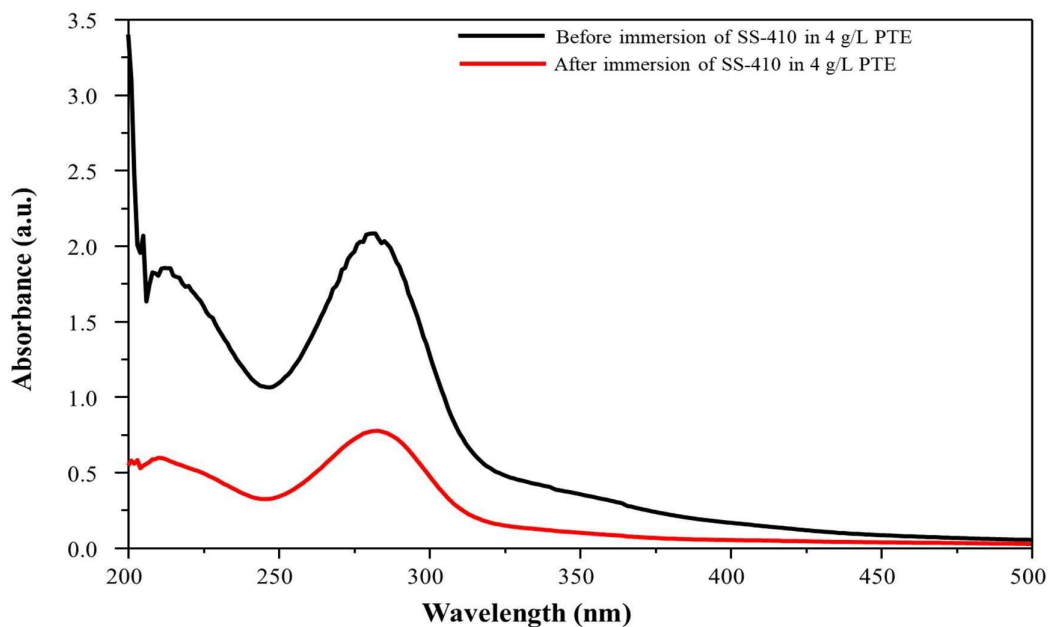


Figure 4.2.3 UV-visible spectra of *P. tremula* extract (PTE).

#### 4.2.3 Weight loss and Electrochemical Study

The corrosion inhibition efficiency of *P. tremula* extract extract for S.S.-410 in 15% HCl solution were obtained by using weight loss, and electrochemical measurements (Tafel and EIS) at various concentrations (1-4 g/L) at 298K. All the key parameters have been mentioned in table 4.2.1. As the concentration of *P. tremula* extract extract increases, the value of corrosion rate decreases in weight loss measurement, thus leading to increase in corrosion inhibition efficiency. The decrease in value of corrosion rate is due to adsorption of *P. tremula* extract phytochemicals on the surface of SS-410. Maximum 92.64 % corrosion inhibition efficiency was obtained using 4 g/L *P. tremula* extract extract. The linear correlation coefficients 0.994 was near to 1, which confirms the adsorption of *P. tremula* extract extract obeys Langmuir adsorption isotherm (Figure 4.2.4) [205].

As the concentration of *P. tremula* extract extract increases in the corrosive media, the value of corrosion current density decreases, that designate the increase in corrosion inhibition efficiency. The shift of 85 mV value in corrosion potential ( $E_{\text{corr}}$ ) from blank to optimum concentration shows that inhibitor behaves as mixed (anodic or cathodic inhibition) type [206-207]. So, *P. tremula* extract extract has mixed type of inhibition

behavior. From the potentiodynamic polarization, 82.06 % corrosion inhibition efficiency was recorded at concentration of 4 g/L *P. tremula* extract in 15% HCl solution (Figure 4.2.5(a)) [208].

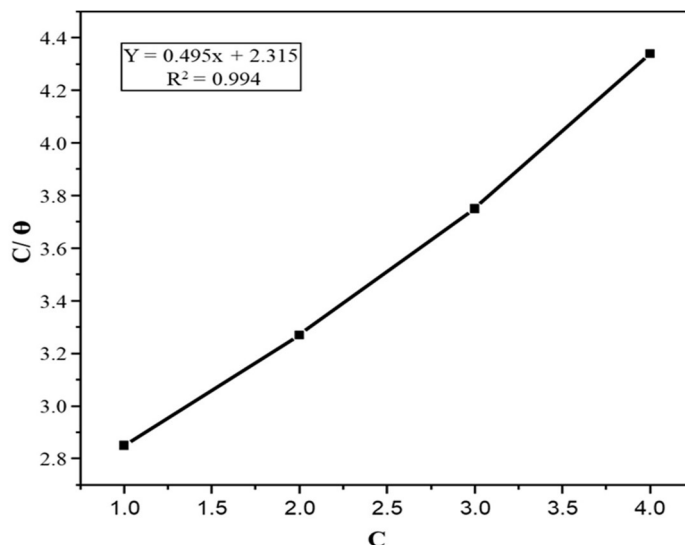


Figure 4.2.4: Langmuir adsorption isotherm for *P. tremula* extract with the help of weight loss measurement.

A maximum 92.80 % corrosion inhibition efficiency was as shown in electrochemical impedance plot (Figure 4.2.5(b)). A layer formation was proven from the Rct value that increases with increases the *P. tremula* extract concentration [209]. The Bode plot has been shown in (Figure 4.2.5(c)) The *P. tremula* get adsorbed on the surface of SS-410 by involving  $\pi$  electrons of its aromatic ring or the hetero atoms from the plant extract with the free electrons of vacant d-orbital of iron from steel. This process leads to efficient anti-corrosive property of *P. tremula*. The Bode plot support iron *P. tremula* get adsorbed on the surface of SS-410. This process leads to efficient anticorrosive property of *P. tremula* [210-211]. The presence of inhibitors shows the process of charge transfer resistance which started on the interface between electrode and electrolyte as clear from phase angles graph is shown in Figure (4.2.5(d)). The inhibition was due to the adsorption of phytochemicals on the surface of steel and a protective film is formed. The increment in the values of phase angle with the presence of increasing concentration of *P. tremula* can be attributed to a decrease in the

capacitance at the surface of steel which makes the steel surface less prone to dissolution in the presence of corrosive media [212].

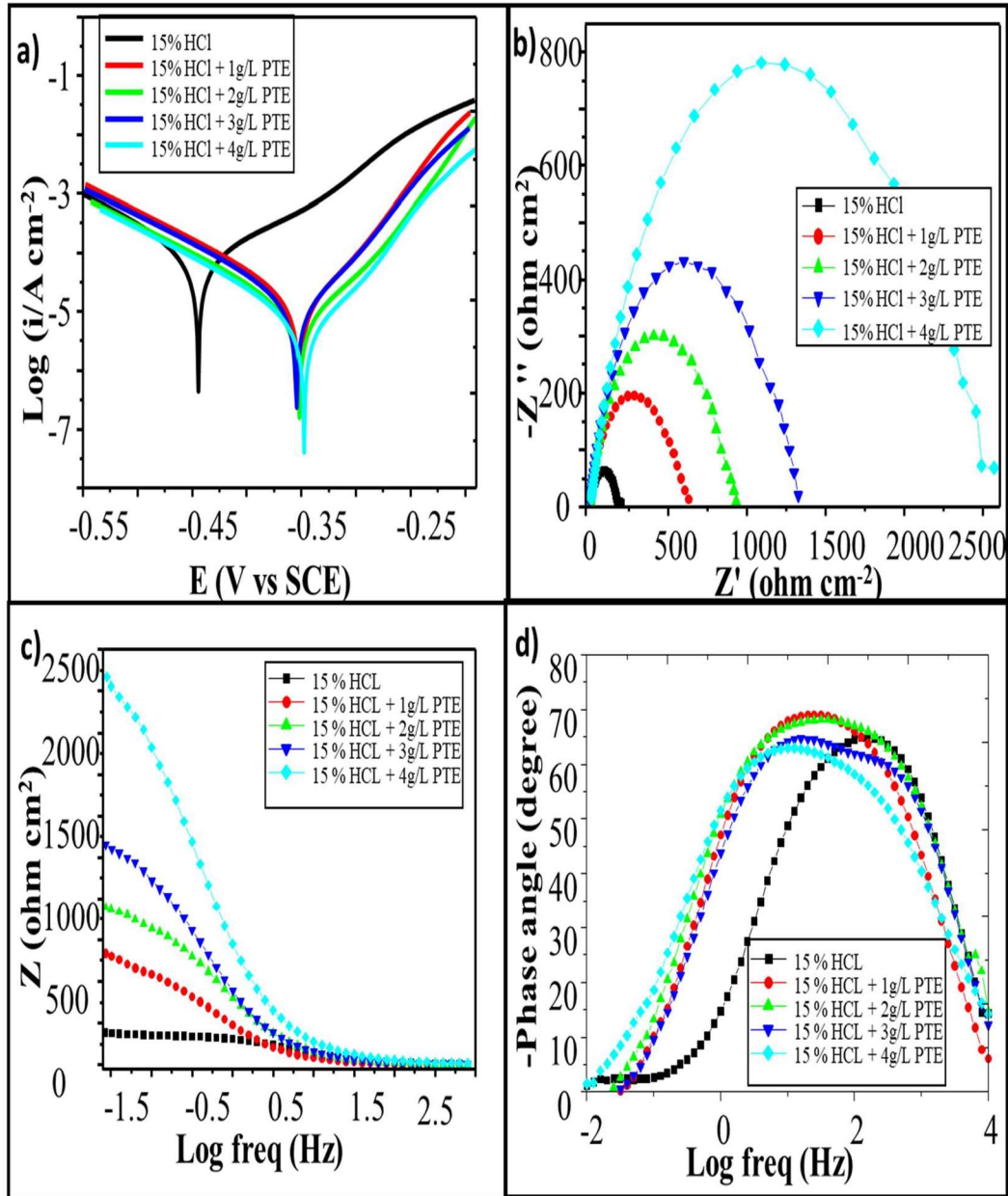


Figure 4.2.5: (a) Potentiodynamic polarization plot (b) Electrochemical impedance plot (c) Bode plot (d) Phase angle plot for different concentration of *P. tremula* extract (PTE).



Table 4.2.1: Corrosion parameters from weight loss, and electrochemical experiments for S.S.-410 in 15% HCl with different concentrations of *P. tremula* extract (PTE).

Weight loss			PDP			EIS	
C (g/L)	C <sub>R</sub> (mmy <sup>-1</sup> )	I.E. (%)	E <sub>corr</sub> (mV vs. SCE)	I <sub>corr</sub> (A cm <sup>-2</sup> )	I.E. (%)	R <sub>ct</sub> (Ω cm <sup>2</sup> )	I.E. (%)
15% HCl	39.01		-474.1	0.000054003		180.21	
15% HCl + 1 g/L PTE	25.30	35.12	-351.9	0.000024489	54.65	665.11	72.90
15% HCl + 2 g/L PTE	15.05	61.41	-354.4	0.000021558	60.07	935.34	80.73
15% HCl + 3 g/L PTE	7.45	80.88	-352.0	0.000013497	75.00	1328.38	86.40
15% HCl + 4 g/L PTE	2.87	92.64	347.4	0.000009662	82.06	2494.67	92.80

#### 4.2.4 SEM and AFM analysis

The SEM and AFM micrographs of the S.S.-410, S.S.-410 immersed in 15% HCl and S.S.-410 immersed in 15% HCl solution in the presence of *P. tremula* extract are shown in Figure 4.2.6. SEM of S.S.-410 coupons after 24 h immersion in 15 % HCl solution at 298 K shows a severely harmed surface. From AFM studies, the average surface roughness for abraded S.S.- 410 is 26.83 nm and for S.S.- 410 immersed in 15 % HCl, AFM micrographs of the average surface roughness is 939.14 nm. The surface of steel sample which is immersed in acid solution with the presence of *P. tremula* extract show very less roughness as comparative smooth surface with respect to S.S.-410 immersed

in only 15% HCl solution. The surface of S.S.-410 sample exposed to acid solution in the presence of *P. tremula* extract show average surface roughness value of 315.28 nm through AFM, which is very less as compared to roughness value of steel immersed in only 15% HCl solution. This change in surface morphology is attributed to the adsorption of some molecules from the *P. tremula* extract on the steel surface which act as corrosion inhibitor by forming a protective layer on the steel surface and thus prevents corrosion. The mentioned SEM and AFM micrograph have been compared with SEM and AFM micrograph of S.S.-410 immersed in 15% HCl solution [213-217].

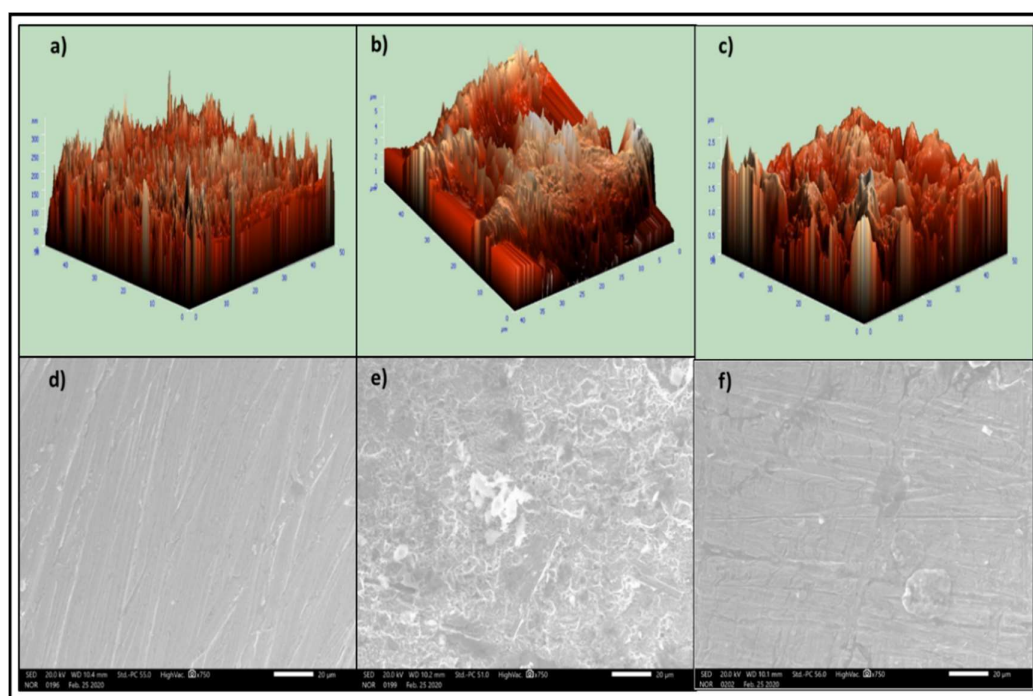


Fig. 4.2.6 Fig. 4.1.6 (a) AFM micrographs of S.S.-410 (b) AFM micrographs of S.S.-410 immersed in 15% HCl solution (c) AFM micrographs of S.S.-410 immersed in 15% HCl solution with *P. tremula* extract (d) SEM micrographs of S.S.-410 (e) SEM micrographs of S.S.-410 immersed in 15% HCl solution (f) SEM micrographs of S.S.-410 immersed in 15% HCl solution with *P. tremula* extract.

#### 4.2.5 Quantum Chemical Calculations

The frontier molecular orbital density distributions (LUMO and HOMO) with optimum structures of phytochemicals presents in *P. tremula* were shown in Fig. 4.2.7.  $E_{\text{HOMO}}$  and  $E_{\text{LUMO}}$  and  $(\Delta E)$  are the key parameters of theoretical study, as mentioned in table

4.1.2 [218-222]. The energy gap of molecular orbital follows the order: Salicin < Tremuloidin < Salicortin. Hence, the inhibition effect follows the order Salicin > Tremuloidin > Salicortin. So, Salicin can be assumed to be the most essential phytochemical in the corrosion inhibition behaviour of the *P. tremula*.

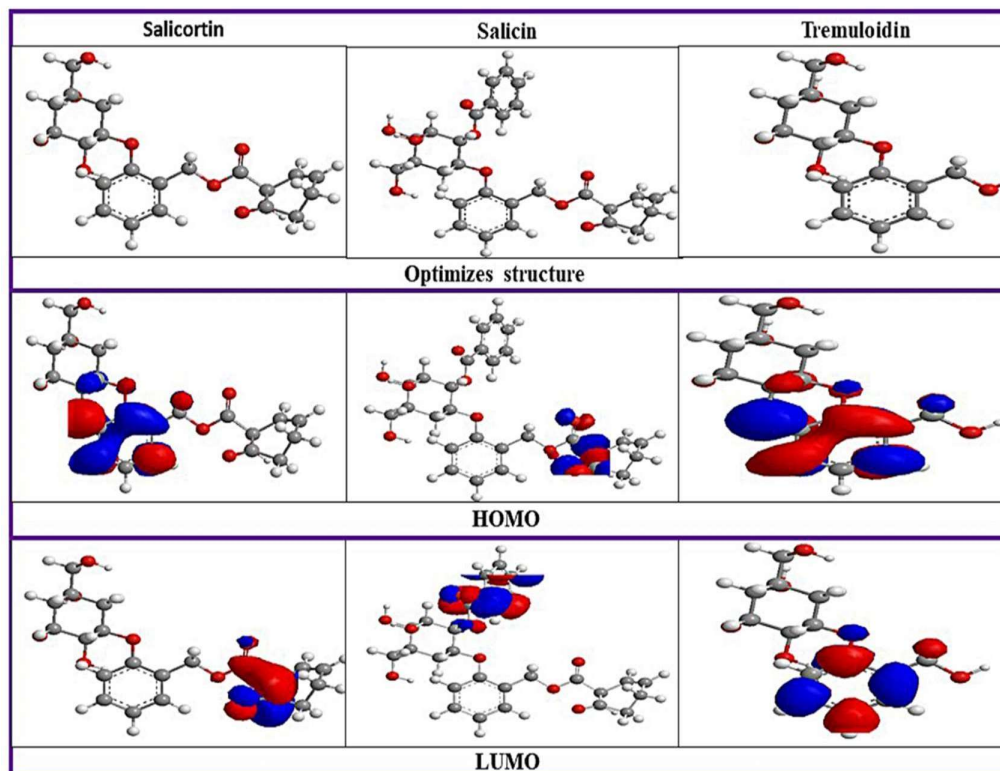


Figure 4.2.7: Optimized structures, HOMO and LUMO of phytochemicals present in *P. tremula* extract.

Table 4.2.2: Calculated quantum chemical parameters of phytochemicals of *P. tremula* extract

S.No	Phytochemicals	$E_{HOMO}$ (eV)	$E_{LUMO}$ (eV)	$\Delta E$ (eV)
1	Salicortin	-10.56	-3.98	6.85
2	Salicin	-4.56	-1.65	2.89
3	Tremuloidin	-4.91	-0.23	4.68

### 4.3 *Triticum aestivum*

*T. aestivum* is a genus of grass family belonging to the botanical tribe Triticeae in the grass family of Gramineae (Poaceae) [229]. *T. aestivum* is commonly known as wheat or bread wheat which is the common form of cultivated wheat species. It constitute 95% of the total wheat production globally [230]. After harvesting seeds most of the vegetative residues are unutilized and pile up as waste. Most of the residues are burned in India due to lack of strategies to utilize it completely and thus accounts for environmental pollution. The *T. aestivum* residues majorly contain various types of phytochemicals namely alkaloids, flavonoids, saponins, terpenoids, steroids, glycosides and tannins as mentioned in Figure 4.3.1 [231-232].

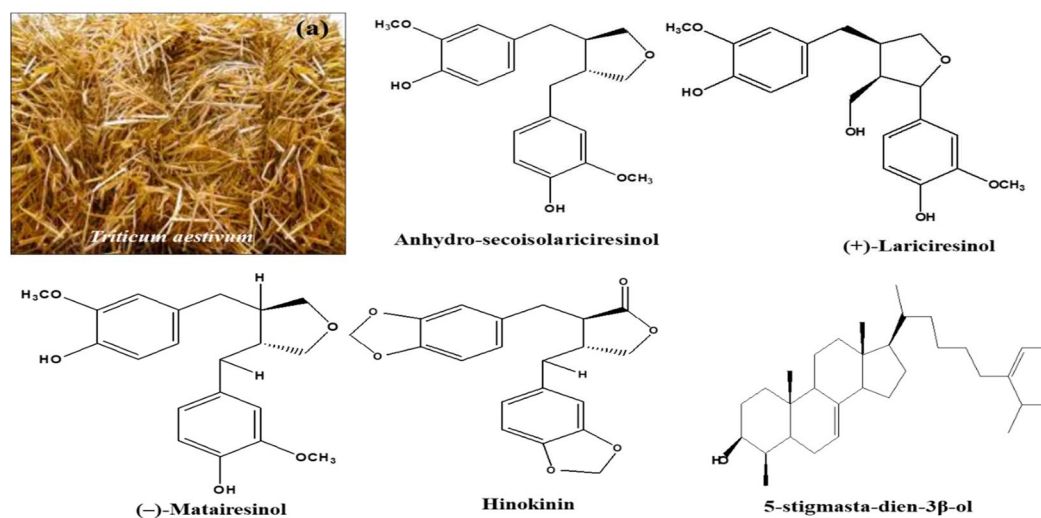


Figure 4.3.1: *T. aestivum* plant and molecular structure of phytochemicals present in *Triticum aestivum* extract.

#### 4.3.1 FTIR analysis of *T. aestivum*

FTIR spectrum was used to identify the possible phytochemicals present in *T. aestivum* extract and is shown in Fig. 4.3.2. The peaks were seen at 3311.88, 2943.47, 2830.63, 2359.98, 1663.65, 1448.58, 1209.40, 1019.41, 850.63, and 612.41  $\text{cm}^{-1}$ . The peak observed at 3311.88  $\text{cm}^{-1}$  is due to stretching of OH group from alcohol and phenol (hydrogen bonded), the characteristic peak observed at 2943.47, 2830.63 and 2359.98

$\text{cm}^{-1}$  are attributed to stretching of C-H of alkanes, the peak observed at 1663.65 and 1448.58  $\text{cm}^{-1}$  are assigned to the stretching of C=O of carbonyl group. The peaks observed at 1209.40 and 1019.41  $\text{cm}^{-1}$  are assigned to the C-O bonding (alcohols, esters, carboxylic acids). The peak observed at 850.63, and 612.41  $\text{cm}^{-1}$  are attributed to the presence of bending of C-H group of alkanes. These phytochemicals present in the peel extract of *T. aestivum* extract contains heteroatoms which are adsorbed on the steel surface and forms bonds with the  $\text{Fe}^{2+}$  ions present on the steel surface and act as potent corrosion inhibitors [233-236].

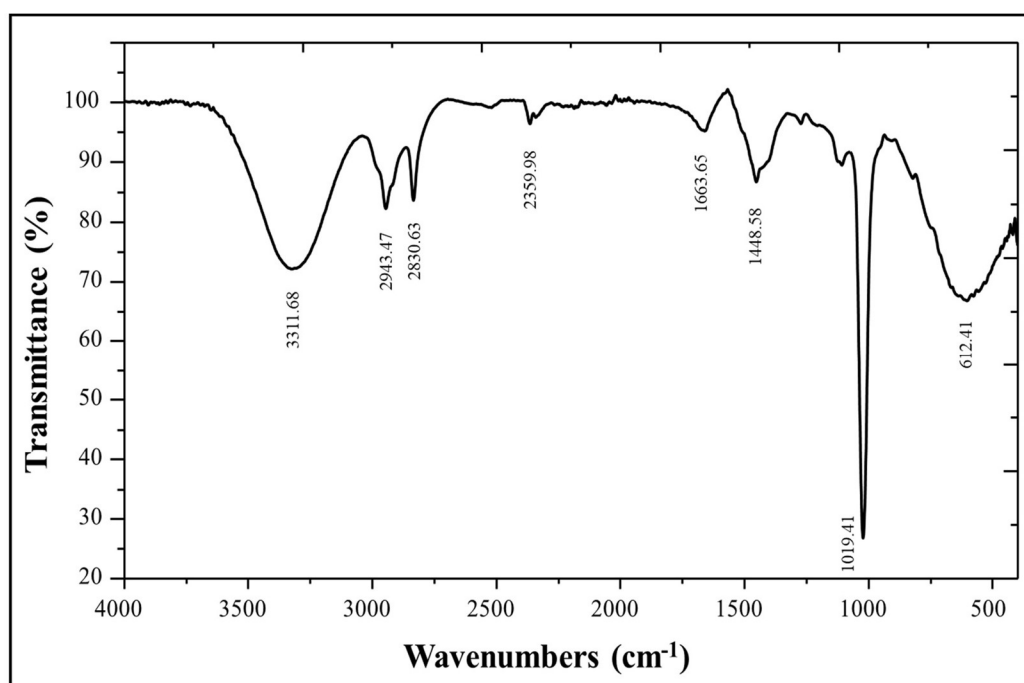


Figure 4.3.2: FT-IR spectra of *T. aestivum* extract.

#### 4.3.2 UV visible spectroscopic study

The UV- visible spectra of *T. aestivum* extract dissolved in 15% HCl before and after immersion of SS-410 specimen is shown in Fig. 4.3.3. The presence of adsorption peaks at 273 nm were due to  $n - \pi^*$  transition. The solution in which SS-410 samples were not immersed show higher peak absorbance with respect to the solution in which steel samples were immersed and further there was shift in the value of adsorption maxima in latter samples. The phytochemicals from the plant extract leads to the shift in

absorption wavelength and lower adsorption peak intensity of steel sample exposed acidic solution indicating the adsorption on the surface of S.S.-410 and the formation of bonds between the  $\text{Fe}^{2+}$  particles of steel and plant extract molecules. So, when S.S.-410 specimen is immersed in the 15% HCl solution containing plant extract, the molecules get absorb on the surface of S.S.-410 and make complexes with the surface atoms of substrate surface thus slow down the corrosion process and act as good corrosion inhibitors [202-204].

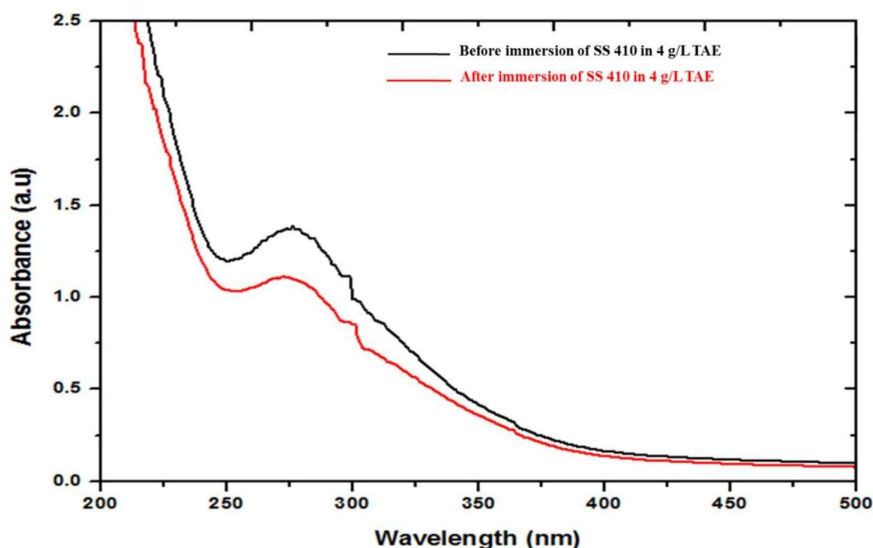


Figure 4.3.3: UV-visible spectra of *T. aestivum* extract (TAE).

#### 4.3.3 Weight loss and Electrochemical Study

The corrosion inhibition efficiency of *T. aestivum* extract extract for S.S.-410 in 15% HCl solution were obtained by using weight loss, and electrochemical measurements (Tafel and EIS) at various concentrations (1-4 g/L) at 298K. All the key parameters have been mentioned in table 4.3.1. As the concentration of *T. aestivum* extract extract increases, the value of corrosion rate decreases in weight loss measurement, thus leading to increase in corrosion inhibition efficiency. The decrease in value of corrosion rate is due to adsorption of *T. aestivum* extract phytochemicals on the surface of SS-410. Maximum 89.28 % corrosion inhibition efficiency was obtained using 4 g/L *T. aestivum* extract extract. The linear correlation coefficients 0.993 was near to 1, which confirms the adsorption of *T. aestivum* extract extract obeys Langmuir adsorption isotherm (Figure 4.3.4) [205].

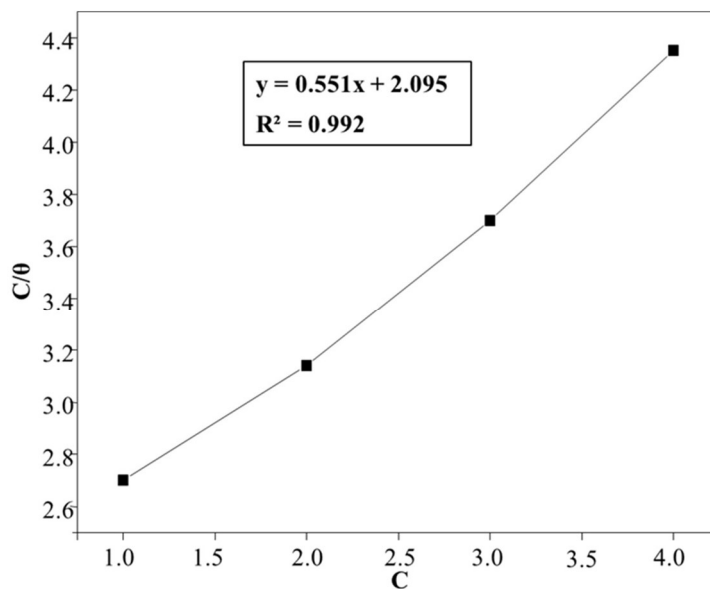


Figure 4.3.4: Langmuir adsorption isotherm for *T. aestivum* extract with the help of weight loss measurement.

As the concentration of *T. aestivum* extract increases in the corrosive media, the value of corrosion current density decreases, that designate the increase in corrosion inhibition efficiency. So, *T. aestivum* extract has mixed type of inhibition behavior. From the potentiodynamic polarization, 92.69 % corrosion inhibition efficiency was recorded at concentration of 4 g/L *T. aestivum* extract in 15% HCl solution (Figure 4.3.5(a)) [208].

A maximum 92.43 % corrosion inhibition efficiency was as shown in electrochemical impedance plot (Figure 4.3.5(b)). A layer formation was proven from the Rct value that increases with increases the *T. aestivum* extract concentration [209].

The Bode plot has been shown in (Figure 4.3.5(c)) the *T. aestivum* get adsorbed on the surface of SS-410 by involving  $\pi$  electrons of its aromatic ring or the hetero atoms from the plant extract with the free electrons of vacant d-orbital of iron from steel. This process leads to efficient anti-corrosive property of *T. aestivum*. The Bode plot support iron *T. aestivum* get adsorbed on the surface of SS-410. This process leads to efficient anticorrosive property of *T. aestivum* [210-211].

The presence of inhibitors shows the process of charge transfer resistance which started

on the interface between electrode and electrolyte as clear from phase angles graph is shown in Figure (4.3.5(d)). The inhibition was due to the adsorption of phytochemicals on the surface of steel and a protective film is formed. The increment in the values of phase angle with the presence of increasing concentration of *T. aestivum* can be attributed to a decrease in the capacitance at the surface of steel which makes the steel surface less prone to dissolution in the presence of corrosive media [212].

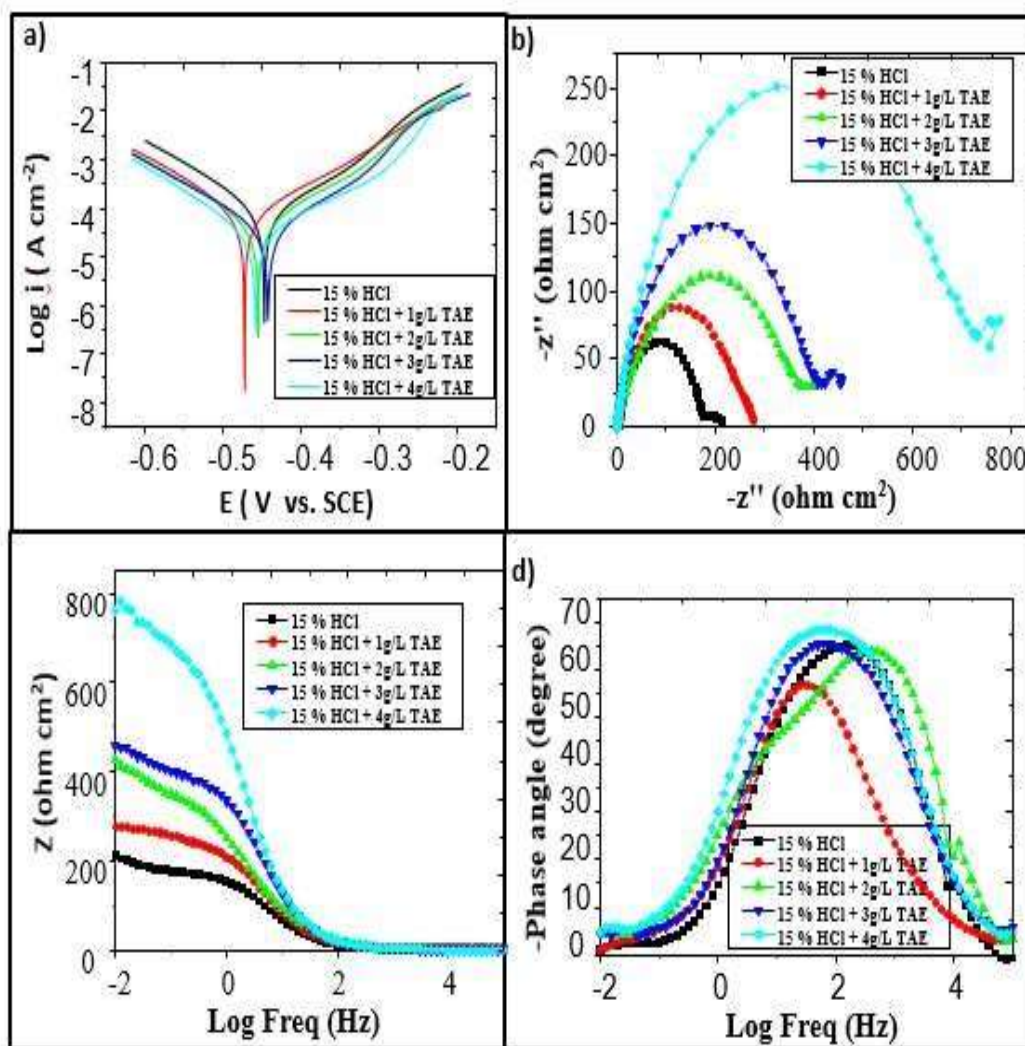


Figure 4.3.5: (a) Potentiodynamic polarization plot (b) Electrochemical impedance plot (c) Bode plot (d) Phase angle plot for different concentration of *T. aestivum* extract (TAE).



Table 4.3.1: Corrosion parameters from weight loss, and electrochemical experiments for S.S.-410 in 15% HCl with different concentrations of *T. aestivum* extract (TAE).

Weight loss			PDP			EIS	
C (g/L)	C <sub>R</sub> (mmy <sup>-1</sup> )	I.E. (%)	E <sub>corr</sub> (mV vs. SCE)	I <sub>corr</sub> (A cm <sup>-2</sup> )	I.E. (%)	R <sub>ct</sub> (Ω cm <sup>2</sup> )	I.E. (%)
15% HCl	39.01		-474.1	0.000054003		180.21	
15% HCl + 1 g/L TAE	24.56	37.03	-447.6	0.000033810	37.39	260.47	50.85
15% HCl + 2 g/L TAE	14.16	63.69	-458.5	0.000018919	64.96	366.66	60.41
15% HCl + 3 g/L TAE	7.38	81.08	-463.5	0.000006608	87.76	455.20	76.24
15% HCl + 4 g/L TAE	3.14	91.95	-443.2	0.000003942	92.69	757.87	30.81

#### 4.3.4 SEM and AFM analysis

The SEM and AFM micrographs of the S.S.-410, S.S.-410 immersed in 15% HCl and S.S.-410 immersed in 15% HCl solution in the presence of *T. aestivum* extract are shown in Figure 4.3.6. SEM of S.S.-410 coupons after 24 h immersion in 15% HCl solution at 298 K shows a severely harmed surface. From AFM studies, the average surface roughness for abraded S.S.-410 is 26.83 nm and for S.S.-410 immersed in 15% HCl, AFM micrographs of the average surface roughness is 939.14 nm. The surface of steel sample which is immersed in acid solution with the presence of *T. aestivum* extract show very less roughness as comparative smooth surface with respect to S.S.-410 immersed in only 15% HCl solution. The surface of S.S.-410 sample exposed to acid solution in the presence of

*T. aestivum* extract show average surface roughness value of 332.41 nm through AFM, which is very less as compared to roughness value of steel immersed in only 15% HCl solution. This change in surface morphology is attributed to the adsorption of some molecules from the *T. aestivum* extract on the steel surface which act as corrosion inhibitor by forming a protective layer on the steel surface and thus prevents corrosion. The mentioned SEM and AFM micrograph have been compared with SEM and AFM micrograph of S.S.-410 immersed in 15% HCl solution [213-217].

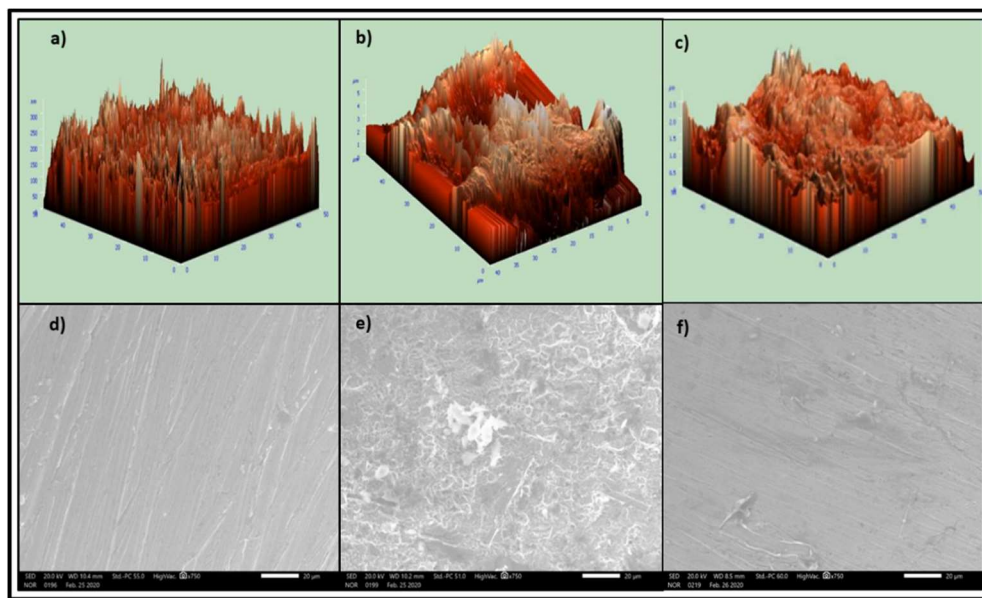


Fig. 4.3.6 (a) AFM micrographs of S.S.-410 (b) AFM micrographs of S.S.-410 immersed in 15% HCl solution (c) AFM micrographs of S.S.-410 immersed in 15% HCl solution with *T. aestivum* extract (d) SEM micrographs of S.S.-410 (e) SEM micrographs of S.S.-410 immersed in 15% HCl solution (f) SEM micrographs of S.S.-410 immersed in 15% HCl solution with *T. aestivum* extract.

#### 4.3.5 Quantum Chemical Calculations

The frontier molecular orbital density distributions (LUMO and HOMO) with optimum structures of phytochemicals presents in *T. aestivum* were shown in Fig. 4.3.7.  $E_{\text{HOMO}}$  and  $E_{\text{LUMO}}$  and  $(\Delta E)$  are the key parameters of theoretical study, have been mentioned in table 4.3.2 [218-222]. The energy gap of molecular orbital follows the order: (+)-Lariciresinol < Anhydro-ecoisolariciresinol < Hinokinin < 5-stigmasta-dien-3 $\beta$ -ol < (-)-Matairesinol. Hence, the inhibition effect follows the order: (+)-Lariciresinol >

Anhydro-ecoisolariciresinol > Hinokinin > 5-stigmasta-dien-3 $\beta$ -ol > (-)-Matairesinol.  
 So, (+)-Lariciresinol can be assumed to be the most essential phytochemical in the corrosion inhibition behaviour of the *T. aestivum*.

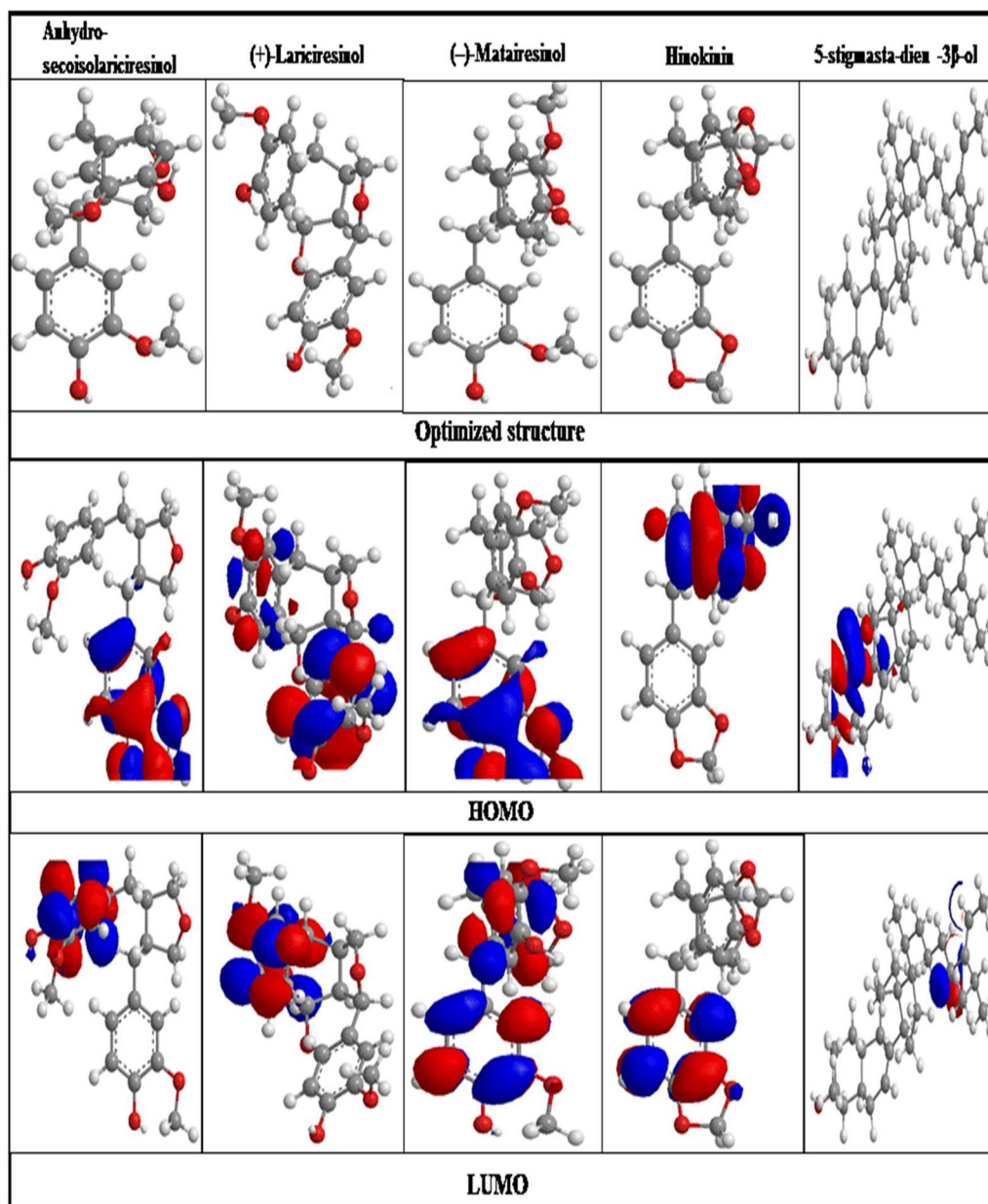


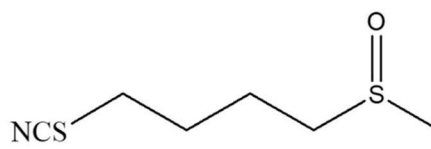
Figure 4.3.7: Optimized structures, HOMO and LUMO of phytochemicals present in *T. aestivum* extract.

Table 4.3.2: Calculated quantum chemical parameters of phytochemicals of *T. aestivum* extract

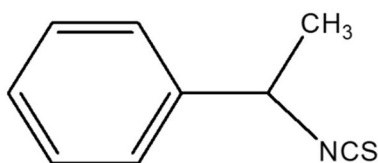
S.No	Phytochemicals	E <sub>HOMO</sub> (eV)	E <sub>LUMO</sub> (eV)	ΔE (eV)
1	Anhydro-secoisolariciresinol	-10.09	-0.88	9.21
2	(+)-Lariciresinol	-0.69	-0.46	0.57
3	(-)-Matairesinol	-11.00	-0.88	11.27
4	Hinokinin	-10.74	-0.89	9.85
5	5-stigmasta-dien-3β-ol	-10.87	-1.74	9.13

#### 4.4 *Brassica nigra*

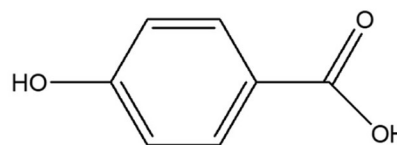
*B. nigra*, is a genus of plant belongs to Brassicaceae family. *B. nigra*, is commonly known as sarso in India. It's black and brown seed is used as spice [237-238]. The *B. nigra* residues contain various types of phytochemicals as mentioned in figure 4.4.1 [239]. After harvesting seeds most of the vegetative residues are unutilized and pile up as waste. Most of the residues are burned in India due to lack of strategies to utilize it completely and thus accounts for environmental pollution. The main aim of this study is to investigate the use of *B. nigra* waste as corrosion inhibitor. Main focus is on exploring the adsorptive and anticorrosion properties of *B. nigra*.



**Sulforaphane**



**Phenyl Isothiocyanate**



**p-hydroxybenzoic acid**

Figure 4.4.1: *B. nigra* plant and molecular structure of phytochemicals present in *B. nigra* extract.

#### 4.4.1 FTIR analysis of *B. nigra*

FTIR spectrum was used to identify the possible phytochemicals present in *B. nigra* extract and is shown in Fig. 4.4.2. The peaks were seen at 3439.19, 3186.50, 2885.60, 2729.36, 2343.58, 1631.83, 1367.57, 1039.81, 981.79, and 513.12  $\text{cm}^{-1}$ . The peak observed at 3439.19 and 3186.50  $\text{cm}^{-1}$  are due to stretching of OH group from alcohol and phenol (hydrogen bonded), the characteristic peak observed at 2885.60, 2729.36 and 2343.58  $\text{cm}^{-1}$  are attributed to stretching of C-H of alkanes, the peak observed at 2152.40 is corresponds to NCS group, the peak observed at 1631.83 and 1367.57  $\text{cm}^{-1}$  are assigned to the stretching of C=O of carbonyl group. The peaks observed at 1039.81  $\text{cm}^{-1}$  is assigned to the C-O bonding (alcohols, esters, carboxylic acids). The peak observed at 981.79, and 513.12  $\text{cm}^{-1}$  are attributed to the presence of bending of C-H group of alkanes. These phytochemicals present in the peel extract of *B. nigra* extract contains heteroatoms which are adsorbed on the steel surface and forms bonds with the  $\text{Fe}^{2+}$  ions present on the steel surface and act as potent corrosion inhibitors [240-243].

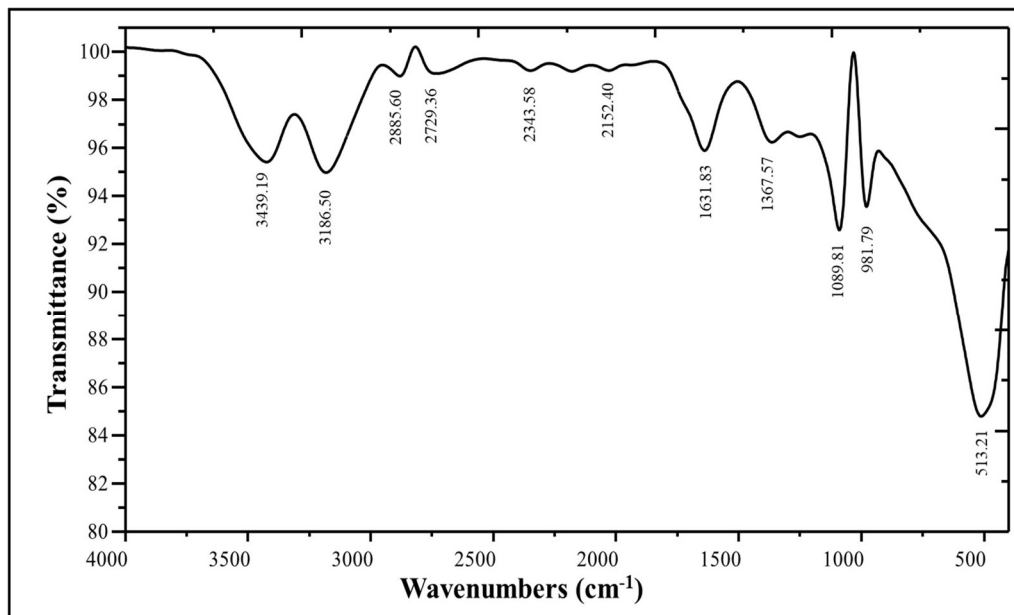


Figure 4.4.2: FT-IR spectra of *B. nigra* extract.

#### 4.4.2 UV visible spectroscopic study

The UV- visible spectra of *B. nigra* extract dissolved in 15% HCl before and after immersion of SS-410 specimen is shown in Fig. 4.4.3. The presence of adsorption peaks at 215.43 and 280.89 nm representing  $\pi - \pi^*$  and  $n - \pi^*$  transition. The solution in which SS-410 samples were not immersed show higher peak absorbance with respect to the solution in which steel samples were immersed and further there was shift in the value of adsorption maxima in latter samples. The phytochemicals from the plant extract leads to the shift in absorption wavelength and lower adsorption peak intensity of steel sample exposed acidic solution indicating the adsorption on the surface of S.S.-410 and the formation of bonds between the  $Fe^{2+}$  particles of steel and plant extract molecules. So, when S.S.-410 specimen is immersed in the 15% HCl solution containing plant extract, the molecules get absorb on the surface of S.S.-410 and make complexes with the surface atoms of substrate surface thus slow down the corrosion process and act as good corrosion inhibitors [202-204].

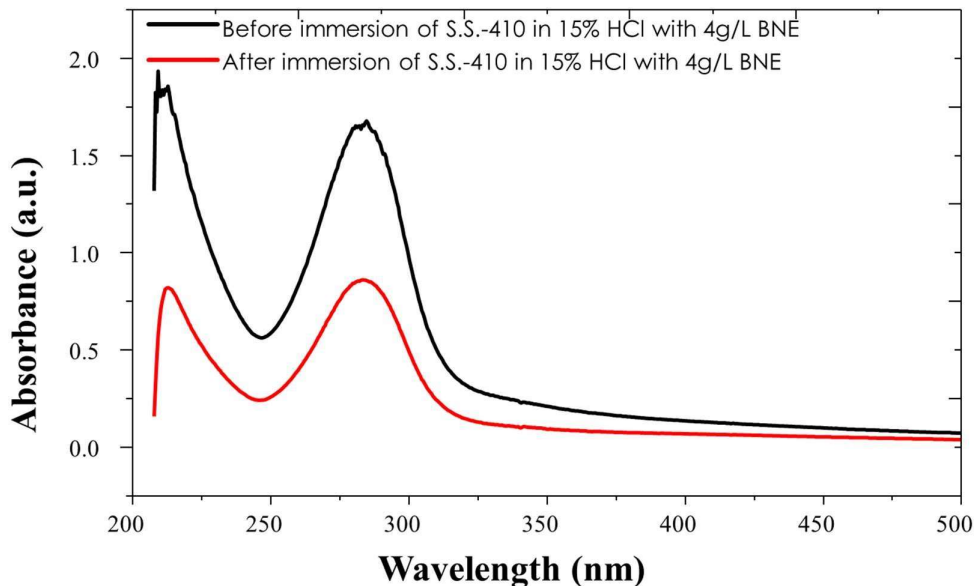


Figure 4.4.3: UV-visible spectra of *B. nigra* extract (BNE).

#### 4.4.3 Weight loss and Electrochemical Study

The corrosion inhibition efficiency of *B. nigra* extract extract for S.S.-410 in 15% HCl solution were obtained by using weight loss, and electrochemical measurements (Tafel and EIS) at various concentrations (1-4 g/L) at 298K. All the key parameters have been mentioned in table 4.4.1. As the concentration of *B. nigra* extract extract increases, the value of corrosion rate decreases in weight loss measurement, thus leading to increase in corrosion inhibition efficiency. The decrease in value of corrosion rate is due to adsorption of *B. nigra* extract phytochemicals on the surface of SS-410. Maximum 91.69 % corrosion inhibition efficiency was obtained using 4 g/L *B. nigra* extract. The linear correlation coefficients 0.9959 was near to 1, which confirms the adsorption of *B. nigra* extract obeys Langmuir adsorption isotherm (Figure 4.4.4) [205].

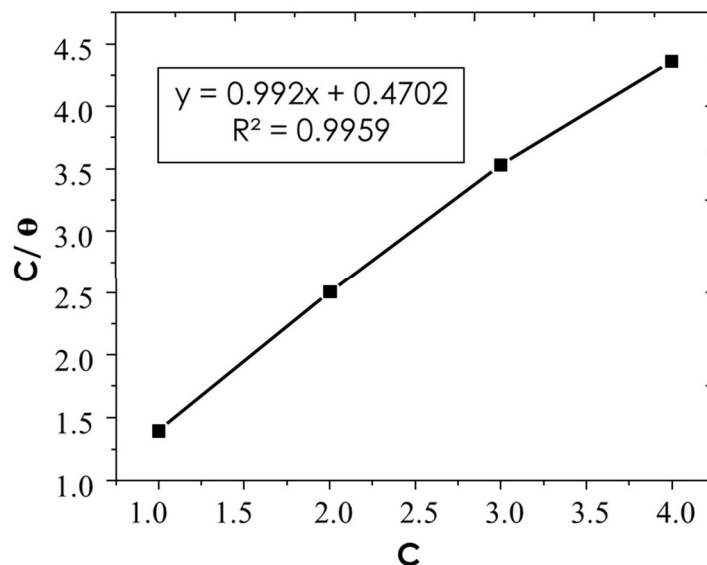


Figure 4.5.4: Langmuir adsorption isotherm of *B. nigra* extract with the of weight loss measurements.

So, *B. nigra* extract has mixed type of inhibition behavior. From the potentiodynamic polarization, 94.50 % corrosion inhibition efficiency was recorded at concentration of 4 g/L *B. nigra* extract in 15% HCl solution (Figure 4.4.5(a)) [208].

A maximum 99.68 % corrosion inhibition efficiency was as shown in electrochemical impedance plot (Figure 4.4.5(b)). A layer formation was proven from the  $R_{ct}$  value that increases with increases the *B. nigra* extract concentration [209]. The Bode plot has been shown in (Figure 4.4.5(c)) the *B. nigra* get adsorbed on the surface of SS-410 by involving  $\pi$  electrons of its aromatic ring or the hetero atoms from the plant extract with the free electrons of vacant d-orbital of iron from steel. This process leads to efficient anti-corrosive property of *B. nigra*. The Bode plot support iron *B. nigra* get adsorbed on the surface of SS-410. This process leads to efficient anticorrosive property of *B. nigra* [210-211]. The presence of inhibitors shows the process of charge transfer resistance which started on the interface between electrode and electrolyte as clear from phase angles graph is shown in Figure (4.4.5(d)).

The inhibition was due to the adsorption of phytochemicals on the surface of steel and a protective film is formed. The increment in the values of phase angle with the presence



of increasing concentration of *B. nigra* can be attributed to a decrease in the capacitance at the surface of steel which makes the steel surface less prone to dissolution in the presence of corrosive media [212].

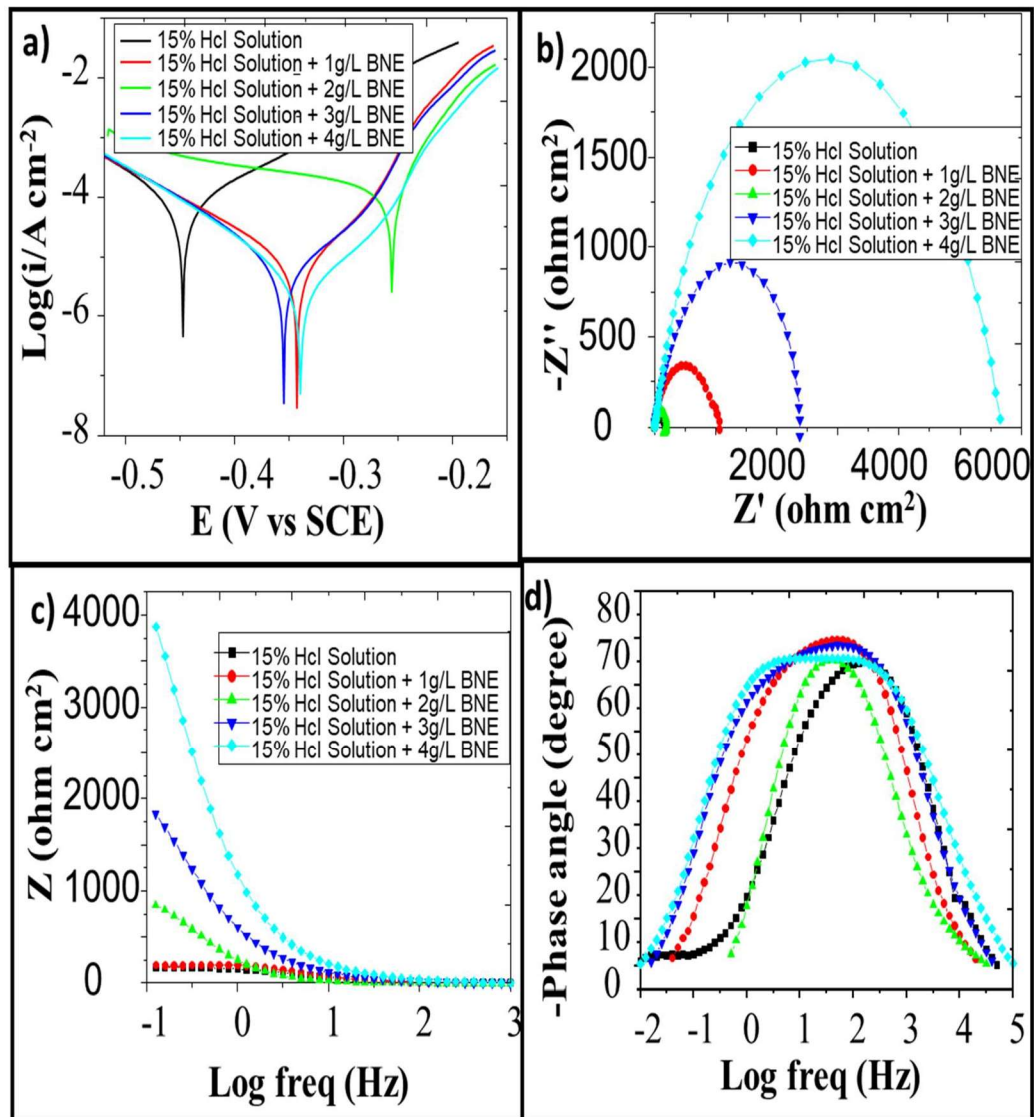


Figure 4.4.5: (a) Potentiodynamic polarization plot (b) Electrochemical impedance plot (c) Bode plot (d) phase angle plot for different concentration of *B. nigra* extract (BNE).

Table 4.4.1: Corrosion parameters from weight loss, and electrochemical experiments for S.S.-410 in 15% HCl with different concentrations of *B. nigra* extract (BNE).

Weight loss			PDP			EIS	
C (g/L)	C <sub>R</sub> (mmy <sup>-1</sup> )	I.E. (%)	E <sub>corr</sub> (mV vs. SCE)	I <sub>corr</sub> (A cm <sup>-2</sup> )	I.E. (%)	R <sub>ct</sub> (Ω cm <sup>2</sup> )	I.E. (%)
15% HCl	39.01		-474.1	.000054003		180.21	
15% HCl + 1 g/L BNE	11.10	71.54	-342.25	.000024503	54.61	250.87	28.16
15% HCl + 2 g/L BNE	7.89	79.77	-255.43	.000021625	59.95	1200.39	84.97
15% HCl + 3 g/L BNE	5.89	84.90	-354.46	.000011329	79.02	2499.47	92.79
15% HCl + 4 g/L BNE	3.24	91.69	-338.59	.000002970	94.50	57301	99.68

#### 4.4.4 SEM and AFM analysis

The SEM and AFM micrographs of the S.S.-410, S.S.-410 immersed in 15% HCl and S.S.-410 immersed in 15% HCl solution in the presence of *B. nigra* extract are shown in Figure 4.4.6. SEM of S.S.-410 coupons after 24 h immersion in 15 % HCl solution at 298 K shows a severely harmed surface. From AFM studies, the average surface roughness for abraded S.S.- 410 is 26.83 nm and for S.S.- 410 immersed in 15 % HCl, AFM micrographs of the average surface roughness is 939.14 nm. The surface of steel sample which is immersed in acid solution with the presence of *B. nigra* extract show very less roughness as comparative smooth surface with respect to S.S.-410 immersed in only 15% HCl solution. The surface of S.S.-410 sample exposed to acid solution in the presence of *B. nigra* extract show average surface roughness value of 368.89 nm through AFM, which is very less as compared to roughness value of steel immersed in only 15% HCl solution.

This change in surface morphology is attributed to the adsorption of some molecules from the *B. nigra* extract on the steel surface which act as corrosion inhibitor by forming a protective layer on the steel surface and thus prevents corrosion. The mentioned SEM and AFM micrograph have been compared with SEM and AFM micrograph of S.S.-410 immersed in 15% HCl solution [213-217].

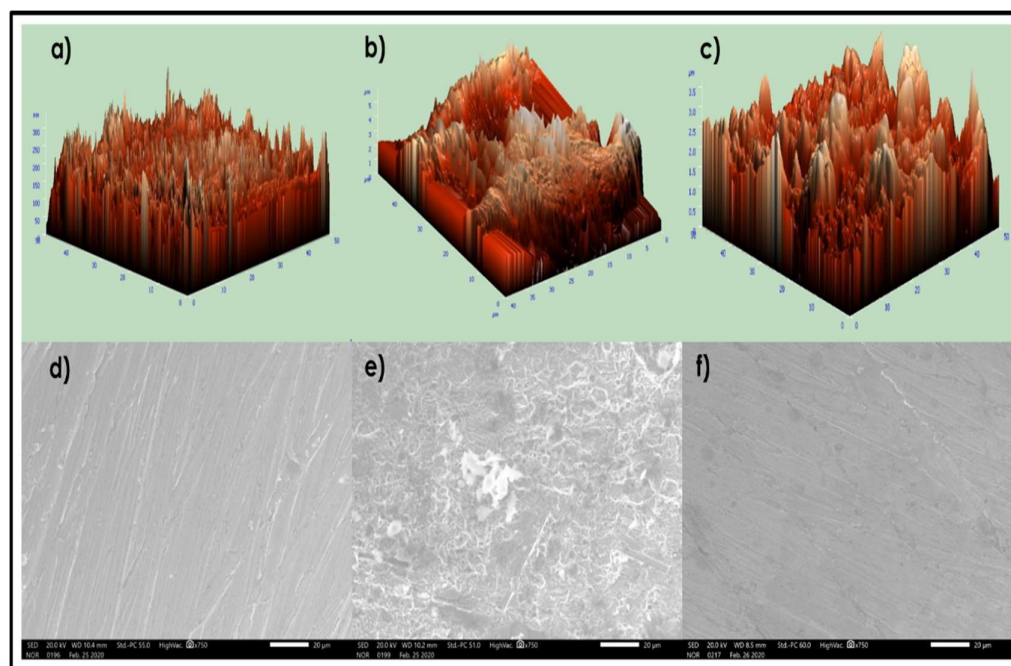


Figure 4.4.6: (a) AFM micrographs of S.S.-410 (b) AFM micrographs of S.S.-410 immersed in 15% HCl solution (c) AFM micrographs of S.S.-410 immersed in 15% HCl solution with *B. nigra* extract (d) SEM micrographs of S.S.-410 (e) SEM micrographs of S.S.-410 immersed in 15% HCl solution (f) SEM micrographs of S.S.-410 immersed in 15% HCl solution with *B. nigra* extract.

#### 4.4.5 Quantum Chemical Calculations:

The frontier molecular orbital density distributions (LUMO and HOMO) with optimum structures of phytochemicals presents in *B. nigra* were shown in Fig. 4.4.7.  $E_{\text{HOMO}}$  and  $E_{\text{LUMO}}$  and  $(\Delta E)$  are the key parameters of theoretical study, have been mentioned in table 4.4.2 [218-222]. The energy gap of molecular orbital follows the order: Phenyl Isothiocyanate < p-hydroxybenzoic acid < Sulforaphane. Hence, the inhibition effect follows the order Phenyl Isothiocyanate > p-hydroxybenzoic acid > Sulforaphane. So,

Phenyl Isothiocyanate can be assumed to be the most essential phytochemical in the corrosion inhibition behaviour of the *B. nigra*.

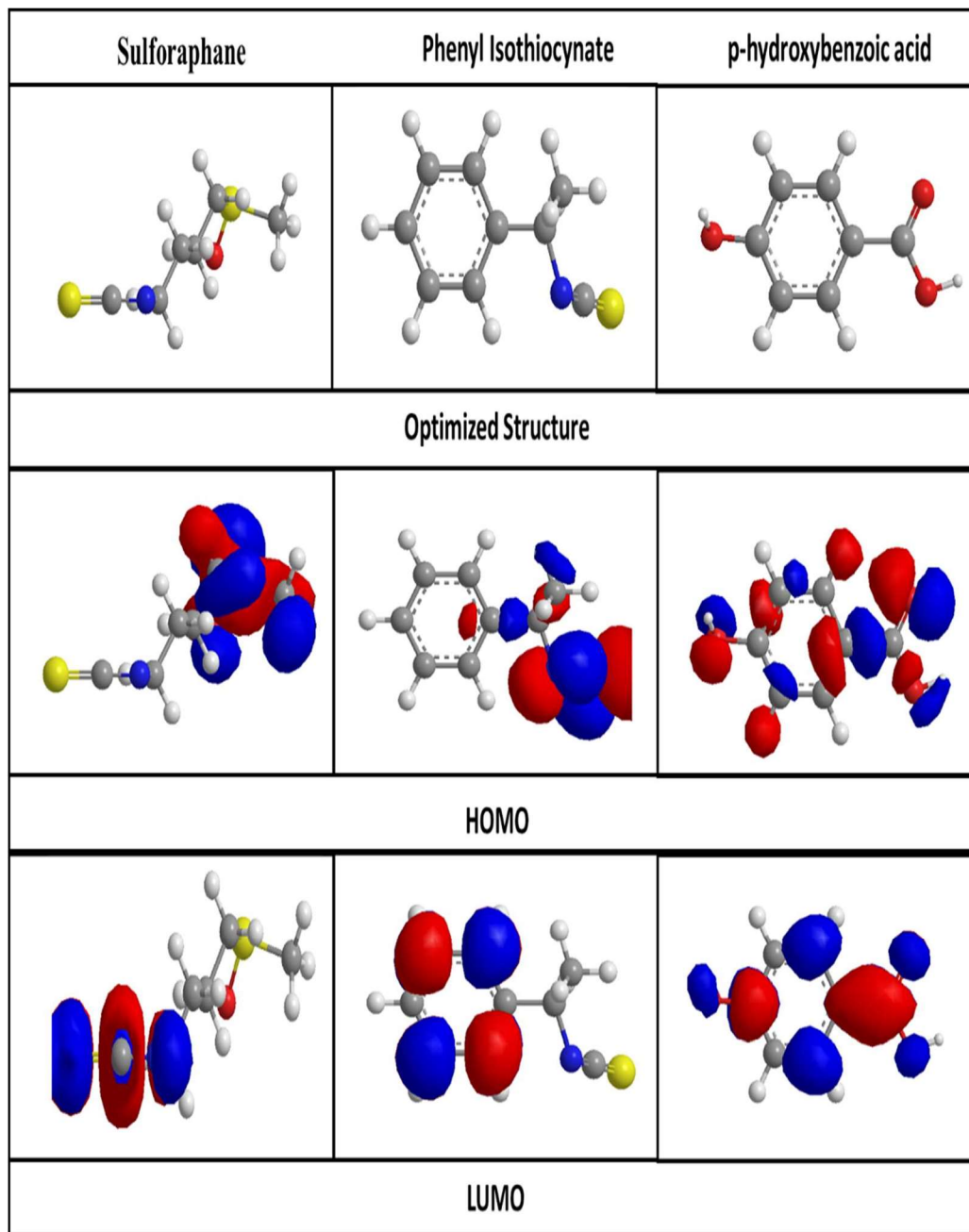


Figure 4.4.7: Optimized structures, HOMO and LUMO of phytochemicals present in *B. nigra* extract.

Table 4.4.2: Calculated quantum chemical parameters of phytochemicals of *B. nigra* extract

S.No	Molecule	E <sub>HOMO</sub> (eV)	E <sub>LUMO</sub> (eV)	ΔE (eV)
1	Sulforaphane	-6.64	4.42	11.06
2	Phenyl Isothiocyanate	-10.50	-1.69	8.81
3	p-hydroxybenzoic acid	-12.66	-3.16	9.5

#### 4.5 *Saccharum officinarum*

*S. officinarum* is a grass diverse genus with 25–30 species of deciduous flowering plants belongs to Poaceae family [244]. *S. officinarum* is commonly known as Ganna in India. The *S. officinarum* residues contain various types of phytochemicals as mentioned in figure 4.5.1 [245]. Most of the residues are burned in India due to lack of strategies to utilize it completely and thus accounts for environmental pollution [246]. The main aim of this study is to investigate the use of *S. officinarum* waste as corrosion inhibitor. Main focus is on exploring the adsorptive and anticorrosion properties of *S. officinarum*.

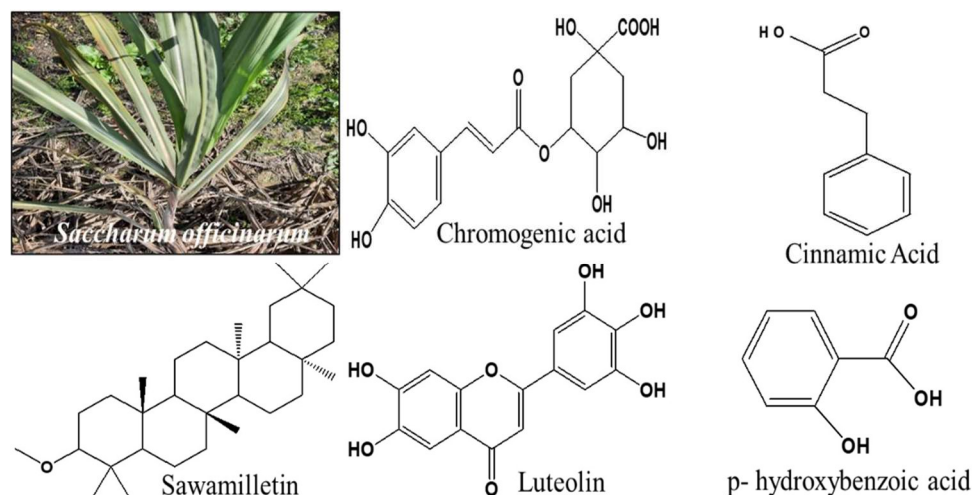


Figure 4.5.1: (a) *S. officinarum* plant (b – f) molecular structure of phytochemicals present in *S. officinarum* extract.

#### 4.5.1 FTIR analysis of *S. officinarum*

FTIR spectrum was used to identify the possible phytochemicals present in *S. officinarum* extract and is shown in Fig. 4.5.2. The peaks were seen at 3485.48, 3147.93, 2926.11, 2353.23, 1714.77, 1327, 1207.47, 1012.66 and 478.36  $\text{cm}^{-1}$ . The peak observed at 3485.48 and 3147.93  $\text{cm}^{-1}$  are due to stretching of OH group from alcohol and phenol (hydrogen bonded), the characteristic peak observed at 2926.11 and 2353.23  $\text{cm}^{-1}$  are attributed to stretching of C-H of alkanes, the peak observed at 1714.77 and 1327  $\text{cm}^{-1}$  are assigned to the stretching of C=O of carbonyl group. The peaks observed at 1207.47 and 1012.66  $\text{cm}^{-1}$  are assigned to the C-O bonding (alcohols, esters, carboxylic acids). The peak observed at 478.36  $\text{cm}^{-1}$  is attributed to the presence of bending of C-H group of alkanes. These phytochemicals present in the peel extract of *S. officinarum* extract contains heteroatoms which are adsorbed on the steel surface and forms bonds with the  $\text{Fe}^{2+}$  ions present on the S.S.-410 surface and act as potent corrosion inhibitors [247-250].

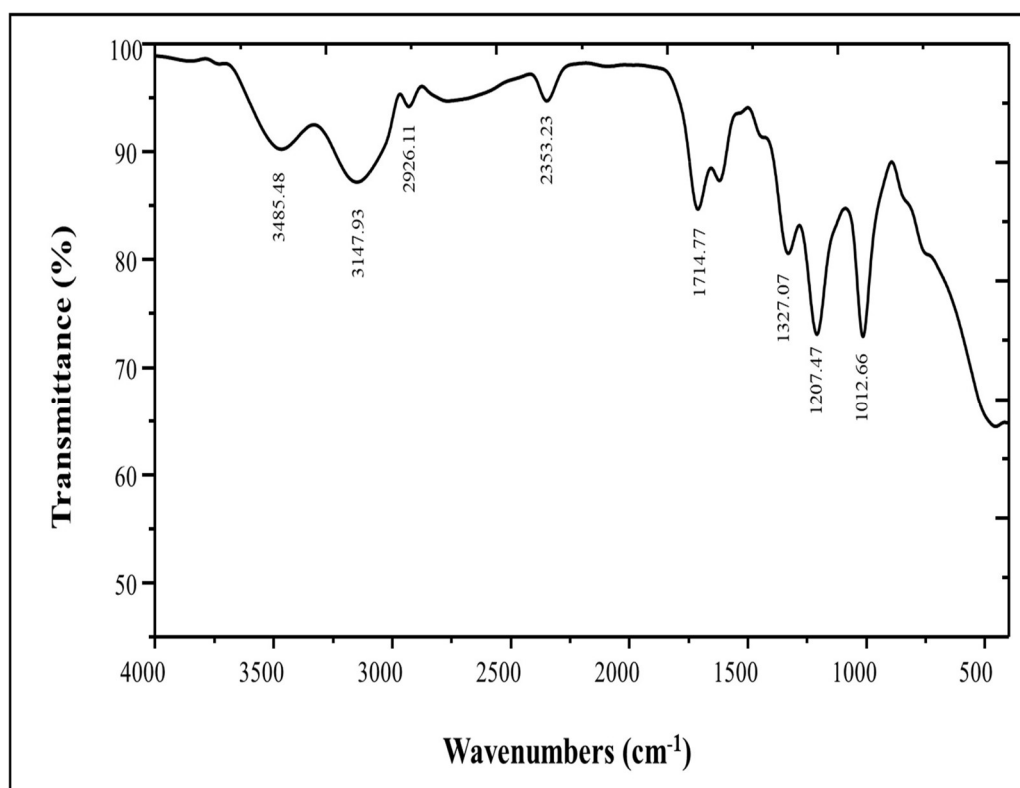


Figure 4.5.2: FT-IR spectra of *S. officinarum* extract.

#### 4.5.2 UV visible spectroscopic study

The UV- visible spectra of *S. officinarum* extract dissolved in 15% HCl before and after immersion of SS-410 specimen is shown in Fig. 4.5.3. The presence of adsorption peaks at 215 and 289 nm representing  $\pi - \pi^*$  and  $n - \pi^*$  transition. The solution in which SS-410 samples were not immersed show higher peak absorbance with respect to the solution in which steel samples were immersed and further there was shift in the value of adsorption maxima in latter samples. The phytochemicals from the plant extract leads to the shift in absorption wavelength and lower adsorption peak intensity of steel sample exposed acidic solution indicating the adsorption on the surface of S.S.-410 and the formation of bonds between the  $Fe^{2+}$  particles of steel and plant extract molecules. So, when S.S.-410 specimen is immersed in the 15% HCl solution containing plant extract, the molecules get absorb on the surface of S.S.-410 and make complexes with the surface atoms of substrate surface thus slow down the corrosion process and act as good corrosion inhibitors [202-204].

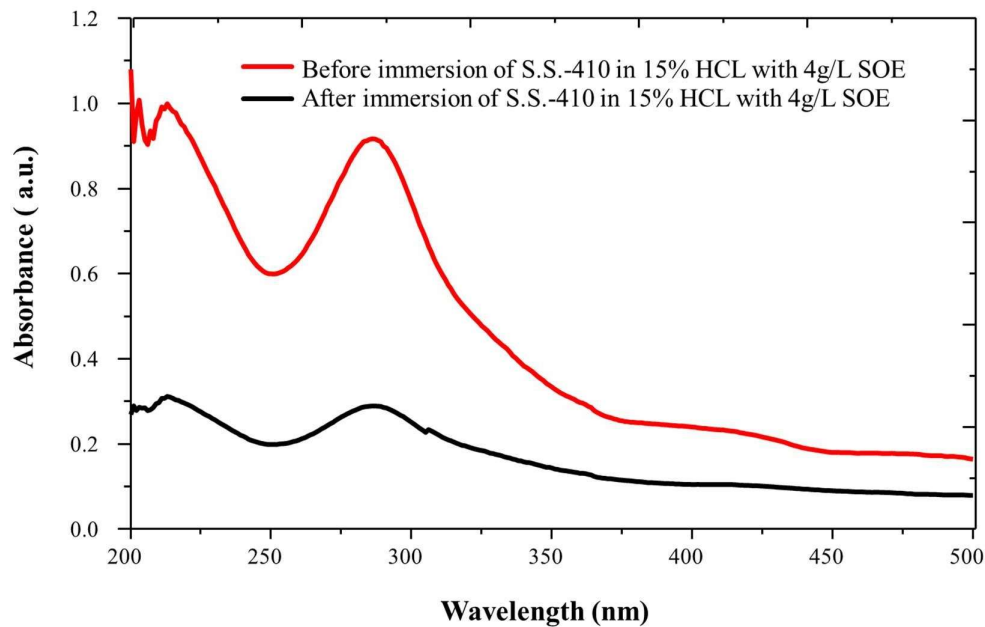


Figure 4.5.3: UV-visible spectra of *S. officinarum* extract (SOE).

#### 4.5.3 Weight loss and Electrochemical Study

The corrosion inhibition efficiency of *S. officinarum* extract for S.S.-410 in

15% HCl solution were obtained by using weight loss, and electrochemical measurements (Tafel and EIS) at various concentrations (1-4 g/L) at 298K. All the key parameters have been mentioned in table 4.5.1. As the concentration of *S. officinarum* extract increases, the value of corrosion rate decreases in weight loss measurement, thus leading to increase in corrosion inhibition efficiency. The decrease in value of corrosion rate is due to adsorption of *S. officinarum* extract phytochemicals on the surface of SS-410. Maximum 95.92 % corrosion inhibition efficiency was obtained using 4 g/L *S. officinarum* extract. The linear correlation coefficient 0.9903 was near to 1, which confirms the adsorption of *S. officinarum* extract obeys Langmuir adsorption isotherm (Figure 4.5.4) [205].

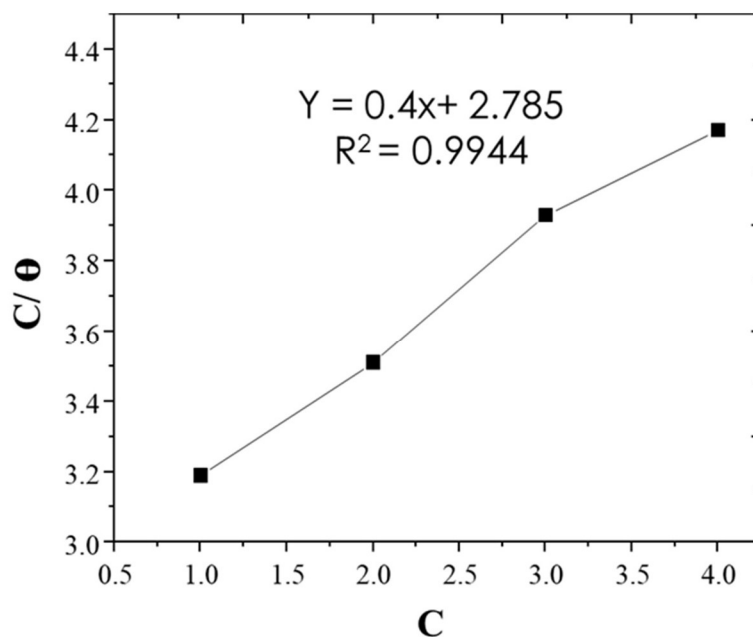


Figure 4.5.4: Langmuir adsorption isotherm of *S. officinarum* extract with the of weight loss measurements.

The shift of 85 mV in corrosion potential ( $E_{corr}$ ) value from blank to optimum concentration shows that inhibitor behaves as mixed (anodic or cathodic inhibition) type [206-207]. So, *S. officinarum* extract has mixed type of inhibition behavior. From the potentiodynamic polarization, 90.21 % corrosion inhibition efficiency was recorded at concentration of 4 g/L *S. officinarum* extract in 15% HCl solution (Figure



4.5.5(a) [208]. A maximum 91.23 % corrosion inhibition efficiency was as shown in electrochemical impedance plot (Figure 4.5.5(b)). A layer formation was proven from the  $R_{ct}$  value that increases with increases the *S. officinarum* extract concentration [209].

The Bode plot has been shown in (Figure 4.5.5(c)) the *S. officinarum* get adsorbed on the surface of SS-410 by involving  $\pi$  electrons of its aromatic ring or the hetero atoms from the plant extract with the free electrons of vacant d-orbital of iron from steel. This process leads to efficient anti-corrosive property of *S. officinarum*. The Bode plot support iron *S. officinarum* get adsorbed on the surface of SS-410. This process leads to efficient anticorrosive property of *S. officinarum* [210-211].

The presence of inhibitors shows the process of charge transfer resistance which started on the interface between electrode and electrolyte as clear from phase angles graph is shown in Figure (4.5.5(d)). The inhibition was due to the adsorption of phytochemicals on the surface of steel and a protective film is formed. The increment in the values of phase angle with the presence of increasing concentration of *S. officinarum* can be attributed to a decrease in the capacitance at the surface of steel which makes the steel surface less prone to dissolution in the presence of corrosive media [212].

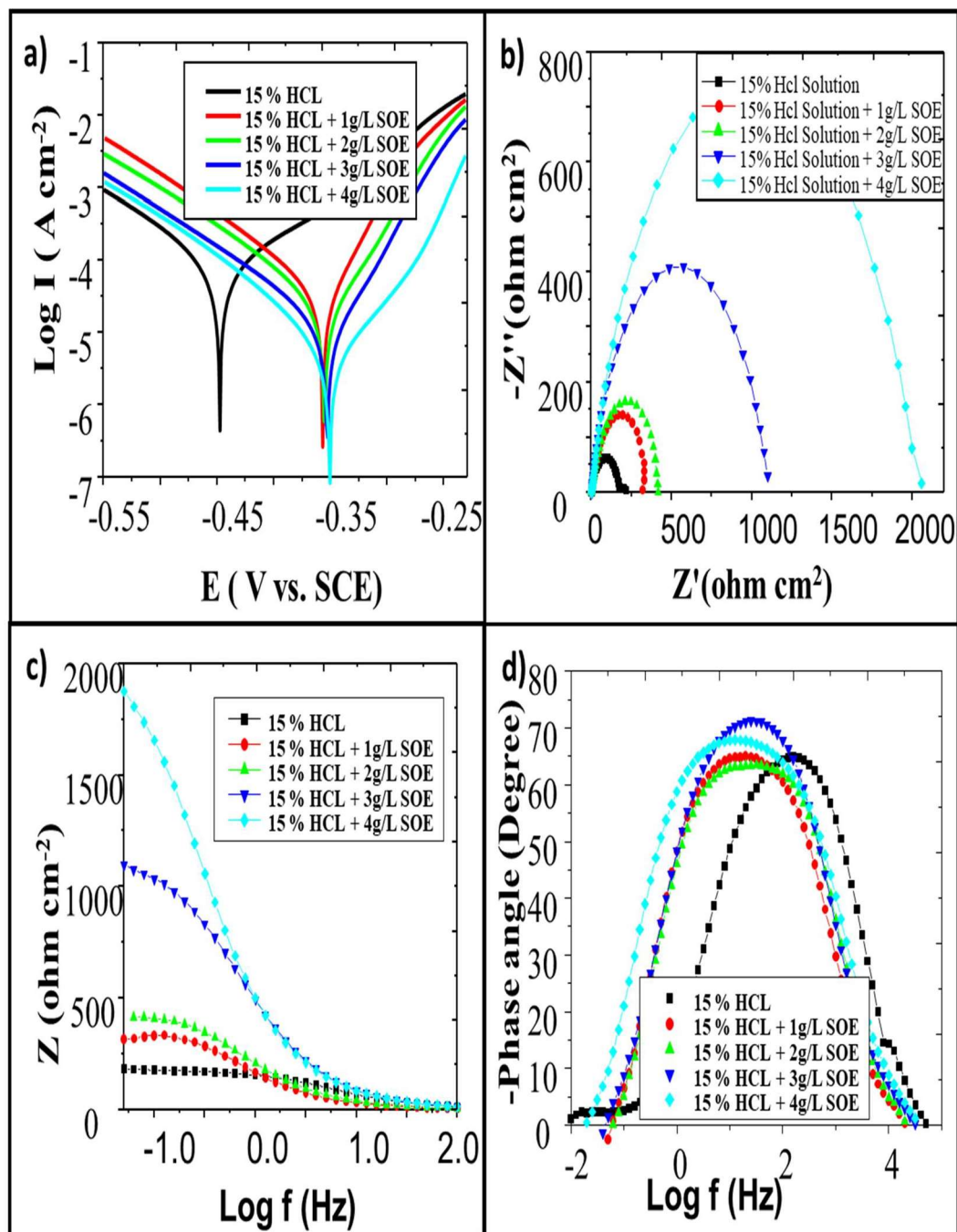


Figure 4.5.5: (a) Potentiodynamic polarization plot (b) Electrochemical impedance plot (c) Bode plot (d) Phase angle plot for different concentration of *S. officinarum* extract (SOE).

Table 4.5.1: Corrosion parameters from weight loss, and electrochemical experiments for S.S.-410 in 15% HCl with different concentrations of *S. officinarum* extract (SOE).

Weight loss			PDP			EIS	
C (g/L)	C <sub>R</sub> (mmy <sup>-1</sup> )	I.E. (%)	E <sub>corr</sub> (mV vs. SCE)	I <sub>corr</sub> (A cm <sup>-2</sup> )	I.E. (%)	R <sub>ct</sub> (Ω cm <sup>2</sup> )	I.E. (%)
15% HCl	39.01		-474.1	0.000054003		180.21	
15% HCl + 1 g/L SOE	26.784	31.34	-356.75	0.0000317052	41.29	319.96	43.67
15% HCl + 2 g/L SOE	16.782	56.98	-355.37	0.0000241285	55.32	415.06	56.58
15% HCl + 3 g/L SOE	9.233	76.33	-352.17	0.0000100014	81.48	1115.89	83.85
15% HCl + 4 g/L SOE	1.591	95.92	-350.49	0.0000052869	90.21	2056.54	91.23

#### 4.5.4 SEM and AFM analysis

The SEM and AFM micrographs of the S.S.-410, S.S.-410 immersed in 15% HCl and S.S.-410 immersed in 15% HCl solution in the presence of *S. officinarum* extract are shown in Figure 4.5.6. SEM of S.S.-410 coupons after 24 h immersion in 15 % HCl solution at 298 K shows a severely harmed surface. From AFM studies, the average surface roughness for abraded S.S.- 410 is 26.83 nm and for S.S.- 410 immersed in 15 % HCl, AFM micrographs of the average surface roughness is 939.14 nm. The surface of steel sample which is immersed in acid solution with the presence of *S. officinarum* extract show very less roughness as comparative smooth surface with respect to S.S.-410 immersed in only 15% HCl solution. The surface of S.S.-410 sample exposed to acid solution in the presence of

*S. officinarum* extract show average surface roughness value of 212.26 nm through AFM, which is very less as compared to roughness value of steel immersed in only 15% HCl solution. This change in surface morphology is attributed to the adsorption of some molecules from the *S. officinarum* extract on the steel surface which act as corrosion inhibitor by forming a protective layer on the steel surface and thus prevents corrosion. The mentioned SEM and AFM micrograph have been compared with SEM and AFM micrograph of S.S.-410 immersed in 15% HCl solution [213-217].

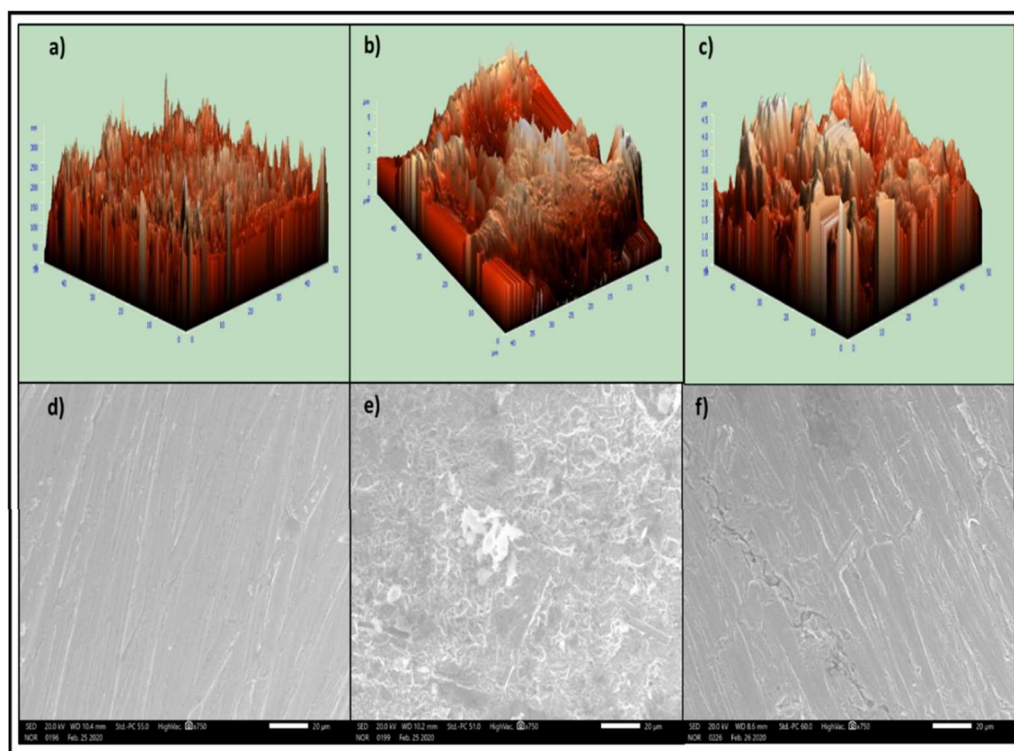


Figure 4.5.6: (a) AFM micrographs of S.S.-410 (b) AFM micrographs of S.S.-410 immersed in 15% HCl solution (c) AFM micrographs of S.S.-410 immersed in 15% HCl solution with *S. officinarum* extract (d) SEM micrographs of S.S.-410 (e) SEM micrographs of S.S.-410 immersed in 15% HCl solution (f) SEM micrographs of S.S.-410 immersed in 15% HCl solution with *S. officinarum* extract.

#### 4.5.5 Quantum Chemical Calculations

The frontier molecular orbital density distributions (LUMO and HOMO) with optimum structures of phytochemicals presents in *S. officinarum* were shown in Fig. 4.5.7.  $E_{\text{HOMO}}$  and  $E_{\text{LUMO}}$  and  $(\Delta E)$  are the key parameters of theoretical study, have been mentioned

in table 4.5.2 [218-222]. The energy gap of molecular orbital follows the order: Luteolin < Chromogenic acid < p- hydroxybenzoic acid < Cinnamic Acid < Sawamilletin. Hence, the inhibition effect follows the order Luteolin > Chromogenic acid > p- hydroxybenzoic acid > Cinnamic Acid > Sawamilletin. So, Luteolin can be assumed to be the most essential phytochemical in the corrosion inhibition behaviour of the *S. officinarum*.

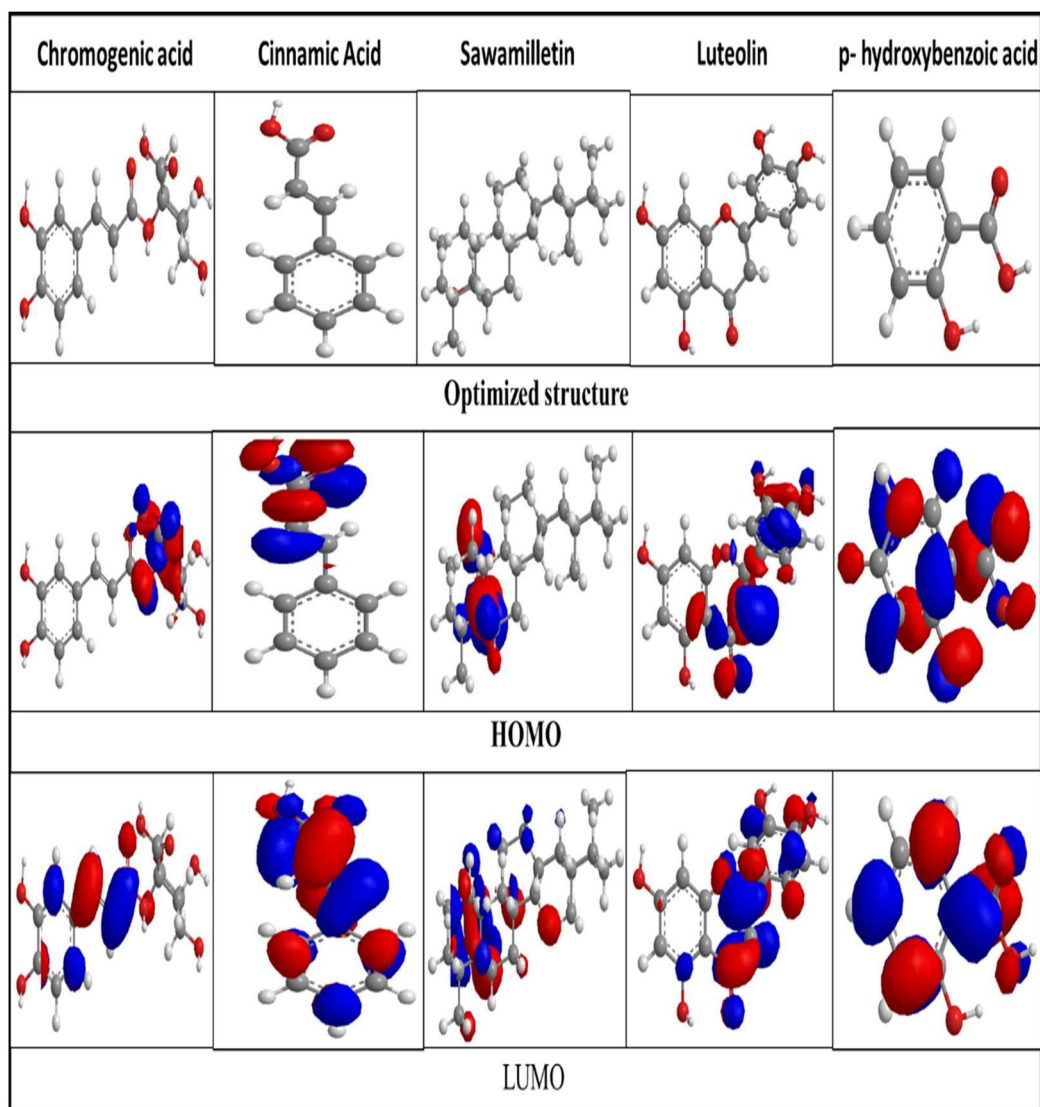


Figure 4.5.7: Optimized structures, HOMO and LUMO of phytochemicals present in *S. officinarum* extract.

Table 4.5.2: Calculated quantum chemical parameters of phytochemicals of *S. officinarum* extract.

S.No	Phytochemicals	E <sub>HOMO</sub> (eV)	E <sub>LUMO</sub> (eV)	ΔE (eV)
1	Chromogenic acid	-10.97	-4.71	6.27
2	Cinnamic Acid	-12.56	-1.70	10.86
3	Sawamilletin	-1.66	21.85	23.51
4	Luteolin	-10.01	-4.04	5.97
5	p- hydroxybenzoic acid	-12.45	-3.65	8.8

#### 4.6 *Beta vulgaris*

*B. vulgaris* is a root vegetable commonly known as red beet. *B. vulgaris* belongs to the family of Amaranthaceae [251] The *B. vulgaris* residues contain various types of phytochemicals as mentioned in figure 4.6.1[252].The main aim of this study is to investigate the use of *B. vulgaris* peel as corrosion inhibitor. Main focus is on exploring the adsorptive and anticorrosion properties of *Beta vulgaris*.

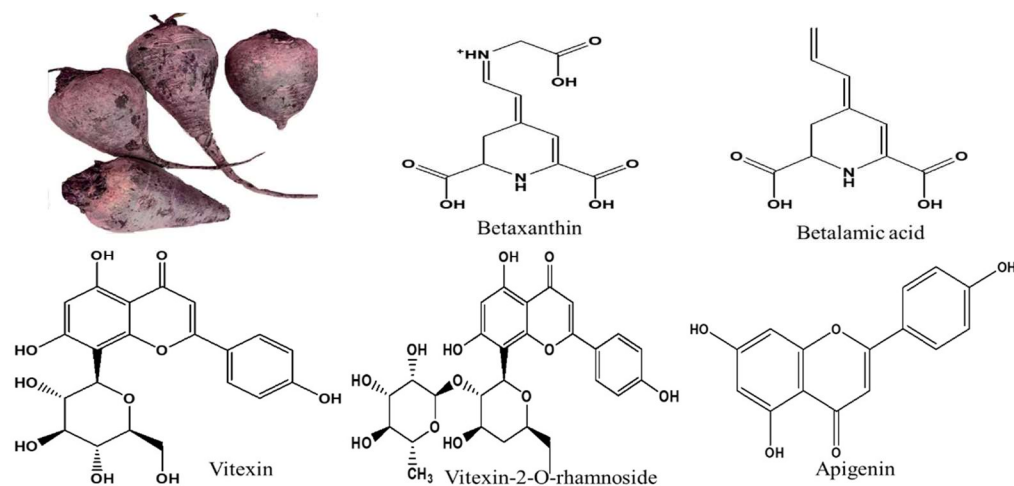


Figure 4.6.1: (a) *B. vulgaris* plant (b – f) molecular structure of phytochemicals present in *B. vulgaris*

#### 4.6.1 FTIR analysis of *B. vulgaris*

FTIR spectrum was used to identify the possible phytochemicals present in *B. vulgaris* extract and is shown in Fig. 4.6.2. The peaks were seen at 3462.33, 3174.93, 2897.17, 2715.86, 2366.73, 1645.33, 1259.55, 1103.31 and 945.15  $\text{cm}^{-1}$ . The peak observed at 3462.33 and 3174.93  $\text{cm}^{-1}$  are due to stretching of OH group from alcohol and phenol (hydrogen bonded), the characteristic peak observed at 2897.17, 2715.86 and 2366.73  $\text{cm}^{-1}$  are attributed to stretching of C-H of alkanes, the peak observed at 1645.33  $\text{cm}^{-1}$  is assigned to the stretching of C=O of carbonyl group. The peaks observed at 1259.55 and 1103.31  $\text{cm}^{-1}$  are assigned to the C-O bonding (alcohols, esters, carboxylic acids). The peak observed at 945.15  $\text{cm}^{-1}$  is attributed to the presence of bending of C-H group of alkanes. These phytochemicals present in the peel extract of *B. vulgaris* extract contains heteroatoms which are adsorbed on the steel surface and forms bonds with the  $\text{Fe}^{2+}$  ions present on the steel surface and act as potent corrosion inhibitors [252-255].

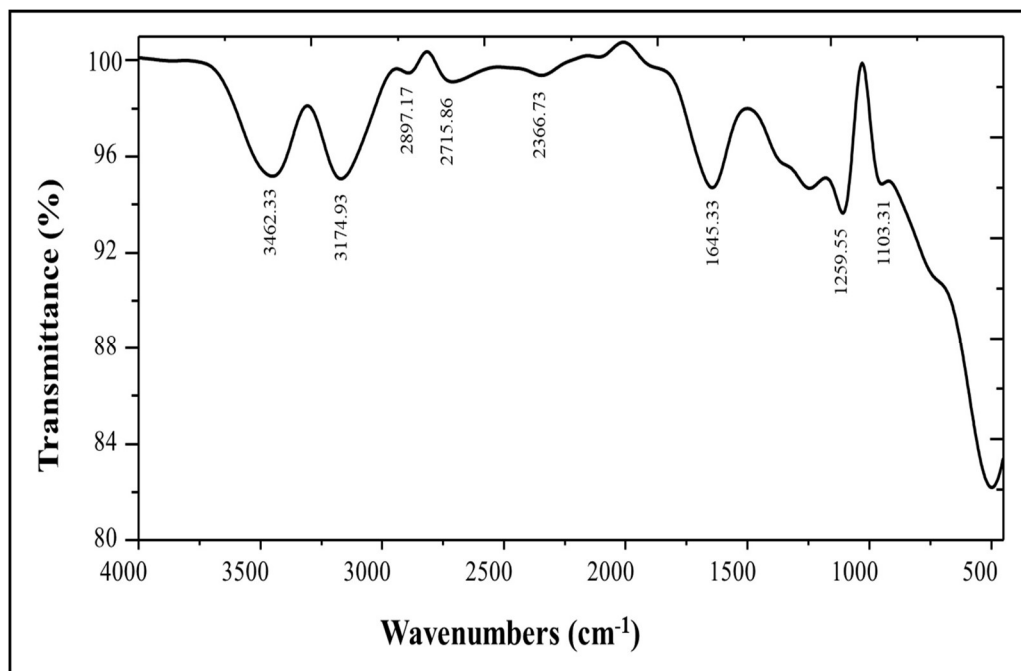


Figure 4.6.2: FT-IR spectra of *B. vulgaris* extract.

#### 4.6.2 UV visible spectroscopic study

The UV- visible spectra of *B. vulgaris* extract dissolved in 15% HCl before and after immersion of S.S.-410 specimen is shown in Fig. 4.6.3. The presence of adsorption peaks at 276.5 nm representing  $n - \pi^*$  transition. The solution in which S.S.-410 samples were not immersed show higher peak absorbance with respect to the solution in which steel samples were immersed and further there was shift in the value of adsorption maxima in latter samples. The phytochemicals from the plant extract leads to the shift in absorption wavelength and lower adsorption peak intensity of steel sample exposed acidic solution indicating the adsorption on the surface of S.S.-410 and the formation of bonds between the  $Fe^{2+}$  particles of steel and plant extract molecules. So, when S.S.-410 specimen is immersed in the 15% HCl solution containing plant extract, the molecules get absorb on the surface of S.S.-410 and make complexes with the surface atoms of substrate surface thus slow down the corrosion process and act as good corrosion inhibitors [202-204].

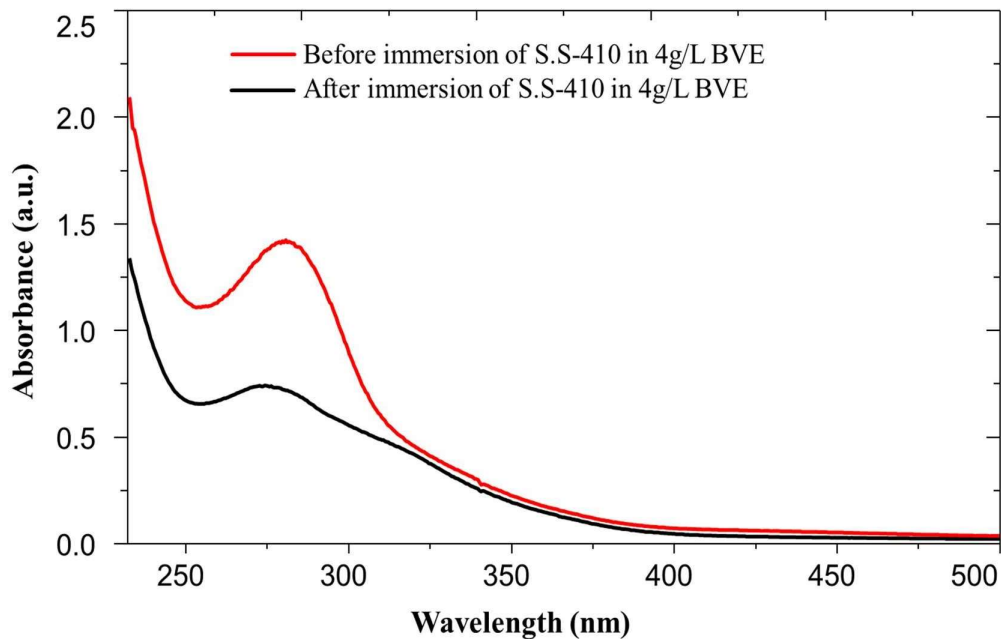


Figure 4.6.3: UV-visible spectra of *B. vulgaris* extract (BVE).

#### 4.6.3 Weight loss and electrochemical Study

The corrosion inhibition efficiency of *B. vulgaris* extract extract for S.S.-410 in 15% HCl solution were obtained by using weight loss, and electrochemical measurements



(Tafel and EIS) at various concentrations (1-4 g/L) at 298K. All the key parameters have been mentioned in table 4.6.1. As the concentration of *B. vulgaris* extract increases, the value of corrosion rate decreases in weight loss measurement, thus leading to increase in corrosion inhibition efficiency. The decrease in value of corrosion rate is due to adsorption of *B. vulgaris* extract phytochemicals on the surface of SS-410. Maximum 90.90 % corrosion inhibition efficiency was obtained using 4 g/L *B. vulgaris* extract. The linear correlation coefficients 0.9944 was near to 1, which confirms the adsorption of *B. vulgaris* extract obeys Langmuir adsorption isotherm (Figure 4.6.4) [205].

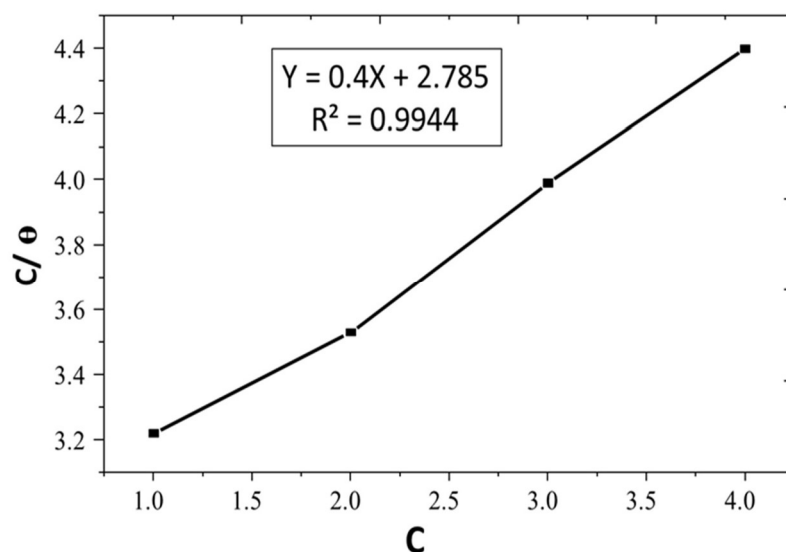


Figure 4.6.4: Langmuir adsorption isotherm of *B. vulgaris* extract with the of weight loss measurements.

Therefore, *B. vulgaris* extract has mixed type of inhibition behavior. From the potentiodynamic polarization, 90.17 % corrosion inhibition efficiency was recorded at concentration of 4 g/L *B. vulgaris* extract in 15% HCl solution (Figure 4.6.5(a)) [208]. A maximum 85.77 % corrosion inhibition efficiency was as shown in electrochemical impedance plot (Figure 4.6.5(b)). A layer formation was proven from the Rct value that increases with increases the *B. vulgaris* extract concentration [209]. The Bode plot has been shown in (Figure 4.6.5(c)) the *B. vulgaris* get adsorbed on the surface of SS-410 by involving  $\pi$  electrons of its aromatic ring or the hetero atoms from the plant extract

with the free electrons of vacant d-orbital of iron from steel. This process leads to efficient anti-corrosive property of *B. vulgaris*. The Bode plot support iron *B. vulgaris* get adsorbed on the surface of SS-10. This process leads to efficient anticorrosive property of *B. vulgaris* [210-211]. The presence of inhibitors shows the process of charge transfer resistance which started on the interface between electrode and electrolyte as clear from phase angles graph is shown in Figure (4.6.5(d)). The inhibition was due to the adsorption of phytochemicals on the surface of steel and a protective film is formed. The increment in the values of phase angle with the presence of increasing concentration of *B. vulgaris* can be attributed to a decrease in the capacitance at the surface of steel which makes the steel surface less prone to dissolution in the presence of corrosive media [212].

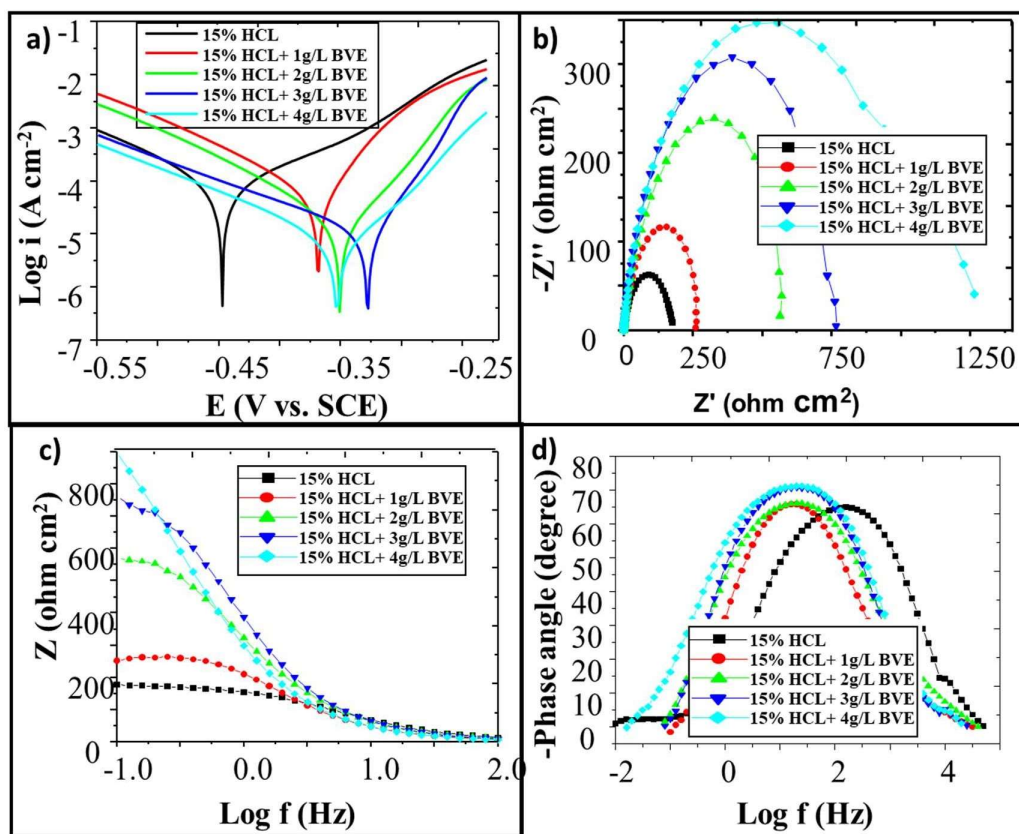


Figure 4.6.5: (a) Potentiodynamic polarization plot (b) Electrochemical impedance plot (c) Bode plot (d) Phase angle plot for different concentration of *B. vulgaris* extract (BVE).

Table 4.6.1: Corrosion parameters from weight loss, and electrochemical experiments for S.S.-410 in 15% HCl with different concentrations of *B. vulgaris* extract (BVE).

Weight loss			PDP			EIS	
C (g/L)	C <sub>R</sub> (mmy <sup>-1</sup> )	I.E. (%)	E <sub>corr</sub> (mV vs. SCE)	I <sub>corr</sub> (A cm <sup>-2</sup> )	I.E. (%)	R <sub>ct</sub> (Ω cm <sup>2</sup> )	I.E. (%)
15% HCl	39.01		-474.1	0.000054003		180.21	
15% HCl + 1 g/L BVE	26.897	31.05	-368.04	0.0000338652	37.29	259.28	30.49
15% HCl + 2 g/L BVE	16.910	56.65	-351.01	0.0000247387	54.19	566.19	50.29
15% HCl + 3 g/L BVE	9.682	75.18	-327.91	0.0000108924	79.83	767.41	76.51
15% HCl + 4 g/L BVE	3.549	90.90	-353.24	0.0000053084	90.17	1266.49	85.77

#### 4.6.4 SEM and AFM analysis

The SEM and AFM micrographs of the S.S.-410, S.S.-410 immersed in 15% HCl and S.S.-410 immersed in 15% HCl solution in the presence of *B. vulgaris* extract are shown in Figure 4.6.6. SEM of S.S.- 410 coupons after 24 h immersion in 15 % HCl solution at 298 K shows a severely harmed surface. From AFM studies, the average surface roughness for abraded S.S.- 410 is 26.83 nm and for S.S.- 410 immersed in 15 % HCl, AFM micrographs of the average surface roughness is 939.14 nm. The surface of steel sample which is immersed in acid solution with the presence of *B. vulgaris* extract show very less roughness as comparative smooth surface with respect to S.S.-410 immersed in only 15% HCl solution. The surface of S.S.-410 sample exposed to acid solution in the presence of *B. vulgaris* extract show average surface roughness value of 310.14 nm

through AFM, which is very less as compared to roughness value of steel immersed in only 15% HCl solution. This change in surface morphology is attributed to the adsorption of some molecules from the *B. vulgaris* extract on the steel surface which act as corrosion inhibitor by forming a protective layer on the steel surface and thus prevents corrosion. The mentioned SEM and AFM micrograph have been compared with SEM and AFM micrograph of S.S.-410 immersed in 15% HCl solution [218-222].

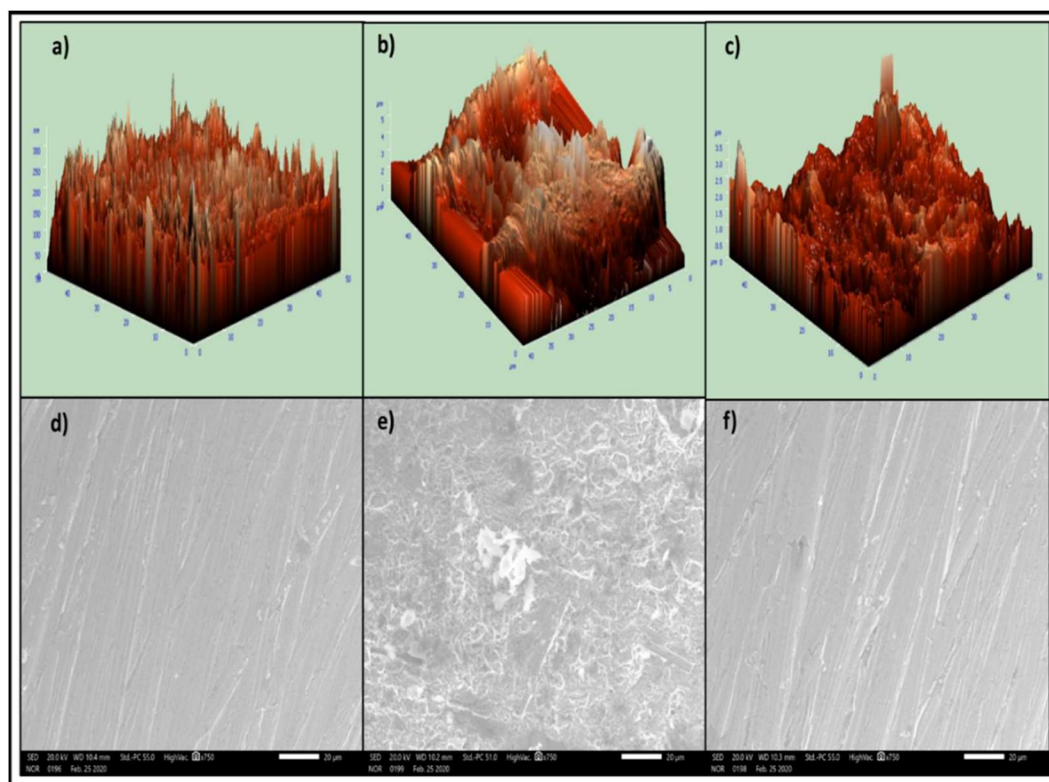


Figure 4.6.6: (a) AFM micrographs of S.S.-410 (b) AFM micrographs of S.S.-410 immersed in 15% HCl solution (c) AFM micrographs of S.S.-410 immersed in 15% HCl solution with *B. vulgaris* extract (d) SEM micrographs of S.S.-410 (e) SEM micrographs of S.S.-410 immersed in 15% HCl solution (f) SEM micrographs of S.S.-410 immersed in 15% HCl solution with *B. vulgaris* extract.

#### 4.6.5. Quantum Chemical Calculations

The frontier molecular orbital density distributions (LUMO and HOMO) with optimum structures of phytochemicals presents in *B. vulgaris* were shown in Fig. 4.6.7.  $E_{HOMO}$ ,  $E_{LUMO}$  and  $\Delta E$  are the key parameters of quantum chemical calculations have been

mentioned in table 4.6.2 [218-222]. The energy gap of molecular orbital follows the order: Vitexin < Betaxanthin < Betalamic acid < Vitexin-2-O-rhamnoside < Apigenin. Hence, the inhibition effect follows the order Vitexin > Betaxanthin > Betalamic acid > Vitexin-2-O-rhamnoside > pigenin. So, Vitexin can be assumed to be the most essential phytochemical in the corrosion inhibition behaviour of the *Beta vulgaris*.

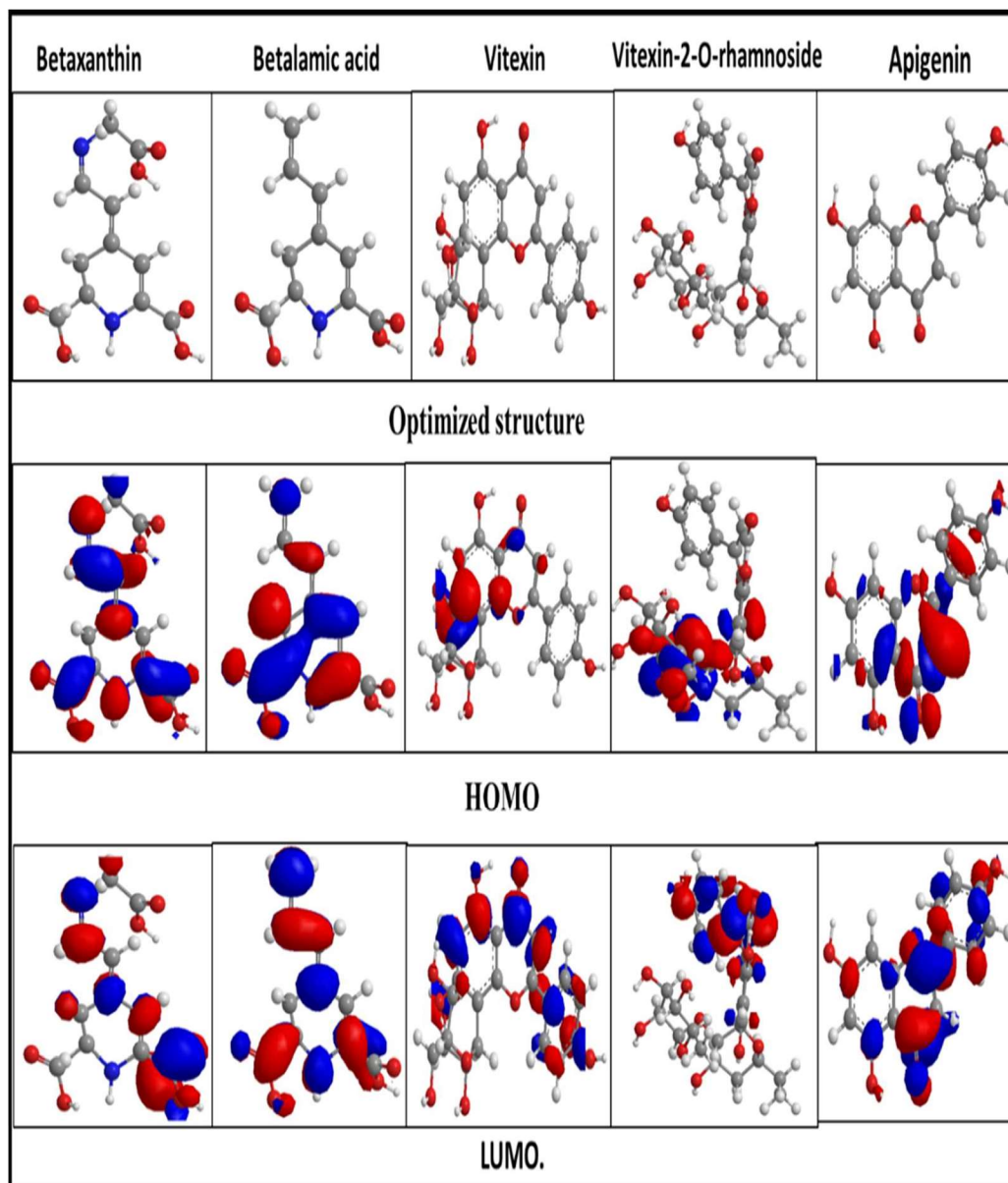


Figure 4.6.7: Optimized structures, HOMO and LUMO of phytochemicals present in *B. vulgaris* extract.

Table 4.6.2: Calculated quantum chemical parameters of phytochemicals of *B. vulgaris* extract.

S.No	Phytochemicals	E <sub>HOMO</sub> (eV)	E <sub>LUMO</sub> (eV)	ΔE (eV)
1	Betaxanthin	-2.55	-0.13	2.42
2	Betalamic acid	-5.53	-2.82	2.71
3	Vitexin	-1.05	0.56	1.61
4	Vitexin-2-O-rhamnoside	-9.60	-4.13	5.47
5	Apigenin	-10.15	-3.79	6.36

#### 4.7 *Phyllanthus emblica*

*P. emblica* a genetically diverse genus with 25–30 species of deciduous flowering plants belongs to Salicaceae family [256]. *P. emblica* is commonly known as Ambla in India. The *P. emblica* residues contain various types of phytochemicals namely, lignins, flavonoids, anthocyanins, salicylate-like phenolic glycosides (PGs), and tannins [257-259]. Till now there is no report present in literature on corrosion inhibition application of *P. emblica* extract. The major phytochemicals present in *P. emblica* as mentioned in figure 4.7.1

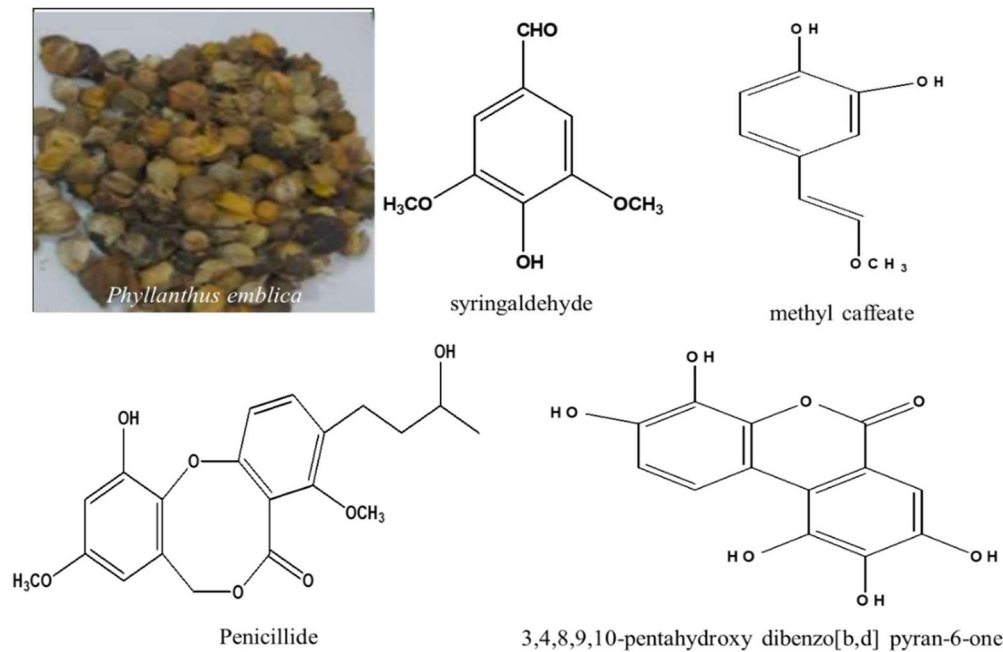


Figure 4.7.1: (a) *P. emblica* plant (b – e) molecular structure of phytochemicals present in *P. emblica* extract.

#### 4.7.1 FTIR analysis of *P. emblica*

FTIR spectrum was used to identify the possible phytochemicals present in *P. emblica* extract and is shown in Fig. 4.7.2. The peaks were seen at 3240.51, 2995.55, 2806.52, 1637.61, 1400.36, 1022.30 and 771.55  $\text{cm}^{-1}$ . The peak observed at 3240.51  $\text{cm}^{-1}$  is due to stretching of OH group from alcohol and phenol (hydrogen bonded), the characteristic peak observed at 2995.55 and 2806.52  $\text{cm}^{-1}$  are attributed to stretching of C-H of alkanes. The peaks observed at 1022.30  $\text{cm}^{-1}$  is assigned to the C-O bonding (alcohols, esters, carboxylic acids). The peak observed at 771.55  $\text{cm}^{-1}$  is attributed to the presence of bending of C-H group of alkanes. These phytochemicals present in the peel extract of *P. emblica* extract contains heteroatoms which are adsorbed on the steel surface and forms bonds with the  $\text{Fe}^{2+}$  ions present on the steel surface and act as potent corrosion inhibitors [260-262].

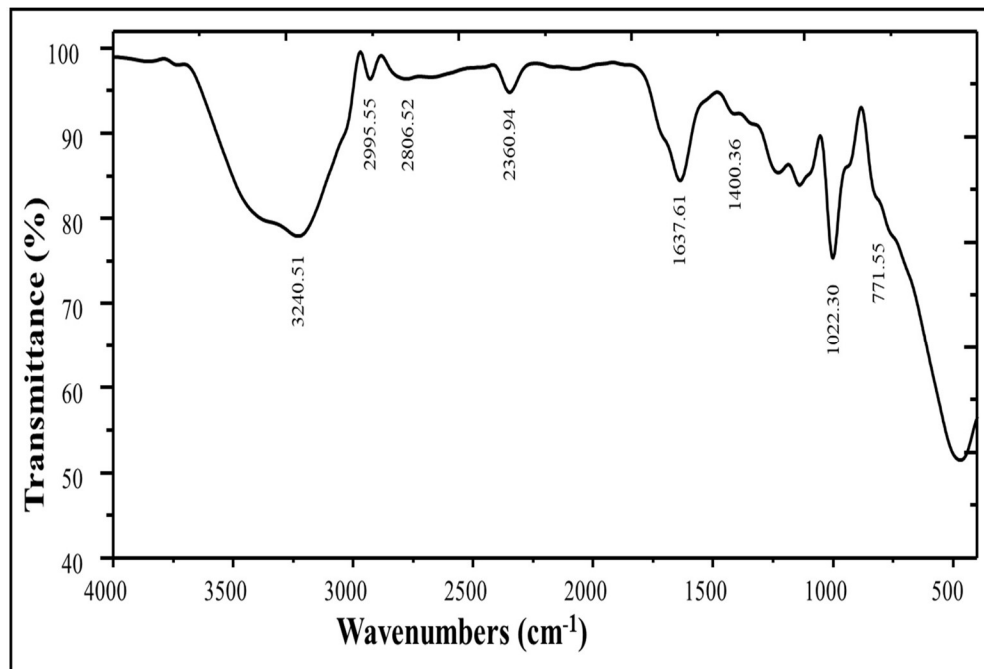


Figure 4.7.2: FT-IR spectra of *P. embelica* extract.

#### 4.7.2 UV visible spectroscopic study

The UV- visible spectra of *P. embelica* extract dissolved in 15% HCl before and after immersion of S.S.-410 specimen is shown in Fig. 4.7.3. The presence of adsorption peaks at 212 and 285 nm representing  $\pi - \pi^*$  and  $n - \pi^*$  transition. The solution in which SS-410 samples were not immersed show higher peak absorbance with respect to the solution in which steel samples were immersed and further there was shift in the value of adsorption maxima in latter samples. The phytochemicals from the plant extract leads to the shift in absorption wavelength and lower adsorption peak intensity of steel sample exposed acidic solution indicating the adsorption on the surface of S.S.-410 and the formation of bonds between the  $Fe^{2+}$  particles of steel and plant extract molecules. So, when S.S.-410 specimen is immersed in the 15% HCl solution containing plant extract, the molecules get absorb on the surface of S.S.-410 and make complexes with the surface atoms of substrate surface thus slow down the corrosion process and act as good corrosion inhibitors [202-204].



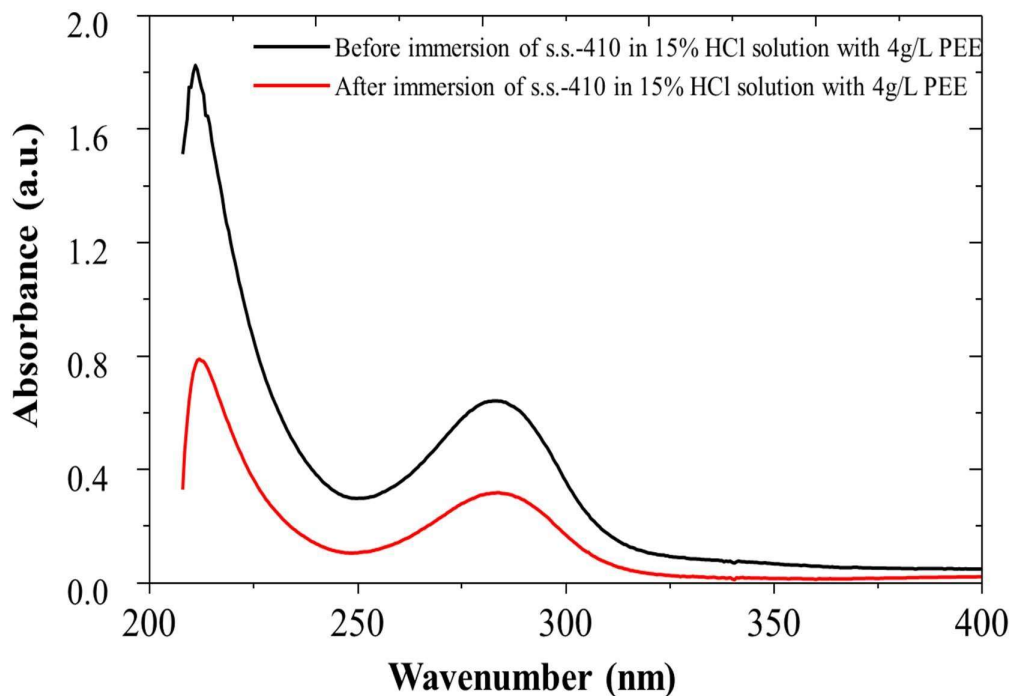


Figure 4.7.3: UV-visible spectra of *P. emblica* extract (PEE).

#### 4.7.3 Weight loss and electrochemical Study

The corrosion inhibition efficiency of *P. emblica* extract for S.S.-410 in 15% HCl solution were obtained by using weight loss, and electrochemical measurements (Tafel and EIS) at various concentrations (1-4 g/L) at 298K. All the key parameters have been mentioned in table 4.7.1. As the concentration of *P. emblica* extract increases, the value of corrosion rate decreases in weight loss measurement, thus leading to increase in corrosion inhibition efficiency. The decrease in value of corrosion rate is due to adsorption of *P. emblica* extract phytochemicals on the surface of SS-410. Maximum 89.28 % corrosion inhibition efficiency was obtained using 4 g/L *P. emblica* extract. The linear correlation coefficients 0.9938 was near to 1, which confirms the adsorption of *P. emblica* extract obeys Langmuir adsorption isotherm (Figure 4.6.4) [205].

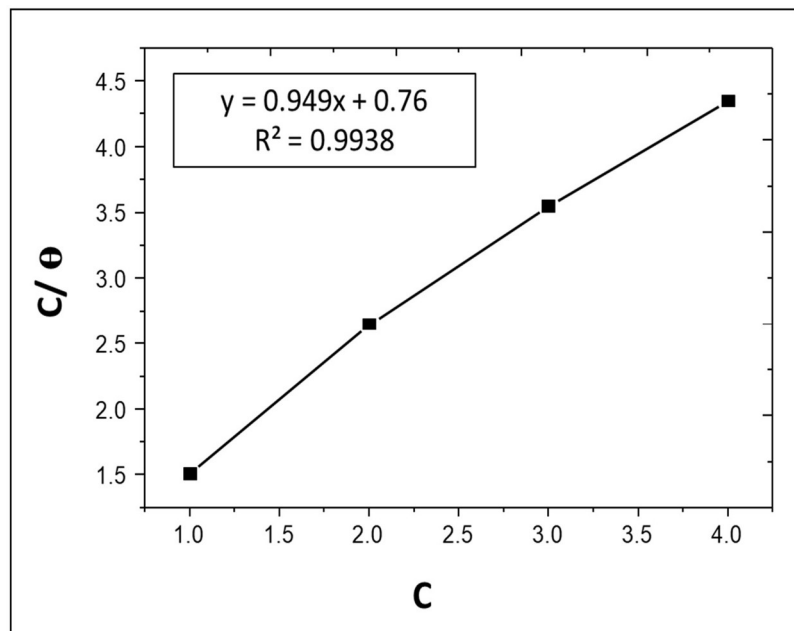


Figure 4.7.4: Langmuir adsorption isotherm of *P. emblica* extract with the of weight loss measurements.

So, *P. emblica* is extract has mixed type of inhibition behavior. From the potentiodynamic polarization, 90.08 % corrosion inhibition efficiency was recorded at concentration of 4 g/L *P. emblica* extract in 15% HCl solution (Figure 4.7.5(a)) [208]. A maximum 89.28 % corrosion inhibition efficiency was as shown in electrochemical impedance plot (Figure 4.7.5(b)). A layer formation was proven from the Rct value that increases with increases the *P. emblica* extract concentration [209]. The Bode plot has been shown in (Figure 4.7.5(c)) the *P. emblica* get adsorbed on the surface of SS-410 by involving  $\pi$  electrons of its aromatic ring or the hetero atoms from the plant extract with the free electrons of vacant d-orbital of iron from steel. This process leads to efficient anti-corrosive property of *P. emblica*. The Bode plot support iron *P. emblica* get adsorbed on the surface of SS-410. This process leads to efficient anticorrosive property of *P. emblica* [210-211].

The presence of inhibitors shows the process of charge transfer resistance which started on the interface between electrode and electrolyte as clear from phase angles graph is shown in Figure (4.7.5(d)). The inhibition was due to the adsorption of phytochemicals on the surface of steel and a protective film is formed. The increment in the values of

phase angle with the presence of increasing concentration of *P. emblica* can be attributed to a decrease in the capacitance at the surface of steel which makes the steel surface less prone to dissolution in the presence of corrosive media [212].

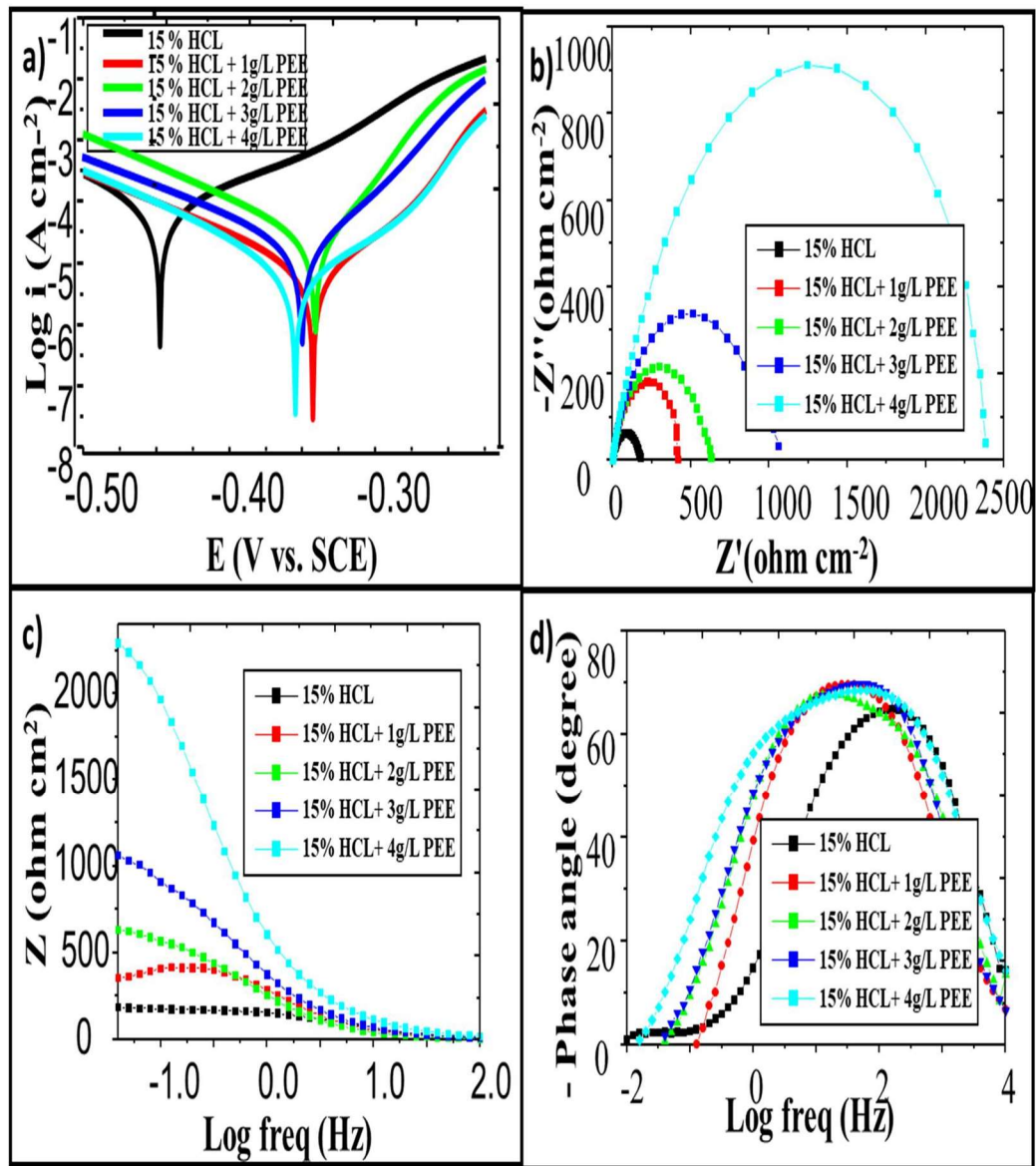


Figure 4.7.5: (a) Potentiodynamic polarization plot (b) Electrochemical impedance plot (c) Bode plot (d) Phase angle plot for different concentration of *P. emblica* extract (PEE).

Table 4.7.1: Corrosion parameters from weight loss, and electrochemical experiments for S.S.-410 in 15% HCl with different concentrations of *P. embelica* extract (PEE).

Weight loss			PDP			EIS	
C (g/L)	C <sub>R</sub> (mmy <sup>-1</sup> )	I.E. (%)	E <sub>corr</sub> (mV vs. SCE)	I <sub>corr</sub> (A cm <sup>-2</sup> )	I.E. (%)	R <sub>ct</sub> (Ω cm <sup>2</sup> )	I.E. (%)
15% HCl	39.01		-474.1	0.000054003		180.21	
15% HCl + 1 g/L PEE	14.9330	61.72	-342.55	0.000027734	48.64	418.79	57.04
15% HCl + 2 g/L PEE	10.7433	72.46	-340.57	0.000021826	59.58	630.30	71.40
15% HCl + 3 g/L PEE	7.1232	81.74	-349.58	0.000011324	79.03	1067.34	83.11
15% HCl + 4 g/L PEE	4.1818	89.28	-354.44	0.000004956	90.08	2381.02	92.43

#### 4.7.4 SEM and AFM analysis

The SEM and AFM micrographs of the S.S.-410, S.S.-410 immersed in 15% HCl and S.S.-410 immersed in 15% HCl solution in the presence of *P. embelica* extract are shown in Figure 4.6.6. SEM of S.S.- 410 coupons after 24 h immersion in 15 % HCl solution at 298 K shows a severely harmed surface. From AFM studies, the average surface roughness for abraded S.S.- 410 is 26.83 nm and for S.S.- 410 immersed in 15 % HCl, AFM micrographs of the average surface roughness is 939.14 nm. The surface of steel sample which is immersed in acid solution with the presence of *P. embelica* extract show very less roughness as comparative smooth surface with respect to S.S.-410 immersed in only 15% HCl solution. The surface of S.S.-410 sample exposed to acid solution in the presence of

*P. embelica* extract show average surface roughness value of 338.24 nm through AFM, which is very less as compared to roughness value of steel immersed in only 15% HCl solution. This change in surface morphology is attributed to the adsorption of some molecules from the *P. embelica* extract on the steel surface which act as corrosion inhibitor by forming a protective layer on the steel surface and thus prevents corrosion. The mentioned SEM and AFM micrograph have been compared with SEM and AFM micrograph of S.S.-410 immersed in 15% HCl solution [213-217].

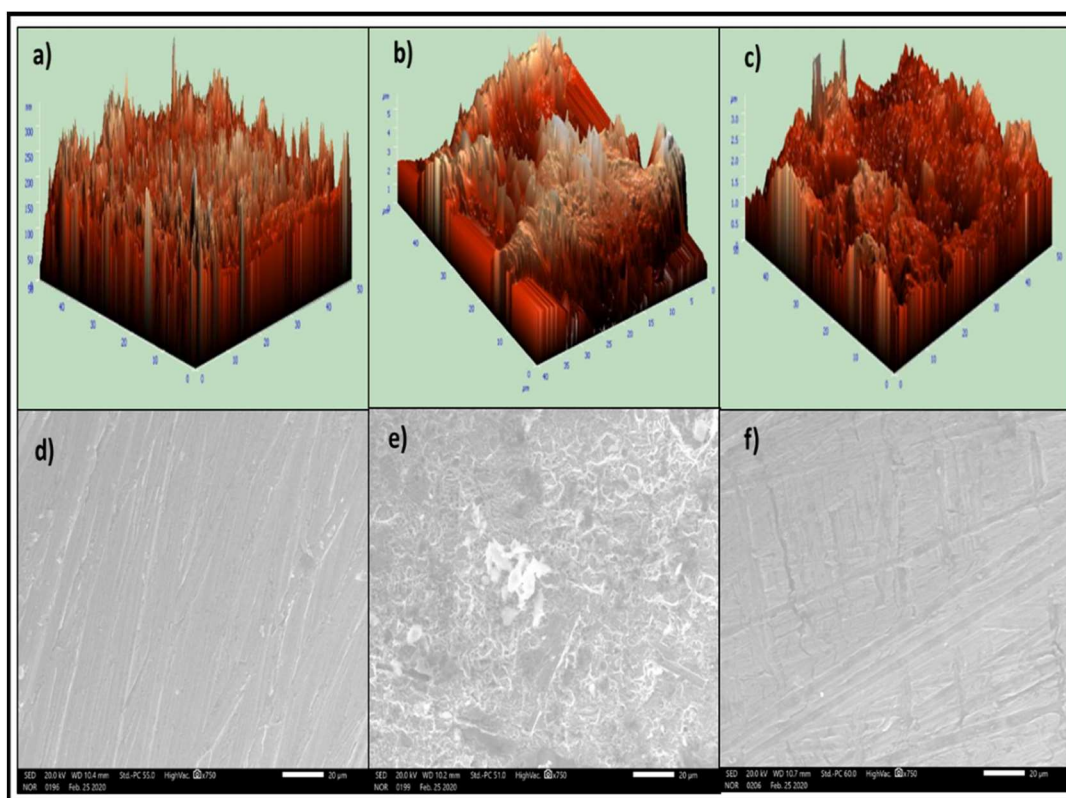


Figure 4.7.6: (a) AFM micrographs of S.S.-410 (b) AFM micrographs of S.S.-410 immersed in 15% HCl solution (c) AFM micrographs of S.S.-410 immersed in 15% HCl solution with *P. embelica* extract (d) SEM micrographs of S.S.-410 (e) SEM micrographs of S.S.-410 immersed in 15% HCl solution (f) SEM micrographs of S.S.-410 immersed in 15% HCl solution with *P. embelica* extract.

#### 4.7.5 Quantum Chemical Calculations

The frontier molecular orbital density distributions (LUMO and HOMO) with optimum structures of phytochemicals presents in *P. embelica* were shown in Fig. 4.7.7.  $E_{\text{HOMO}}$ ,

$E_{LUMO}$  and  $\Delta E$  are the key parameters of quantum chemical calculations have been mentioned in table 4.7.2 [218-222]. The energy gap of molecular orbital follows the order: 3,4,8,9,10-pentahydroxy-dibenzo[b,d] pyran-6-one < Syringaldehyde < methyl caffeate < Penicillide. So, 3,4,8,9,10-pentahydroxy-dibenzo[b,d] pyran-6-one. Hence, the inhibition effect follows the order 3,4,8,9,10-pentahydroxy-dibenzo[b,d] pyran-6-one >Syringaldehyde >methyl caffeate>Penicillide. So, 3,4,8,9,10-pentahydroxy-dibenzo[b,d] pyran-6-one can be assumed to be the most essential phytochemical in the corrosion inhibition behaviour of the *P. embelica*.

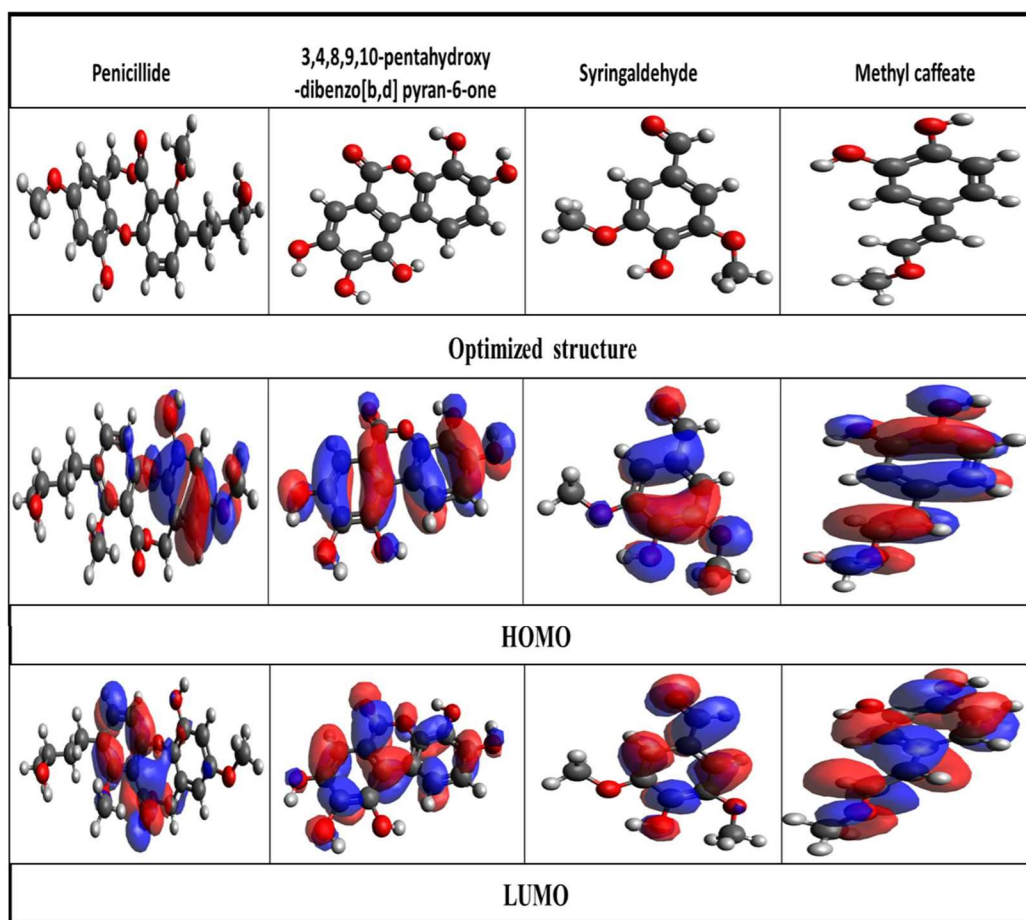


Figure 4.7.7: Optimized structures, HOMO and LUMO of phytochemicals present in *P. embelica* extract.

Table 4.7.2: Calculated quantum chemical parameters of phytochemicals of *P. embelica* extract.

S. No	Phytochemicals	E <sub>HOMO</sub> (eV)	E <sub>LUMO</sub> (eV)	ΔE (eV)
1	Penicillide	-5.709	-1.008	4.701
2	3,4,8,9,10-pentahydroxy-dibenzo[b,d] pyran-6-one	-5.57	-1.335	4.235
3	Syringaldehyde	-5.696	-1.239	4.457
4	methyl caffeate	-4.879	-0.217	4.662

#### 4.8 Comparative study

Table 4.8.1 shows the comparative corrosion rate and inhibition efficiency of pre-coated SS without and with the existing synthetic paints and selected inhibitors. Paint coated SS of synthetic paint sample 1 and 2 along with the selected natural inhibitor have been used as a coating material. Here, inhibitor samples were coated on the SS surface and then weight loss experiments were carried out.

As per the Table 4.8.1, it is very clear that there is a small difference in inhibition efficiency between the synthetic paint samples and selected natural extracts at the same concentration and environment. The advances to use the natural extract as a green inhibitor are; 1) Natural products are eco-friendly and non-hazardous to the environment as well as for the human being. 2) Convert waste products to a useful material with negligible production cost.

Table 4.8: Inhibition efficiency and corrosion rate of the paint-coated S.S.-410 without and with selected inhibitors

S. No.	Sample	C <sub>R</sub> (mmy <sup>-1</sup> )	IE (%)
1	15% HCl Solution	39.01	-
2	Synthetic paint sample 1	1.62	95.84
3	Synthetic paint sample 2	1.68	95.69
4	<i>Oryza Sativa</i>	3.15	91.92
5	<i>P. tremula</i>	2.87	92.64
6	<i>Triticum aestivum</i>	3.14	91.95
7	<i>B. nigra</i>	3.24	91.69
8	<i>Saccharum officinarum</i>	1.59	95.92
9	<i>Beta vulgaris</i>	3.54	90.90
10	<i>Phyllanthus embelica</i>	4.18	89.28



## CHAPTER 05: SUMMARY AND CONCLUSION

### 5.1 Summary

The present study aimed at investigation of corrosion restraint effectiveness of some inhibitors for S.S.-410 in HCl solution. The FTIR spectrum for the pure inhibitors indicates the presence of various functional groups. These groups contain various heteroatoms like oxygen, nitrogen, etc. along with conjugated systems. These can easily donate their non-bonding electrons to the metal and can create coordination bonds or electrostatic interaction is also possible.

UV-visible spectroscopy indicates adsorption of active molecules of the plant extract on the S.S.-410 surface. The EIS techniques showed all the selected plant extracts have been found to act as excellent corrosion inhibitors for S.S.-410 in acidic media.

Weight loss analysis studies revealed that there is an increase in inhibition efficiency by increasing inhibitor concentration. The increase in inhibition efficiency occurred as a result of the development of a defensive layer that decreases the corrosion procedure. The slope and correlation coefficient of straight line obtained by plotting  $C/\theta$  against  $C$  comes near unity, suggesting that the inhibitors obey the Langmuir adsorption isotherm and form a mono-layer on the S.S.-410 surface.

The inhibition efficiency increases as the concentration of the inhibitor increases and corrosion potential values indicated the mixed type of inhibition. The Tafel slope values have been found to be irregular indicating the inhibitory effect of all inhibitors is not only due to the adsorption alone but due to the mixed effect of blocking of active sites by the involvement of some other anions present in the solution.

In EIS, there is a remarkable increase in the diameter of the semicircle in the presence of inhibitors in comparison to the only acid solution. The higher charge transfer resistance values in the presence of inhibitors in aggressive acidic solution indicated the formation of protective layer of inhibitor molecules on the S.S.-410 surface. The inhibition efficiencies obtained from EIS are in agreement with those obtained from the PDP technique.

In SEM studies, the corrosion is maximum in the acidic media (blank) and shows

badly damaged surface of the S.S.-410. Significant reduction in corrosion is observed in the presence of all the inhibitors and shows remarkably improved surface of the S.S.-410.

AFM analysis revealed deterioration over the surface of S.S.-410 in acidic media leading to rough surface. The surface roughness parameters were found to be significantly lower in the presence of tested plant extract inhibitors, which confirmed that all the selected inhibitors as excellent corrosion inhibitors.

Comparative studies have been carried out to between some existing synthetic paints and selected plants (*Oryza sativa*, *Populus tremula*, *Triticum aestivum*, *Brassica nigra*, *Saccharum officinarum*, *Beta vulgaris* and *Phyllanthus emblica*) extract. There was a small differences in the inhibition efficiency between the synthetic paint sample and selected plants extract. The advances to use the natural extract as a green inhibitor are: 1) Natural products are eco-friendly and non-hazardous to the environment as well as to the human being; 2) Using waste materials as a useful material with negligible production cost.

## **5.2 Conclusion**

Corrosion is referred to as the deterioration of materials and its properties change by chemical process as well as by interaction with environmental conditions. Corrosion has a significant impact on infrastructure, utilities, transport and other critical sectors of the society. With the dynamic progress in the science and technology, researches developed better criteria of corrosion mitigation that behaves best as inhibitors, make corrosion resistant alloys so that materials can last for much longer time. The use of natural inhibitors in the deterrence of corrosion has proved to be an extremely effective, eco-friendly and economically viable option. Thus, the present work has been under taken to study the influence of selected plant extract for inhibiting the corrosion of S.S.-410 in HCl solution.

The selected plant extracts have been characterized as corrosion resisting agents for S.S.-410 in 15% HCl at different concentration. The effectiveness of these compounds was investigated with the help of weight-loss, temperature and kinetic studies, potentiodynamic polarization and electrochemical impedance spectroscopic

techniques. The outcomes of above studies were supplemented by FTIR, UV-vis., SEM, AFM and DFT method

### 5.3 Scope for future work

The inhibitors studied here are good inhibitors for protection of the S.S.-410 in HCl solution. They may be tried for other metals in acid solutions. The inhibitors may be applied for corrosion inhibition of other metals in different corrosive media other than acids.

**List of publications: (Citations: 126, h-index: 7, i10-index: 5 as per the Google scholar on October, 2021)**

#### A. Published articles:

- [1] **Bhardwaj, N., Sharma, P., Guo, L., Dagdag, O., & Kumar, V. (2021).** Molecular dynamic simulation and quantum chemical calculation of phytochemicals present in *Beta vulgaris* and electrochemical behaviour of Beta vulgaris peel extract as green corrosion inhibitor for stainless steel (SS-410) in acidic medium. *Colloids and Surfaces A: Physicochemical and Engineering Aspects*. **(Accepted)**
- [2] **Bhardwaj, N., Sharma, P., & Kumar, V. (2021).** *Triticum aestivum* Extract as Corrosion Inhibitor for Stainless Steel (SS-410) In Acidic Media: Experimental and Theoretical Study. *Current Research in Green and Sustainable Chemistry*. **(Accepted)**
- [3] **Bhardwaj, N., Sharma, P., & Kumar, V. (2021).** *O. sativa* plant extract as green Corrosion Inhibitor in 15 % hydrochloric acid for stainless steel-410 surface. *Tenside Surfactants Detergents*. **(Accepted)**
- [4] **Bhardwaj, N., Sharma, P., & Kumar, V. (2021).** Corrosion inhibition property and adsorption behaviour of *P. tremula* leaf extract in acidic media for steel used in petroleum industry (S.S.- 410). *Protection of Metals and Physical Chemistry of Surfaces*. **(Accepted)**
- [5] **Bhardwaj, N., Sharma, P., Singh, K., Rana, D., & Kumar, V. (2021).** *Phyllanthus emblica* seed extract as corrosion inhibitor for stainless steel used in petroleum industry (SS-410) in acidic medium. *Chemical Physics Impact*.3, 100038.
- [6] **Bhardwaj, N., Sharma, P., & Kumar, V. (2021).** Anti-corrosive behaviour of *S. officinarum* plant extract in 15 % hydrochloric acid for stainless steel-410 surface.

*Asian Journal of chemistry*, 33(6),1389-1395

- [7] **Bhardwaj, N.**, Sharma, P., & Kumar, V. (2021). Phytochemicals as steel corrosion inhibitor: an insight into mechanism. *Corrosion Reviews*, 39(1), 27-41.
- [8] Sharma, P. **Bhardwaj, N.**, & Kumar, V., (2021). “*Swertia chirata* extract mediated synthesis of iron oxide nanoparticles and its use as corrosion inhibitor for stainless steel 316 L in Ringer’s solution” *Advances in Natural Sciences: Nano science and Nanotechnology (Accepted)*
- [9] Sharma, P. **Bhardwaj, N.**, & Kumar, V., (2021). *Swertia chirata* extract synthesized iron oxide nanoparticles as corrosion inhibitor for ss-316 l in hank’s solution. *Asian Journal of chemistry*, 33(8), 1824-1830
- [10] Sharma, P. **Bhardwaj, N.**, & Kumar, V., (2020). Defence applications Of Nanotechnology: Development and Strategies. *European Journal of Molecular & Clinical Medicine*, 7(7), 4310-4316.
- [11] **Bhardwaj, N.**, Sharma, P., & Kumar, V. (2018). Types of corrosion due to rusting of steel used in petroleum industries: A Review. *Journal of Emerging Technology and Innovative Research*, 5(12), 503-508.
- [12] Sharma, P. **Bhardwaj, N.**, & Kumar, V. "Nanotechnology in corrosion control of biomaterials." *Journal of Emerging Technologies and Innovative Research* , vol. 5 (2018)509-513.
- [13] **Bhardwaj, N.**, Prasad, D., & Haldhar, R. (2018). Study of the *Aegle marmelos* as a green corrosion inhibitor for mild steel in acidic medium: experimental and theoretical approach. *Journal of Bio-and Tribo-Corrosion*, 4(4), 1-10.
- [14] Saxena, A., Thakur, K. K., & **Bhardwaj, N.** (2020). Electrochemical studies and surface examination of low carbon steel by applying the extract of *Musa acuminata*. *Surfaces and Interfaces*, 18, 100436.
- [15] Saxena, A., Sharma, V., Thakur, K. K., & **Bhardwaj, N.** (2020). Electrochemical studies and the surface examination of low carbon steel by applying the extract of *citrus sinensis*. *Journal of Bio-and Tribo-Corrosion*, 6(2), 1-11.
- [16] Haldhar, R., Prasad, D., & **Bhardwaj, N.** (2019). Extraction and experimental studies of *Citrus aurantifolia* as an economical and green corrosion inhibitor for mild steel in acidic media. *Journal of Adhesion Science and Technology*, 33(11),

1169-1183.

- [17] Haldhar, R., Prasad, D., & **Bhardwaj, N.** (2020). Surface adsorption and corrosion resistance performance of *Acacia concinna* pod extract: An efficient inhibitor for mild steel in acidic environment. *Arabian Journal for Science and Engineering*, 45(1), 131-141.
- [18] Haldhar, R., Prasad, D., & **Bhardwaj, N.** (2020). Experimental and theoretical evaluation of *acacia catechu* extract as a natural, economical and effective corrosion inhibitor for mild steel in an acidic environment. *Journal of Bio-and Tribo-Corrosion*, 6, 1-11.
- [19] Haldhar, R., Prasad, D., & **Bhardwaj, N.** (2020) Experimental and Theoretical Evolution of *Apium graveolens* Extract as an Eco-friendly Corrosion Inhibitor for Mild Steel in 1 M HCl Medium. *CORCON*.

#### **B. Conferences and workshop**

- [1] Oral presentation on “Tamarindus indica Seed Extract as Corrosion Inhibitor for S.S.-410(SS-410) In Acidic Media: Experimental and Theoretical Study” in the International Conference on Recent Advances in Fundamental and Applied Sciences on November 5 to 6, 2019.
- [2] Oral presentation on “Brassica nigra (L) Extract as Corrosion Inhibitor for S.S.-410(SS-410) in Acidic Media: Experimental and Theoretical Study” in the International Conference on Modern Emerging Trends: Future of Chemical Sciences on April 23 to 24, 2021.
- [3] Oral presentation on “*T natans* extract as Corrosion Inhibitor for S.S.-410(SS-410) in Acidic Media: Experimental and Theoretical Study” in International Conference on Recent Advances in Applied Sciences, Technology & Health on March 3<sup>rd</sup> & 4<sup>th</sup>, 2021
- [4] Participation in the International Conference on 106th Indian Science Conference on January 3 to 7, 2019.
- [5] National Workshop on Advanced Instrumentation at Lovely Professional University on April, 20, 2019

## Bibliography

- [1] Xie, Z. H., & Wu, L. (2020). Corrosion inhibition of layered double hydroxide coating for Mg alloy in acidic corrosive environments. *Materials and Corrosion*, 71(1), 118-124.
- [2] Baena, L. M., Gómez, M., & Calderón, J. A. (2012). Aggressiveness of a 20% bioethanol–80% gasoline mixture on autoparts: I behavior of metallic materials and evaluation of their electrochemical properties. *Fuel*, 95, 320-328.
- [3] Abdeen, D. H., El Hachach, M., Koc, M., & Atieh, M. A. (2019). A review on the corrosion behaviour of nanocoatings on metallic substrates. *Materials*, 12(2), 210.
- [4] Shifler, D. A. (2005). Understanding material interactions in marine environments to promote extended structural life. *Corrosion Science*, 47(10), 2335-2352.
- [5] Goyal, A., Pouya, H. S., Ganjian, E., & Claisse, P. (2018). A review of corrosion and protection of steel in concrete. *Arabian Journal for Science and Engineering*, 43(10), 5035-5055.

- [6] Alcántara, J., Chico, B., Simancas, J., Díaz, I., & Morcillo, M. (2017). Marine atmospheric corrosion of carbon steel: a review. *Materials*, *10*(4), 406.
- [7] Malik, M. A., Hashim, M. A., Nabi, F., Al-Thabaiti, S. A., & Khan, Z. (2011). Anti-corrosion ability of surfactants: a review. *Int. J. Electrochem. Sci*, *6*(6), 1927-1948.
- [8] Kermani, M. B., & Harrop, D. (1996). The impact of corrosion on oil and gas industry. *SPE Production & Facilities*, *11*(03), 186-190.
- [9] Koch, G. (2017). Cost of corrosion. *Trends in oil and gas corrosion research and technologies*, 3-30.
- [10] Lindell, M. K., & Prater, C. S. (2003). Assessing community impacts of natural disasters. *Natural hazards review*, *4*(4), 176-185.
- [11] Pang, J. W., & Bond, I. P. (2005). A hollow fibre reinforced polymer composite encompassing self-healing and enhanced damage visibility. *Composites Science and Technology*, *65*(11-12), 1791-1799.
- [12] De Seranno, T., Lambrechts, E., Verliefde, A. R. D., Depover, T., & Verbeke, K. (2021). Mechanistic interpretation on acidic stress-corrosion cracking of NiCrMoV steam turbine steel. *Materials Science and Engineering: A*, *802*, 140433.
- [13] Neufeld, A. K., Cole, I. S., Bond, A. M., & Furman, S. A. (2002). The initiation mechanism of corrosion of zinc by sodium chloride particle deposition. *Corrosion Science*, *44*(3), 555-572.
- [14] Grundmeier, G., Schmidt, W., & Stratmann, M. J. E. A. (2000). Corrosion protection by organic coatings: electrochemical mechanism and novel methods of investigation. *Electrochimica Acta*, *45*(15-16), 2515-2533.
- [15] Carrasco, J., Hodgson, A., & Michaelides, A. (2012). A molecular perspective of water at metal interfaces. *Nature materials*, *11*(8), 667-674.
- [16] Elboujdaini, M., & Revie, R. W. (2009). Metallurgical factors in stress corrosion cracking (SCC) and hydrogen-induced cracking (HIC). *Journal of solid state electrochemistry*, *13*(7), 1091-1099.
- [17] Guérin, M., Andrieu, E., Odemer, G., Alexis, J., & Blanc, C. (2014). Effect of varying conditions of exposure to an aggressive medium on the corrosion behavior of the 2050 Al–Cu–Li alloy. *Corrosion science*, *85*, 455-470.

- [18] Fajobi, M. A., Loto, R. T., & Oluwole, O. O. (2019). Corrosion in crude distillation overhead system: A review. *Journal of Bio-and Tribo-Corrosion*, 5(3), 1-9.
- [19] Al-Sherrawi, M. H., Lyashenko, V., Edaan, E. M., & Sotnik, S. (2018). Corrosion of metal construction structures.
- [20] Bauer, S., Schmuki, P., Von Der Mark, K., & Park, J. (2013). Engineering biocompatible implant surfaces: Part I: Materials and surfaces. *Progress in Materials Science*, 58(3), 261-326.
- [21] Parthipan, P., Elumalai, P., Karthikeyan, O. P., Ting, Y. P., & Rajasekar, A. (2017). A review on biodegradation of hydrocarbon and their influence on corrosion of carbon steel with special reference to petroleum industry. *Journal of Environment & Biotechnology Research*, 6(1), 12-33.
- [22] Al-Janabi, Y. T. (2020). An overview of corrosion in oil and gas industry: upstream, midstream, and downstream sectors. *Corrosion Inhibitors in the Oil and Gas Industry*, 1-39.
- [23] Prabha, S. S., Rathish, R. J., Dorothy, R., Brindha, G., Pandiarajan, M., Al-Hashem, A., & Rajendran, S. (2014). Corrosion problems in petroleum industry and their solution. *Eur. Chem. Bull*, 3(3), 300-307.
- [24] Askari, M., Aliofkhaezai, M., Ghaffari, S., & Hajizadeh, A. (2018). Film former corrosion inhibitors for oil and gas pipelines-A technical review. *Journal of Natural Gas Science and Engineering*, 58, 92-114.
- [25] Bellemans, I., De Wilde, E., Moelans, N., & Verbeken, K. (2018). Metal losses in pyrometallurgical operations-A review. *Advances in colloid and interface science*, 255, 47-63.
- [26] Smith, C. S., & Ellis, I. I. (1983). *Addendum to material selection guidelines for geothermal energy-utilization systems. Part I. Extension of the field experience data base. Part II. Proceedings of the geothermal engineering and materials (GEM) program conference (San Diego, CA, 6-8 October 1982)* (No. DOE/ET/27026-2; CONF-821075-). Radian Corp., Austin, TX (US).
- [27] Le, H. N. T., Garcia, B., Deslouis, C., & Le Xuan, Q. (2001). Corrosion protection and conducting polymers: polypyrrole films on iron. *Electrochimica acta*, 46(26-27), 4259-4272.



- [28] Alvarez-Armas, I. (2008). Duplex stainless steels: brief history and some recent alloys. *Recent Patents on Mechanical Engineering*, 1(1), 51-57.
- [29] Shahriari, A., Khaksar, L., Nasiri, A., Hadadzadeh, A., Amirkhiz, B. S., & Mohammadi, M. (2020). Microstructure and corrosion behavior of a novel additively manufactured maraging stainless steel. *Electrochimica Acta*, 339, 135925.
- [30] Vafadar, A., Guzzomi, F., Rassau, A., & Hayward, K. (2021). Advances in metal additive manufacturing: a review of common processes, industrial applications, and current challenges. *Applied Sciences*, 11(3), 1213.
- [31] Talebian, M., Raeissi, K., Atapour, M., Fernández-Pérez, B. M., Betancor-Abreu, A., Llorente, I., & Souto, R. M. (2019). Pitting corrosion inhibition of 304 S.S.in NaCl solution by three newly synthesized carboxylic Schiff bases. *Corrosion Science*, 160, 108130.
- [32] Alamri, A. H. (2020). Localized Corrosion and Mitigation Approach of Steel Materials Used in Oil and Gas Pipelines-An overview. *Engineering Failure Analysis*, 104735.
- [33] Esmaily, M., Svensson, J. E., Fajardo, S., Birbilis, N., Frankel, G. S., Virtanen, S., & Johansson, L. G. (2017). Fundamentals and advances in magnesium alloy corrosion. *Progress in Materials Science*, 89, 92-193.
- [34] Khan, M. M., Nemati, A., Rahman, Z. U., Shah, U. H., Asgar, H., & Haider, W. (2018). Recent advancements in bulk metallic glasses and their applications: a review. *Critical Reviews in Solid State and Materials Sciences*, 43(3), 233-268.
- [35] Rahmani, K., Jadidian, R., & Haghtalab, S. (2016). Evaluation of inhibitors and biocides on the corrosion, scaling and biofouling control of carbon steel and copper–nickel alloys in a power plant cooling water system. *Desalination*, 393, 174-185.
- [36] Cho, C. P., Kwon, O. S., & Lee, Y. J. (2014). Effects of the sulfur content of liquefied petroleum gas on regulated and unregulated emissions from liquefied petroleum gas vehicle. *Fuel*, 137, 328-334.
- [37] Calderón, J. A., Jiménez, J. P., & Zuleta, A. A. (2016). Improvement of the erosion-corrosion resistance of magnesium by electroless Ni-P/Ni (OH) 2-ceramic nanoparticle composite coatings. *Surface and Coatings Technology*, 304, 167-178.

- [38] Du, D., Chen, K., Lu, H., Zhang, L., Shi, X., Xu, X., & Andresen, P. L. (2016). Effects of chloride and oxygen on stress corrosion cracking of cold worked 316/316L austenitic S.S.in high temperature water. *Corrosion Science*, *110*, 134-142.
- [39] Palanisamy, G. (2019). Corrosion inhibitors. *Corrosion inhibitors*, 1-24.
- [40] Izionworu, V., Ukpaka, C., & Oguzie, E. (2020). Green and eco-benign corrosion inhibition agents: alternatives and options to chemical based toxic corrosion inhibitors. *Chemistry International*, *6*(4), 232-259.
- [41] Taghavikish, M., Dutta, N. K., & Roy Choudhury, N. (2017). Emerging corrosion inhibitors for interfacial coating. *Coatings*, *7*(12), 217.
- [42] Solomon, M. M., Umoren, S. A., Quraishi, M. A., & Mazumder, M. J. (2019). Corrosion inhibition of N80 steel in simulated acidizing environment by N-(2-(2-pentadecyl-4, 5-dihydro-1H-imidazol-1-yl) ethyl) palmitamide. *Journal of Molecular Liquids*, *273*, 476-487.
- [43] Oguzie, E. E., Adindu, C. B., Enenebeaku, C. K., Ogukwe, C. E., Chidiebere, M. A., & Oguzie, K. L. (2012). Natural products for materials protection: mechanism of corrosion inhibition of mild steel by acid extracts of Piper guineense. *The Journal of Physical Chemistry C*, *116*(25), 13603-13615.
- [44] Marzorati, S., Verotta, L., & Trasatti, S. P. (2019). Green corrosion inhibitors from natural sources and biomass wastes. *Molecules*, *24*(1), 48.
- [45] Khan, A., Qurashi, A., Badeghaish, W., Noui-Mehidi, M. N., & Aziz, M. (2020). Frontiers and Challenges in Electrochemical Corrosion Monitoring; Surface and Downhole Applications. *Sensors*, *20*(22), 6583.
- [46] Xhanari, K., Finšgar, M., Hrnčič, M. K., Maver, U., Knez, Ž., & Seiti, B. (2017). Green corrosion inhibitors for aluminium and its alloys: a review. *RSC advances*, *7*(44), 27299-27330.
- [47] Singh, A., Singh, V. K., & Quraishi, M. A. (2010). Effect of fruit extracts of some environmentally benign green corrosion inhibitors on corrosion of mild steel in hydrochloric acid solution. *Journal of materials and environmental science*, *1*(3), 162-174.

- [48] Fiori-Bimbi, M. V., Alvarez, P. E., Vaca, H., & Gervasi, C. A. (2015). Corrosion inhibition of mild steel in HCL solution by pectin. *Corrosion Science*, *92*, 192-199.
- [49] Aljourani, J., Raeissi, K., & Golozar, M. A. (2009). Benzimidazole and its derivatives as corrosion inhibitors for mild steel in 1M HCl solution. *Corrosion science*, *51*(8), 1836-1843.
- [50] Popoola, L. T. (2019). Organic green corrosion inhibitors (OGCIs): a critical review. *Corrosion Reviews*, *37*(2), 71-102.
- [51] Dar, M. A. (2011). A review: plant extracts and oils as corrosion inhibitors in aggressive media. *Industrial Lubrication and Tribology*, *63*(4), 227-233.
- [52] Sangeetha, M., Rajendran, S., Sathiyabamaa, J., & Krishnavenic, A. (2013). Inhibition of corrosion of aluminium and its alloys by extracts of green inhibitors. *Portugaliae Electrochimica Acta*, *31*(1), 44-45.
- [53] Bobina, M., Kellenberger, A., Millet, J. P., Muntean, C., & Vaszilcsin, N. (2013). Corrosion resistance of carbon steel in weak acid solutions in the presence of l-histidine as corrosion inhibitor. *Corrosion Science*, *69*, 389-395.
- [54] Al-Moubaraki, A. H., & Obot, I. B. (2021). Top of the Line Corrosion: Causes, Mechanisms, and Mitigation Using Corrosion Inhibitors. *Arabian Journal of Chemistry*, *14*, 103116.
- [55] Mo, S., Luo, H. Q., & Li, N. B. (2016). Plant extracts as “green” corrosion inhibitors for steel in sulphuric acid. *Chemical Papers*, *70*(9), 1131-1143.
- [56] Arndt, N., Kesler, S., & Ganino, C. (2015). Classification, distribution and uses of ores and ore deposits. *In Metals and society*, 15-40
- [57] Umoren, S. A., & Solomon, M. M. (2019). Protective polymeric films for industrial substrates: A critical review on past and recent applications with conducting polymers and polymer composites/nanocomposites. *Progress in Materials Science*, *104*, 380-450.
- [58] Akbarzadeh, E., Ibrahim, M. M., & Rahim, A. A. (2011). Corrosion inhibition of mild steel in near neutral solution by kraft and soda lignins extracted from oil palm empty fruit bunch. *Int. J. Electrochem. Sci*, *6*(11), 5396-5416.

- [59] Bhardwaj, N., Sharma, P., & Kumar, V. (2021). Phytochemicals as steel corrosion inhibitor: an insight into mechanism. *Corrosion Reviews*, 39(1), 27-41
- [60] Altemimi, A., Lakhssassi, N., Baharlouei, A., Watson, D. G., & Lightfoot, D. A. (2017). Phytochemicals: Extraction, isolation, and identification of bioactive compounds from plant extracts. *Plants*, 6(4), 42.
- [61] Asmara, Y. P., Kurniawan, T., Sutjipto, A. G. E., & Jafar, J. (2018). Application of plants extracts as green corrosion inhibitors for steel in concrete-a review. *Indonesian Journal of Science and Technology*, 3(2), 158-170.
- [62] Kesavan, D., Gopiraman, M., & Sulochana, N. (2012). Green inhibitors for corrosion of metals: a review. *Chemical Science Review and Letters*, 1(1), 1-8.
- [63] Tourabi, M., Nohair, K., Traisnel, M., Jama, C., & Bentiss, F. (2013). Electrochemical and XPS studies of the corrosion inhibition of carbon steel in hydrochloric acid pickling solutions by 3, 5-bis (2-thienylmethyl)-4-amino-1, 2, 4-triazole. *Corrosion Science*, 75, 123-133.
- [64] Singh, A., Ansari, K. R., Quraishi, M. A., Lgaz, H., & Lin, Y. (2018). Synthesis and investigation of pyran derivatives as acidizing corrosion inhibitors for N80 steel in hydrochloric acid: theoretical and experimental approaches. *Journal of Alloys and Compounds*, 762, 347-362.
- [65] Popoola, L. T. (2019). Progress on pharmaceutical drugs, plant extracts and ionic liquids as corrosion inhibitors. *Heliyon*, 5(2), 1143.
- [66] Finšgar, M., & Jackson, J. (2014). Application of corrosion inhibitors for steels in acidic media for the oil and gas industry: A review. *Corrosion science*, 86, 17-41.
- [67] Rajeev, P., Surendranathan, A. O., & Murthy, C. S. (2012). Corrosion mitigation of the oil well steels using organic inhibitors—a review. *Journal of Materials and Environmental Science*, 3(5), 856-869.
- [68] Yadav, M., Behera, D., & Sharma, U. (2016). Nontoxic corrosion inhibitors for N80 steel in hydrochloric acid. *Arabian Journal of Chemistry*, 9, S1487-S1495.
- [69] Kamal, M. S., Hussein, I., Mahmoud, M., Sultan, A. S., & Saad, M. A. (2018). Oilfield scale formation and chemical removal: A review. *Journal of petroleum science and engineering*, 171, 127-139.

- [70] Ituen, E., Akaranta, O., James, A., & Sun, S. (2017). Green and sustainable local biomaterials for oilfield chemicals: *Griffonia simplicifolia* extract as steel corrosion inhibitor in hydrochloric acid. *Sustainable Materials and Technologies*, 11, 12-18.
- [71] Raja, P. B., Qureshi, A. K., Rahim, A. A., Osman, H., & Awang, K. (2013). *Neolamarckia cadamba* alkaloids as eco-friendly corrosion inhibitors for mild steel in 1 M HCl media. *Corrosion Science*, 69, 292-301.
- [72] El Bribri, A., Tabyaoui, M., Tabyaoui, B., El Attari, H., & Bentiss, F. (2013). The use of *Euphorbia falcata* extract as eco-friendly corrosion inhibitor of carbon steel in hydrochloric acid solution. *Materials Chemistry and Physics*, 141(1), 240-247.
- [73] Hamdy, A., & El-Gendy, N. S. (2013). Thermodynamic, adsorption and electrochemical studies for corrosion inhibition of carbon steel by *henna* extract in acid medium. *Egyptian Journal of Petroleum*, 22(1), 17-25.
- [74] Shalabi, K., Abdallah, Y. M., Hassan, H. M., & Fouda, A. S. (2014). Adsorption and corrosion inhibition of *Atropa Belladonna* extract on carbon steel in 1 M HCl solution. *International Journal of Electrochemical Science*, 9, 1468-1487.
- [75] Soltani, N., Tavakkoli, N., Kashani, M. K., Mosavizadeh, A. E. E. O., Oguzie, E. E., & Jalali, M. R. (2014). *Silybum marianum* extract as a natural source inhibitor for 304 S.S.corrosion in 1.0 M HCl. *Journal of Industrial and Engineering Chemistry*, 20(5), 3217-3227.
- [76] Rajeswari, V., Kesavan, D., Gopiraman, M., Viswanathamurthi, P., Poonkuzhali, K., & Palvannan, T. (2014). Corrosion inhibition of *Eleusine aegyptiaca* and *Croton rotleri* leaf extracts on cast iron surface in 1 M HCl medium. *Applied surface science*, 314, 537-545.
- [77] Faustin, M., Maciuk, A., Salvin, P., Roos, C., & Lebrini, M. (2015). Corrosion inhibition of C38 steel by alkaloids extract of *Geissospermum laeve* in 1 M hydrochloric acid: electrochemical and phytochemical studies. *Corrosion Science*, 92, 287-300.

- [78] Anupama, K. K., Ramya, K., Shainy, K. M., & Joseph, A. (2015). Adsorption and electrochemical studies of *Pimenta dioica* leaf extracts as corrosion inhibitor for mild steel in hydrochloric acid. *Materials Chemistry and Physics*, 167, 28-41.
- [79] Prabakaran, M., Kim, S. H., Kalaiselvi, K., Hemapriya, V., & Chung, I. M. (2016). Highly efficient *Ligularia fischeri* green extract for the protection against corrosion of mild steel in acidic medium: electrochemical and spectroscopic investigations. *Journal of the Taiwan Institute of Chemical Engineers*, 59, 553-562.
- [80] Anupama, K. K., Ramya, K., & Joseph, A. (2016). Electrochemical and computational aspects of surface interaction and corrosion inhibition of mild steel in hydrochloric acid by *Phyllanthus amarus* leaf extract (PAE). *Journal of Molecular Liquids*, 216, 146-155.
- [81] Rose, K., Kim, B. S., Rajagopal, K., Arumugam, S., & Devarayan, K. (2016). Surface protection of steel in acid medium by *Tabernaemontana divaricata* extract: physicochemical evidence for adsorption of inhibitor. *Journal of Molecular Liquids*, 214, 111-116.
- [82] Anupama, K. K., Ramya, K., & Joseph, A. (2017). Electrochemical measurements and theoretical calculations on the inhibitive interaction of *Plectranthus amboinicus* leaf extract with mild steel in hydrochloric acid. *Measurement*, 95, 297-305.
- [83] Azzaoui, K., Mejdoubi, E., Jodeh, S., Lamhamdi, A., Rodriguez-Castellón, E., Algarra, M., & Lgaz, H. (2017). Eco friendly green inhibitor Gum Arabic (GA) for the corrosion control of mild steel in hydrochloric acid medium. *Corrosion Science*, 129, 70-81.
- [84] Alibakhshi, E., Ramezanzadeh, M., Bahlakeh, G., Ramezanzadeh, B., Mahdavian, M., & Motamedi, M. (2018). *Glycyrrhiza glabra* leaves extract as a green corrosion inhibitor for mild steel in 1 M hydrochloric acid solution: experimental, molecular dynamics, Monte Carlo and quantum mechanics study. *Journal of Molecular Liquids*, 255, 185-198.
- [85] Umoren, S. A., Obot, I. B., Israel, A. U., Asuquo, P. O., Solomon, M. M., Eduok, U. M., & Udoh, A. P. (2014). Inhibition of mild steel corrosion in acidic medium using coconut coir dust extracted from water and methanol as solvents. *Journal of Industrial and Engineering Chemistry*, 20(5), 3612-3622.

- [86] Liao, L. L., Mo, S., Luo, H. Q., & Li, N. B. (2017). Longan seed and peel as environmentally friendly corrosion inhibitor for mild steel in acid solution: experimental and theoretical studies. *Journal of Colloid and Interface Science*, 499, 110-119.
- [87] Mobin, M., & Rizvi, M. (2017). Polysaccharide from *Plantago* as a green corrosion inhibitor for carbon steel in 1 M HCl solution. *Carbohydrate Polymers*, 160, 172-183.
- [88] Srivastava, M., Tiwari, P., Srivastava, S. K., Kumar, A., Ji, G., & Prakash, R. (2018). Low cost aqueous extract of *Pisum sativum* peels for inhibition of mild steel corrosion. *Journal of Molecular Liquids*, 254, 357-368.
- [89] Hassannejad, H., & Nouri, A. (2018). Sunflower seed hull extract as a novel green corrosion inhibitor for mild steel in HCl solution. *Journal of Molecular Liquids*, 254, 377-382.
- [90] Biswas, A., Pal, S., & Udayabhanu, G. (2015). Experimental and theoretical studies of xanthan gum and its graft co-polymer as corrosion inhibitor for mild steel in 15% HCl. *Applied Surface Science*, 353, 173-183.
- [91] Eissen, M., Metzger, J. O., Schmidt, E., & Schneidewind, U. (2002). 10 years after Rio—concepts on the contribution of chemistry to a sustainable development. *Angewandte Chemie International Edition*, 41(3), 414-436.
- [92] Anastas, P. T., & Kirchhoff, M. M. (2002). Origins, current status, and future challenges of green chemistry. *Accounts of Chemical Research*, 35(9), 686-694.
- [93] Sheldon, R. A. (2018). Metrics of green chemistry and sustainability: past, present, and future. *ACS Sustainable Chemistry & Engineering*, 6(1), 32-48.
- [94] Ismail, M., Abdulrahman, A. S., & Hussain, M. S. (2011). Solid waste as environmental benign corrosion inhibitors in acid medium. *International Journal of Engineering Science and Technology*, 3(2), 1742-1748.
- [95] Odewunmi, N. A., Umoren, S. A., & Gasem, Z. M. (2015). Watermelon waste products as green corrosion inhibitors for mild steel in HCl solution. *Journal of Environmental Chemical Engineering*, 3(1), 286-296.
- [96] Ismail, M., Abdulrahman, A. S., & Hussain, M. S. (2011). Solid waste as environmental benign corrosion inhibitors in acid medium. *International Journal of Engineering Science and Technology*, 3(2), 1742-1748.

- [97] Chen, G., Zhang, M., Pang, M., Hou, X. Q., Su, H., & Zhang, J. (2013). Extracts of *Punica granatum* Linne husk as green and eco-friendly corrosion inhibitors for mild steel in oil fields. *Research on Chemical Intermediates*, 39(8), 3545-3552.
- [98] Tiwari, P., Srivastava, M., Mishra, R., Ji, G., & Prakash, R. (2018). Economic use of waste *Musa paradisiaca* peels for effective control of mild steel loss in aggressive acid solutions. *Journal of Environmental Chemical Engineering*, 6(4), 4773-4783.
- [99] Ji, G., Dwivedi, P., Sundaram, S., & Prakash, R. (2016). Aqueous extract of *Argemone mexicana* roots for effective protection of mild steel in an HCl environment. *Research on Chemical Intermediates*, 42(2), 439-459.
- [100] . (2018). Optimization of an efficient, economic and eco-friendly inhibitor based on *Sesbania grandiflora* leaf extract for the mild steel corrosion in aggressive HCl environment. *Anti-Corrosion Methods and Materials*, 65(2), 210-216
- [101] Al-Senani, G. M. (2016). Corrosion inhibition of carbon steel in acidic chloride medium by *Cucumis sativus* (cucumber) peel extract. *International Journal of Electrochemical Science*, 11(1) 291 - 302.
- [102] Da Rocha, J. C., Gomes, J. A. D. C. P., & D'Elia, E. (2010). Corrosion inhibition of carbon steel in hydrochloric acid solution by fruit peel aqueous extracts. *Corrosion Science*, 52(7), 2341-2348.
- [103] Umoren, S. A., Gasem, Z. M., & Obot, I. B. (2013). Natural products for material protection: inhibition of mild steel corrosion by date palm seed extracts in acidic media. *Industrial & Engineering Chemistry Research*, 52(42), 14855-14865.
- [104] Ferreira, K. C. R., Cordeiro, R. F. B., Nunes, J. C., Orofino, H., Magalhães, M., Torres, A. G., & D'Elia, E. (2016). Corrosion inhibition of carbon steel in HCl solution by aqueous brown onion peel extract. *International Journal of Electrochemical Science*, 11, 406-418.
- [105] Rangel, M. A., & Vogl, T. S. (2019). Agricultural fires and health at birth. *Review of Economics and Statistics*, 101(4), 616-630.
- [106] Fares, M. M., Maayta, A. K., & Al-Qudah, M. M. (2012). Pectin as promising green corrosion inhibitor of aluminum in hydrochloric acid solution. *Corrosion Science*, 60, 112-117.



- [107] Chen, J., Li, C., Ristovski, Z., Milic, A., Gu, Y., Islam, M. S., & Dumka, U. C. (2017). A review of biomass burning: Emissions and impacts on air quality, health and climate in China. *Science of the Total Environment*, 579, 1000-1034.
- [108] Andreae, M. O., & Merlet, P. (2001). Emission of trace gases and aerosols from biomass burning. *Global Biogeochemical Cycles*, 15(4), 955-966.
- [109] Jain, N., Bhatia, A., & Pathak, H. (2014). Emission of air pollutants from crop residue burning in India. *Aerosol and Air Quality Research*, 14(1), 422-430.
- [110] Erenstein, O. (2011). Cropping systems and crop residue management in the Trans-Gangetic Plains: Issues and challenges for conservation agriculture from village surveys. *Agricultural Systems*, 104(1), 54-62.
- [111] Keyword, M., Kanakidou, M., Stohl, A., Dentener, F., Grassi, G., Meyer, C. P., & Burrows, J. (2013). Fire in the air: Biomass burning impacts in a changing climate. *Critical Reviews in Environmental Science and Technology*, 43(1), 40-83.
- [112] Engling, G., & Gelencsér, A. (2010). Atmospheric brown clouds: From local air pollution to climate change. *Elements*, 6(4), 223-228.
- [113] Hmamou, D. B., Salghi, R., Zarrouk, A., Zarrok, H., Benali, O., Errami, M., & Hammouti, B. (2013). Inhibition effect of horehound (*Marrubium vulgare* L.) extract towards C38 steel corrosion in HCl solution. *Research on Chemical Intermediates*, 39(7), 3291-3302.51
- [114] Raghavendra, N., & Bhat, J. I. (2016). Green approach to inhibition of corrosion of aluminum in 0.5 M HCl medium by *tender arecanut* seed extract: insight from gravimetric and electrochemical studies. *Research on Chemical Intermediates*, 42(7), 6351-6372.
- [115] Cui, R., Gu, N., & Li, C. (2011). Polyaspartic acid as a green corrosion inhibitor for carbon steel. *Materials and Corrosion*, 62(4), 362-369.
- [116] Fares, M. M., Maayta, A. K., & Al-Qudah, M. M. (2012). Pectin as promising green corrosion inhibitor of aluminum in hydrochloric acid solution. *Corrosion Science*, 60, 112-117.
- [117] Nasibi, M., Zaarei, D., Rashed, G., & Ghasemi, E. (2013). Chamomile (*Matricaria recutita*) extract as a corrosion inhibitor for mild steel in hydrochloric acid solution. *Chemical Engineering Communications*, 200(3), 367-378.

- [118] Ghazi, Z., ELmssellem, H., Ramdani, M., Chetouani, A., Rmil, R., Aouniti, A., ... & Hammouti, B. (2014). Corrosion inhibition by naturally occurring substance containing *Opuntia-Ficus Indica* extract on the corrosion of steel in hydrochloric acid. *Journal of Chemical and Pharmaceutical Research*, 6, 14171425.
- [119] Umoren, S., Obot, I. B., Gasem, Z., & Odewunmi, N. A. (2015). Experimental and theoretical studies of red apple fruit extract as green corrosion inhibitor for mild steel in HCl solution. *Journal of Dispersion Science and Technology*, 36(6), 789-802.
- [120] Halambek, J., Žutinić, A., & Berković, K. (2013). Ocimum basilicum L. oil as corrosion inhibitor for aluminium in hydrochloric acid solution. *International Journal of Electrochemical Science*, 8, 11201-11214.
- [121] Kumar, H., & Yadav, V. (2016). Citrus sinensis peels as a green corrosion inhibitor for mild steel in 5.0 M hydrochloric acid solution. *Research Journal of Chemical Sciences*, 6(1), 53-60.
- [122] Matos, L. A. C., Taborda, M. C., Alves, G. J. T., Cunha, M. T., Banczek, E. P., Oliveira, M. F., & Rodrigues, P. R. P. (2018). Application of an acid extract of barley agro-industrial waste as a corrosion inhibitor for S.S.AISI 304 in H<sub>2</sub>SO<sub>4</sub>. *International Journal of Electrochemical Science*, 13(2), 1577-93.
- [123] Okeniyi, J. O., Omotosho, O. A., Ogunlana, O. O., Okeniyi, E. T., Owoeye, T. F., Ogbiye, A. S., & Ogunlana, E. O. (2015). Investigating prospects of *Phyllanthus muellerianus* as eco-friendly/sustainable material for reducing concrete steel-reinforcement corrosion in industrial/microbial environment. *Energy Procedia*, 74, 1274-1281.
- [124] Hmamou, D. B., Salghi, R., Zarrouk, A., Al-Deyab, S. S., Zarrok, H., Hammouti, B., & Errami, E. (2012). Verbena extract: an efficient inhibitor of C38 steel corrosion in hydrochloric acid. *International Journal of Electrochemical Science*, 7, 6234-6246.
- [125] Okafor, P. C., & Apebende, E. A. (2014). Corrosion inhibition characteristics of *Thymus vulgaris*, *Xylopi aethiopic a* and *Zingiber officinale* extracts on mild steel in H<sub>2</sub>SO<sub>4</sub> solutions. *Pigment & Resin Technology*, 42:6351–6372

- [126] Loto, R. T. (2017). Study of the corrosion behaviour of S32101 duplex and 410 martensitic S.S.for application in oil refinery distillation systems. *Journal of Materials Research and Technology*, 6(3), 203-212.
- [127] Liu, X., & Wang, X. (2014). The research of oil and gas pipeline corrosion and protection technology. *Advan Petrol Explorat Dev*, 7, 102-5..
- [128] Talha, M., Behera, C. K., & Sinha, O. P. (2013). A review on nickel-free nitrogen containing austenitic stainless steels for biomedical applications. *Materials Science and Engineering: C*, 33(7), 3563-3575.
- [129] Zitelli, C., Folgarait, P., & Di Schino, A. (2019). Laser powder bed fusion of stainless steel grades: a review. *Metals*, 9(7), 731.
- [130] Chakraborty, G., Das, C. R., Albert, S. K., Bhaduri, A. K., Paul, V. T., Panneerselvam, G., & Dasgupta, A. (2015). Study on tempering behaviour of AISI 410 stainless steel. *Materials Characterization*, 100, 81-87.
- [131] Dalmau, A., Richard, C., & Igual–Muñoz, A. (2018). Degradation mechanisms in martensitic stainless steels: Wear, corrosion and tribocorrosion appraisal. *Tribology International*, 121, 167-179.
- [132] Speight, J. G. (2020). Petroleum refining and environmental control and environmental effects. *Fossil Energy*, 101-131.
- [133] Subramanian, C. (2021). Corrosion prevention of crude and vacuum distillation column overheads in a petroleum refinery: A field monitoring study. *Process Safety Progress*, 40(2), e12213.
- [134] Ajeel, A., Mohammed Waadulah, H., & Sultan, D. A. (2012). Effects of H<sub>2</sub>SO<sub>4</sub> and HCl concentration on the corrosion resistance of protected low carbon steel. *Al-Rafidain Engineering Journal*, 20(6), 70-76.
- [135] Ansari, K. R., Chauhan, D. S., Singh, A., Saji, V. S., & Quraishi, M. A. (2020). Corrosion inhibitors for acidizing process in oil and gas sectors. *Corrosion Inhibitors in the Oil and Gas Industry*, 151-176.
- [136] Chambers, B., Srinivasan, S., Yap, K. M., & Yunovich, M. (2011). Corrosion in crude distillation unit overhead operations: a comprehensive review. *Corrosion*, 11360, 5011-21.
- [137] Loto, R. T. (2017). Anti-corrosion performance of 1, 3-benzothiazole on 410 martensitic S.S.in H<sub>2</sub>SO<sub>4</sub>. *Surface Review and Letters*, 24(07), 1750121.

- [138] El-Sayed, H. A., & Gouda, V. K. (1984). Stress Corrosion of 410 S.S.in Boiling Sodium Sulphide Solution. *British Corrosion Journal*, 19(2), 64-69
- [139] Ahmad, A., Xuan, T. D., Minh, T. N., Siddiqui, N. A., & Van Quan, N. (2019). Comparative extraction and simple isolation improvement techniques of active constituents' momilactone A and B from rice husks of *O. sativa* by HPLC analysis and column chromatography. *Saudi pharmaceutical journal*, 27(1), 17-24.
- [140] Chávez-González, M. L., Sepúlveda, L., Verma, D. K., Luna-García, H. A., Rodríguez-Durán, L. V., Iliina, A., & Aguilar, C. N. (2020). Conventional and emerging extraction processes of flavonoids. *Processes*, 8(4), 434.
- [141] Savic, I. M., & Gajic, I. M. S. (2020). Optimization of ultrasound-assisted extraction of polyphenols from wheatgrass (*Triticum aestivum L.*). *Journal of Food Science and Technology*, 57(8), 2809-2818.
- [142] Radha Krishnan, K., Azhagu Saravana Babu, P., Babuskin, S., Sivarajan, M., & Sukumar, M. (2015). Modeling the Kinetics of Antioxidant Extraction from *Origanum vulgare* and *B. nigra*. *Chemical Engineering Communications*, 202(12), 1577-1585.
- [143] Williams, I. O., Onyenweaku, E. O., & Atangwho, I. J. (2016). Nutritional and antimicrobial evaluation of *S. officinarum* consumed in Calabar, Nigeria. *African Journal of Biotechnology*, 15(33), 1789-1795.
- [144] Abbas, A., Iqbal, Z., Abbas, R. Z., Khan, M. K., Khan, J. A., Mahmood, M. S., & Salemi, M. K. (2017). In vivo anticoccidial effects of *B. vulgaris* (sugar beet) in broiler chickens. *Microbial pathogenesis*, 111, 139-144.
- [145] Manikandan, A. P., Akila, S., & Prabu, K. (2019). Production of Polyphenol from *Phyllanthus Emblica* using Soxhlet Extraction Process. *International Journal of Recent Technology and Engineering (IJRTE)*, 8(4), 5010-5012.
- [146] Okafor, P. C., Ebenso, E. E., & Ekpe, U. J. (2010). *Azadirachta indica* extracts as corrosion inhibitor for mild steel in acid medium. *International Journal of Electrochemical Science*, 5(7), 978-993.
- [147] Alamri, A. H., & Obot, I. B. (2019). Highly efficient corrosion inhibitor for C1020 carbon steel during acid cleaning in multistage flash (MSF) desalination plant. *Desalination*, 470, 114100.

- [148] Krishnegowda, P. M., Venkatesha, V. T., Krishnegowda, P. K. M., & Shivayogiraju, S. B. (2013). *Acalypha torta* leaf extract as green corrosion inhibitor for mild steel in hydrochloric acid solution. *Industrial & Engineering Chemistry Research*, 52(2), 722-728.
- [149] Wang, X., Jiang, H., Zhang, D. X., Hou, L., & Zhou, W. J. (2019). *Solanum lasiocarpum* L. Extract as green corrosion inhibitor for A3 steel in 1 M HCl solution *International Journal of Electrochemical Science*, 14, 1178-1196.
- [150] Amin, M. A., Abd El-Rehim, S. S., El-Sherbini, E. E. F., & Bayoumi, R. S. (2007). The inhibition of low carbon steel corrosion in hydrochloric acid solutions by succinic acid: Part I. Weight loss, polarization, EIS, PZC, EDX and SEM studies. *Electrochimica Acta*, 52(11), 3588-3600.
- [151] Singh, A., Lin, Y., Liu, W., Yu, S., Pan, J., Ren, C., & Kuanhai, D. (2014). Plant derived cationic dye as an effective corrosion inhibitor for 7075 aluminum alloy in 3.5% NaCl solution. *Journal of Industrial and Engineering Chemistry*, 20(6), 4276-4285.
- [152] Emranuzzaman, Kumar, T., Vishwanatham, S., & Udayabhanu, G. (2004). Synergistic effects of formaldehyde and alcoholic extract of plant leaves for protection of N80 steel in 15% HCl. *Corrosion Engineering, Science and Technology*, 39(4), 327-332.
- [153] Abdallah, M. (2004). Antibacterial drugs as corrosion inhibitors for corrosion of aluminium in hydrochloric solution. *Corrosion Science*, 46(8), 1981-1996.
- [154] Ituen, E., Akaranta, O., & James, A. (2017). Evaluation of performance of corrosion inhibitors using adsorption isotherm models: an overview. *Chem. Sci. Int. J*, 18(1), 1-34.
- [155] Alvarez, P. E., Fiori-Bimbi, M. V., Neske, A., Brandán, S. A., & Gervasi, C. A. (2018). *Rollinia occidentalis* extract as green corrosion inhibitor for carbon steel in HCl solution. *Journal of Industrial and Engineering Chemistry*, 58, 92-99.
- [156] Biswas, A., Mourya, P., Mondal, D., Pal, S., & Udayabhanu, G. (2018). Grafting effect of gum acacia on mild steel corrosion in acidic medium: Gravimetric and electrochemical study. *Journal of Molecular Liquids*, 251, 470-479.

- [157] Qiang, Y., Zhang, S., Tan, B., & Chen, S. (2018). Evaluation of Ginkgo leaf extract as an eco-friendly corrosion inhibitor of X70 steel in HCl solution. *Corrosion Science*, 133, 6-16.
- [158] Salinas-Solano, G., Porcayo-Calderon, J., de la Escalera, L. M., Canto, J., Casales-Diaz, M., Sotelo-Mazon, O., ... & Martinez-Gomez, L. (2018). Development and evaluation of a green corrosion inhibitor based on rice bran oil obtained from agro-industrial waste. *Industrial Crops and Products*, 119, 111-124.
- [159] Bagherzadeh, M., & Jaberinia, F. (2018). Electrochemical study of Monel alloy corrosion in hydrochloric acid solution and pyrrolidine dithiocarboxylate self-assembled monolayers as its corrosion protector. *Journal of Alloys and Compounds*, 750, 677-686.
- [160] Obot, I. B., Solomon, M. M., Onyechu, I. B., Umoren, S. A., Meroufel, A., Alenazi, A., & Sorour, A. A. (2020). Development of a green corrosion inhibitor for use in acid cleaning of MSF desalination plant. *Desalination*, 495, 114675.
- [161] Chauhan, D. S., Mouaden, K. E., Quraishi, M. A., & Bazzi, L. (2020). Aminotriazolethiol-functionalized chitosan as a macromolecule-based bioinspired corrosion inhibitor for surface protection of S.S.in 3.5% NaCl. *International Journal of Biological Macromolecules*, 152, 234-241.
- [162] Farhadian, A., Rahimi, A., Safaei, N., Shaabani, A., Abdouss, M., & Alavi, A. (2020). A theoretical and experimental study of castor oil-based inhibitor for corrosion inhibition of mild steel in acidic medium at elevated temperatures. *Corrosion Science*, 175, 108871.
- [163] Asfia, M. P., Rezaei, M., & Bahlakeh, G. (2020). Corrosion prevention of AISI 304 S.S.in hydrochloric acid medium using garlic extract as a green corrosion inhibitor: electrochemical and theoretical studies. *Journal of Molecular Liquids*, 315, 113679.
- [164] Bashir, S., Thakur, A., Lgaz, H., Chung, I. M., & Kumar, A. (2020). Corrosion inhibition efficiency of bronopol on aluminium in 0.5 M HCl solution: Insights from experimental and quantum chemical studies. *Surfaces and Interfaces*, 20, 100542.
- [165] Ansari, K. R., Chauhan, D. S., Quraishi, M. A., Mazumder, M. A., & Singh, A. (2020). Chitosan Schiff base: an environmentally benign biological

macromolecule as a new corrosion inhibitor for oil & gas industries. *International Journal of Biological Macromolecules*, 144, 305-315.

[166] Fouda, A. S., Al-Sarawy, A. A., Ahmed, F. S., & El-Abbasy, H. M. (2009). Corrosion inhibition of aluminum 6063 using some pharmaceutical compounds. *Protection of Metals and Physical Chemistry of Surfaces*, 45(5), 635-643.

[167] Hamilton-Amachree, A., & Iroha, N. B. (2020). Corrosion inhibition of API 5L X80 pipeline steel in acidic environment using aqueous extract of *Thevetia peruviana*. *Chemistry International*, 6(3), 117-128.

[168] Ehsani, A., Mahjani, M. G., Hosseini, M., Safari, R., Moshrefi, R., & Shiri, H. M. (2017). Evaluation of *Thymus vulgaris* plant extract as an eco-friendly corrosion inhibitor for S.S.304 in acidic solution by means of electrochemical impedance spectroscopy, electrochemical noise analysis and density functional theory. *Journal of Colloid and Interface Science*, 490, 444-451.

[169] Barbouchi, M., Benzidia, B., Aouidate, A., Ghaleb, A., & El Idrissi, M. (2020). Theoretical modeling and experimental studies of *Terebinth* extracts as green corrosion inhibitor for iron in 3% NaCl medium. *Journal of King Saud University-Science*, 32(7), 2995-3004.

[170] Sedik, A., Lerari, D., Salci, A., Athmani, S., Bachari, K., Gecibesler, İ. H., & Solmaz, R. (2020). *Dardagan* Fruit extract as eco-friendly corrosion inhibitor for mild steel in 1 M HCl: Electrochemical and surface morphological studies. *Journal of the Taiwan Institute of Chemical Engineers*, 107, 189-200.

[171] Onyeachu, I. B., Solomon, M. M., Umoren, S. A., Obot, I. B., & Sorour, A. A. (2020). Corrosion inhibition effect of a benzimidazole derivative on heat exchanger tubing materials during acid cleaning of multistage flash desalination plants. *Desalination*, 479, 114283.

[172] Harb, M. B., Abubshait, S., Etteyeb, N., Kamoun, M., & Dhoub, A. (2020). Olive leaf extract as a green corrosion inhibitor of reinforced concrete contaminated with seawater. *Arabian Journal of Chemistry*, 13(3), 4846-4856.

[173] Dominic, O. O., Chikaodili, A. V., & Sandra, O. C. (2020). Optimum prediction for inhibition efficiency of *Sapium ellipticum* leaf extract as corrosion inhibitor of aluminum alloy (AA3003) in hydrochloric acid solution using

- electrochemical impedance spectroscopy and response surface methodology. *Bulletin of the Chemical Society of Ethiopia*, 34(1), 175-191.
- [174] Pal, A., & Das, C. (2020). A novel use of solid waste extract from tea factory as corrosion inhibitor in acidic media on boiler quality steel. *Industrial Crops and Products*, 151, 112468.
- [175] Dehghani, A., Bahlakeh, G., Ramezanzadeh, B., & Ramezanzadeh, M. (2019). Potential of Borage flower aqueous extract as an environmentally sustainable corrosion inhibitor for acid corrosion of mild steel: electrochemical and theoretical studies. *Journal of Molecular Liquids*, 277, 895-911.
- [176] Keramatnia, M., Ramezanzadeh, B., & Mahdavian, M. (2019). Green production of bioactive components from herbal origins through one-pot oxidation/polymerization reactions and application as a corrosion inhibitor for mild steel in HCl solution. *Journal of the Taiwan Institute of Chemical Engineers*, 105, 134-149.
- [177] Asadi, N., Ramezanzadeh, M., Bahlakeh, G., & Ramezanzadeh, B. (2019). Utilizing Lemon Balm extract as an effective green corrosion inhibitor for mild steel in 1M HCl solution: A detailed experimental, molecular dynamics, Monte Carlo and quantum mechanics study. *Journal of the Taiwan Institute of Chemical Engineers*, 95, 252-272.
- [178] Nikpour, S., Ramezanzadeh, M., Bahlakeh, G., Ramezanzadeh, B., & Mahdavian, M. (2019). Eriobotrya japonica Lindl leaves extract application for effective corrosion mitigation of mild steel in HCl solution: experimental and computational studies. *Construction and Building Materials*, 220, 161-176.
- [179] Chung, I. M., Kim, S. H., Hemapriya, V., Kalaiselvi, K., & Prabakaran, M. (2019). Inhibition behavior of *Tragia involucrata* L. phenolic compounds against acidic medium corrosion in low carbon steel surface. *Chinese Journal of Chemical Engineering*, 27(3), 717-725.
- [180] Yaocheng, Y., Caihong, Y., Singh, A., & Lin, Y. (2019). Electrochemical study of commercial and synthesized green corrosion inhibitors for N80 steel in acidic liquid. *New Journal of Chemistry*, 43(40), 16058-16070.



- [181] Mobin, M., Basik, M., & Aslam, J. (2019). Pineapple stem extract (Bromelain) as an environmental friendly novel corrosion inhibitor for low carbon steel in 1 M HCl. *Measurement*, 134, 595-605.
- [182] Jmiai, A., Tara, A., El Issami, S., Hilali, M., Jbara, O., & Bazzi, L. (2021). A new trend in corrosion protection of copper in acidic medium by using Jujube shell extract as an effective green and environmentally safe corrosion inhibitor: Experimental, quantum chemistry approach and Monte Carlo simulation study. *Journal of Molecular Liquids*, 322, 114509.
- [183] Verma, C. B., Quraishi, M. A., & Singh, A. (2015). 2-Aminobenzene-1, 3-dicarbonitriles as green corrosion inhibitor for mild steel in 1 M HCl: Electrochemical, thermodynamic, surface and quantum chemical investigation. *Journal of the Taiwan Institute of Chemical Engineers*, 49, 229-239.
- [184] Feng, Y., He, J., Zhan, Y., An, J., & Tan, B. (2021). Insight into the anti-corrosion mechanism Veratrum root extract as a green corrosion inhibitor. *Journal of Molecular Liquids*, 334, 116110.
- [185] Tan, B., He, J., Zhang, S., Xu, C., Chen, S., Liu, H., & Li, W. (2021). Insight into anti-corrosion nature of Betel leaves water extracts as the novel and eco-friendly inhibitors. *Journal of Colloid and Interface Science*, 585, 287-301.
- [186] Dahmani, K., Galai, M., Ouakki, M., Cherkaoui, M., Tourir, R., Erkan, S. & El Ibrahimy, B. (2021). Quantum chemical and molecular dynamic simulation studies for the identification of the extracted cinnamon essential oil constituent responsible for copper corrosion inhibition in acidified 3.0 wt% NaCl medium. *Inorganic Chemistry Communications*, 124, 108409.
- [187] Ebenso, E. E., Isabirye, D. A., & Eddy, N. O. (2010). Adsorption and quantum chemical studies on the inhibition potentials of some thiosemicarbazides for the corrosion of mild steel in acidic medium. *International Journal of Molecular Sciences*, 11(6), 2473-2498.
- [188] Manssouri, M., Znini, M., Lakbaibi, Z., Ansari, A., & El Ouadi, Y. (2021). Experimental and computational studies of perillaldehyde isolated from *Ammodaucus leucotrichus* essential oil as a green corrosion inhibitor for mild steel in 1.0 M HCl. *Chemical Papers*, 75(3), 1103-1114.

- [189] Resen, A. M., Hanoon, M. M., Alani, W. K., Kadhim, A., Mohammed, A. A., Gaaz, T. S., & Takriff, M. S. (2021). Exploration of 8-piperazine-1-ylmethylumbelliferone for application as a corrosion inhibitor for mild steel in hydrochloric acid solution. *International Journal of Corrosion and Scale Inhibition*, 10(1), 368-387.
- [190] Abdallah, M., Altass, H. M., Al-Gorair, A. S., Al-Fahemi, J. H., Jahdaly, B. A. A. L., & Soliman, K. A. (2021). Natural nutmeg oil as a green corrosion inhibitor for carbon steel in 1.0 M HCl solution: Chemical, electrochemical, and computational methods. *Journal of Molecular Liquids*, 323, 115036.
- [191] Chen, Z., Fadhil, A. A., Chen, T., Khadom, A. A., Fu, C., & Fadhil, N. A. (2021). Green synthesis of corrosion inhibitor with biomass platform molecule: Gravimetric, electrochemical, morphological, and theoretical investigations. *Journal of Molecular Liquids*, 332, 115852.
- [192] Tasić, Ž. Z., Mihajlović, M. B. P., Radovanović, M. B., Simonović, A. T., & Antonijević, M. M. (2021). Experimental and theoretical studies of paracetamol as a copper corrosion inhibitor. *Journal of Molecular Liquids*, 327, 114817.
- [193] Yadav, M., Behera, D., Kumar, S., & Sinha, R. R. (2013). Experimental and quantum chemical studies on the corrosion inhibition performance of benzimidazole derivatives for mild steel in HCl. *Industrial & Engineering Chemistry Research*, 52(19), 6318-6328.
- [194] Al-Azawi, K. F., Al-Baghdadi, S. B., Mohamed, A. Z., Al-Amiery, A. A., Abed, T. K., Mohammed, S. A., & Mohamad, A. B. (2016). Synthesis, inhibition effects and quantum chemical studies of a novel coumarin derivative on the corrosion of mild steel in a hydrochloric acid solution. *Chemistry Central Journal*, 10(1), 1-9.
- [195] Nwankwo, H. U., Akpan, E. D., Olasunkanmi, L. O., Verma, C., Al-Mohaimed, A. M., Al Farraj, D. A., & Ebenso, E. E. (2021). N-substituted carbazoles as corrosion inhibitors in microbiologically influenced and acidic corrosion of mild steel: Gravimetric, electrochemical, surface and computational studies. *Journal of Molecular Structure*, 1223, 129328.
- [196] Vaughan, D. A., Ge, S., Kaga, A., & Tomooka, N. (2008). Phylogeny and biogeography of the genus *Oryza*. *In Rice biology in the genomics era*, 62, 219-234.

- [197] Malathi, K., & Ramaiah, S. (2017). Ethyl iso-allocholate from a medicinal rice Karungkavuni inhibits dihydropteroate synthase in Escherichia coli: A molecular docking and dynamics study. *Indian Journal of Pharmaceutical Sciences*, 78(6), 780-788.
- [198] Meng, B., Feng, X., Qiu, G., Liang, P., Li, P., Chen, C., & Shang, L. (2011). The process of methylmercury accumulation in rice (*Oryza sativa* L.). *Environmental science & technology*, 45(7), 2711-2717.
- [199] Afzal, S., Sharma, D., & Singh, N. K. (2021). Eco-friendly synthesis of phytochemical-capped iron oxide nanoparticles as nano-priming agent for boosting seed germination in rice (*Oryza sativa* L.). *Environmental Science and Pollution Research*, 1-13.
- [200] Prasad, T. N., Adam, S., Rao, P. V., Reddy, B. R., & Krishna, T. G. (2016). Size dependent effects of antifungal phytochemical silver nanoparticles on germination, growth and biochemical parameters of rice (*Oryza sativa* L), maize (*Zea mays* L) and peanut (*Arachis hypogaea* L). *IET nanobiotechnology*, 11(3), 277-285.
- [201] Anwaar, S., Maqbool, Q., Jabeen, N., Nazar, M., Abbas, F., Nawaz, B., & Hussain, S. Z. (2016). The effect of green synthesized CuO nanoparticles on callogenesis and regeneration of *Oryza sativa* L. *Frontiers in plant science*, 7, 1330.
- [202] Ramakrishnan, P. J., Janardhanan, V. D. K., Sreekumar, R., & Mohan, K. P. (2014). Investigation on the effect of green inhibitors for corrosion protection of mild steel in 1 M NaOH solution. *International Journal of Corrosion*, 2014.
- [203] Leena, P., Zeinul Hukuman, N. H., Biju, A. R., & Jisha, M. (2019). Studies on Methanolic Extract of *Lepidagathis keralensis* as Green Corrosion Inhibitor for Mild Steel in 1M HCl. *Journal of Electrochemical Science and Technology*, 10(2), 231-243.
- [204] Zhang, K., Yang, W., Yin, X., Chen, Y., Liu, Y., Le, J., & Xu, B. (2018). Amino acids modified konjac glucomannan as green corrosion inhibitors for mild steel in HCl solution. *Carbohydrate polymers*, 181, 191-199.

- [205] Chakravarthy, M. P., & Mohana, K. N. (2014). Adsorption and corrosion inhibition characteristics of some nicotinamide derivatives on mild steel in hydrochloric acid solution. *International Scholarly Research Notices*, 2014.
- [206] Zulkifli, F., Yusof, M. S. M., Isa, M. I. N., Yabuki, A., & Nik, W. W. (2017). Henna leaves extract as a corrosion inhibitor in acrylic resin coating. *Progress in Organic Coatings*, 105, 310-319.
- [207] Srivastava, M., Tiwari, P., Srivastava, S. K., Prakash, R., & Ji, G. (2017). Electrochemical investigation of Irbesartan drug molecules as an inhibitor of mild steel corrosion in 1 M HCl and 0.5 M H<sub>2</sub>SO<sub>4</sub> solutions. *Journal of Molecular Liquids*, 236, 184-197.
- [208] Cang, H., Fei, Z., Shao, J., Shi, W., & Xu, Q. (2013). Corrosion inhibition of mild steel by aloes extract in HCl solution medium. *International Journal of Electrochemical Science*, 8(1), 720-734.
- [209] Hamilton-Amachree, A., & Iroha, N. B. (2020). Corrosion inhibition of API 5L X80 pipeline steel in acidic environment using aqueous extract of *Thevetia peruviana*. *Chemistry International*, 6(3), 117-128.
- [210] Oguzie, E. E., Enenebeaku, C. K., Akalezi, C. O., Okoro, S. C., Ayuk, A. A., & Ejike, E. N. (2010). Adsorption and corrosion-inhibiting effect of *Dacryodis edulis* extract on low-carbon-steel corrosion in acidic media. *Journal of Colloid and interface Science*, 349(1), 283-292.
- [211] Singh, P., & Quraishi, M. A. (2016). Corrosion inhibition of mild steel using Novel Bis Schiff's Bases as corrosion inhibitors: electrochemical and surface measurement. *Measurement*, 86, 114-124.
- [212] Chung, I. M., Kim, S. H., & Prabakaran, M. (2020). Evaluation of phytochemical, polyphenol composition and anti-corrosion capacity of *Cucumis anguria* L. leaf extract on metal surface in sulfuric acid medium. *Protection of Metals and Physical Chemistry of Surfaces*, 56(1), 214-224.
- [213] Verma, C., Olasunkanmi, L. O., Ebenso, E. E., Quraishi, M. A., & Obot, I. B. (2016). Adsorption behavior of glucosamine-based, pyrimidine-fused heterocycles as green corrosion inhibitors for mild steel: experimental and theoretical studies. *The Journal of Physical Chemistry C*, 120(21), 11598-11611.

- [214] Yuan, S. J., & Pehkonen, S. O. (2007). Microbiologically influenced corrosion of 304 stainless steel by aerobic *Pseudomonas* NCIMB 2021 bacteria: AFM and XPS study. *Colloids and Surfaces B: Biointerfaces*, 59(1), 87-99.
- [215] Singh, A., Ansari, K. R., Kumar, A., Liu, W., Songsong, C., & Lin, Y. (2017). Electrochemical, surface and quantum chemical studies of novel imidazole derivatives as corrosion inhibitors for J55 steel in sweet corrosive environment. *Journal of Alloys and Compounds*, 712, 121-133.
- [216] Tan, B., Zhang, S., Liu, H., Guo, Y., Qiang, Y., Li, W., ... & Chen, S. (2019). Corrosion inhibition of X65 steel in sulfuric acid by two food flavorants 2-isobutylthiazole and 1-(1, 3-Thiazol-2-yl) ethanone as the green environmental corrosion inhibitors: Combination of experimental and theoretical researches. *Journal of colloid and interface science*, 538, 519-529.
- [217] Singh, P., & Quraishi, M. A. (2016). Corrosion inhibition of mild steel using Novel Bis Schiff's Bases as corrosion inhibitors: electrochemical and surface measurement. *Measurement*, 86, 114-124.
- [218] Gece, G., & Bilgiç, S. (2009). Quantum chemical study of some cyclic nitrogen compounds as corrosion inhibitors of steel in NaCl media. *Corrosion Science*, 51(8), 1876-1878.
- [219] Zhang, Z., Li, W., Zhang, W., Huang, X., Ruan, L., & Wu, L. (2018). Experimental, quantum chemical calculations and molecular dynamics (MD) simulation studies of methionine and valine as corrosion inhibitors on carbon steel in phase change materials (PCMs) solution. *Journal of Molecular Liquids*, 272, 528-538.
- [220] Verma, C., Ebenso, E. E., & Quraishi, M. A. (2017). Ionic liquids as green and sustainable corrosion inhibitors for metals and alloys: an overview. *Journal of Molecular Liquids*, 233, 403-414.
- [221] Godavarthi, S., Porcayo-Calderon, J., Casales-Diaz, M., Vazquez-Velez, E., Neri, A., & Martinez-Gomez, L. (2016). Electrochemical analysis and quantum chemistry of castor oil-based corrosion inhibitors. *Current Analytical Chemistry*, 12(5), 476-488.
- [222] Cui, G., Guo, J., Zhang, Y., Zhao, Q., Fu, S., Han, T., & Wu, Y. (2019). Chitosan oligosaccharide derivatives as green corrosion inhibitors for P110 steel in

a carbon-dioxide-saturated chloride solution. *Carbohydrate polymers*, 203, 386-395.

[223] Kögler, A., Seibt, K. M., Heitkam, T., Morgenstern, K., Reiche, B., Brückner, M., & Schmidt, T. (2020). Divergence of 3' ends as a driver of short interspersed nuclear element (SINE) evolution in the Salicaceae. *The Plant Journal*, 103(1), 443-458.

[224] Holeski, L. M., McKenzie, S. C., Kruger, E. L., Couture, J. J., Rubert-Nason, K., & Lindroth, R. L. (2016). Phytochemical traits underlie genotypic variation in susceptibility of quaking aspen (*Populus tremuloides*) to browsing by a keystone forest ungulate. *Journal of Ecology*, 104(3), 850-863.

[225] Abreu, I. N., Ahnlund, M., Moritz, T., & Albrechtsen, B. R. (2011). UHPLC-ESI/TOFMS determination of salicylate-like phenolic glycosides in *P. tremula* leaves. *Journal of Chemical Ecology*, 37(8), 857-870.

[226] Colom, X., Carrillo, F., Nogués, F., & Garriga, P. (2003). Structural analysis of photodegraded wood by means of FTIR spectroscopy. *Polymer Degradation and Stability*, 80(3), 543-549.

[227] Tka, N., Jabli, M., Saleh, T. A., & Salman, G. A. (2018). Amines modified fibers obtained from natural *P. tremula* and their rapid biosorption of Acid Blue 25. *Journal of Molecular Liquids*, 250, 423-432.

[228] Gorzsás, A., Stenlund, H., Persson, P., Trygg, J., & Sundberg, B. (2011). Cell-specific chemotyping and multivariate imaging by combined FT-IR microspectroscopy and orthogonal projections to latent structures (OPLS) analysis reveals the chemical landscape of secondary xylem. *The Plant Journal*, 66(5), 903-914.

[229] Soreng, R. J., Peterson, P. M., Romaschenko, K., Davidse, G., Zuloaga, F. O., Judziewicz, E. J., & Morrone, O. (2015). A worldwide phylogenetic classification of the *Poaceae* (Gramineae). *Journal of Systematics and Evolution*, 53(2), 117-137.

[230] Faltermaier, A., Waters, D., Becker, T., Arendt, E., & Gastl, M. (2014). Common wheat (*T. aestivum* L.) and its use as a brewing cereal—a review. *Journal of the Institute of Brewing*, 120(1), 1-15.

- [231] Pathak, V., & Shrivastav, S. (2015). Biochemical studies on wheat (*T. aestivum* L.). *Journal of Pharmacognosy and Phytochemistry*, 4(3), 171
- [232] Zhu, Y., & Sang, S. (2017). Phytochemicals in whole grain wheat and their health-promoting effects. *Molecular Nutrition & Food Research*, 61(7), 1600852.
- [233] Wang, J., Zhu, J., Huang, R., & Yang, Y. (2012). Investigation of cell wall composition related to stem lodging resistance in wheat (*T. aestivum* L.) by FTIR spectroscopy. *Plant signaling & behavior*, 7(7), 856-863.
- [234] Barron, C., & Rouau, X. (2008). FTIR and Raman signatures of wheat grain peripheral tissues. *Cereal Chemistry*, 85(5), 619-625.
- [235] Farooq, U., Khan, M. A., Athar, M., & Kozinski, J. A. (2011). Effect of modification of environmentally friendly biosorbent wheat (*Triticum aestivum*) on the biosorptive removal of cadmium (II) ions from aqueous solution. *Chemical Engineering Journal*, 171(2), 400-410.
- [236] Hansen, M. A., Kristensen, J. B., Felby, C., & Jørgensen, H. (2011). Pretreatment and enzymatic hydrolysis of wheat straw (*T. aestivum* L.)—the impact of lignin relocation and plant tissues on enzymatic accessibility. *Bioresource technology*, 102(3), 2804-2811.
- [237] Singh, S., Dey, S. S., Bhatia, R., Kumar, R., & Behera, T. K. (2019). Current understanding of male sterility systems in vegetable Brassicas and their exploitation in hybrid breeding. *Plant reproduction*, 32(3), 231-256.
- [238] Khalid, S., Ibrahim, U., Riaz, S., Naseem, M., Sajjad, M., Khan, W. M., ... & Haq, S. I. U. (2020). 4. A comparative study of the allelopathic effects of *Albizia lebbek* L. and *Ficus virens* on growth and germination of *Brassica campestris* L. *Pure and Applied Biology*, 10(2), 368-377.
- [239] Salehi, B., Quispe, C., Butnariu, M., Sarac, I., Marmouzi, I., Kamle, M., & Martorell, M. (2021). Phytotherapy and food applications from Brassica genus. *Phytotherapy Research*.
- [240] Pandit, R. A. K. S. H. A. (2015). Green synthesis of silver nanoparticles from seed extract of *B. nigra* and its antibacterial activity. *Nusantara Biosci*, 7(1), 15-19.
- [241] Fadhil, A. B., & Abdulahad, W. S. (2014). Transesterification of mustard (*B. nigra*) seed oil with ethanol: purification of the crude ethyl ester with activated

carbon produced from de-oiled cake. *Energy Conversion and Management*, 77, 495-503.

[242] Zafar, H., Abbasi, B. H., & Zia, M. (2019). Physiological and antioxidative response of *B. nigra* (L.) to ZnO nanoparticles grown in culture media and soil. *Toxicological & Environmental Chemistry*, 101(3-6), 281-299.

[243] Nandiyanto, A. B. D., Oktiani, R., & Ragadhita, R. (2019). How to read and interpret FTIR spectroscopy of organic material. *Indonesian Journal of Science and Technology*, 4(1), 97-118.

[244] Negi, A., & Koujalagi, D. (2018). Study of genetic variability, heritability and genetic advance for various yield and quality traits in sugarcane genotypes (*Saccharum officinarum*). *International Journal of Current Microbiology and Applied Sciences*, 7(4), 1464-1472.

[245] Singh, A., Lal, U. R., Mukhtar, H. M., Singh, P. S., Shah, G., & Dhawan, R. K. (2015). Phytochemical profile of sugarcane and its potential health aspects. *Pharmacognosy Reviews*, 9(17), 45.

[246] Bhuvaneshwari, S., Hettiarachchi, H., & Meegoda, J. N. (2019). Crop residue burning in India: Policy challenges and potential solutions. *International Journal of Environmental Research and Public Health*, 16(5), 832.

[247] Kaliannan, D., Palaninaicker, S., Palanivel, V., Mahadeo, M. A., Ravindra, B. N., & Jae-Jin, S. (2019). A novel approach to preparation of nano-adsorbent from agricultural wastes (*Saccharum officinarum* leaves) and its environmental application. *Environmental Science and Pollution Research*, 26(6), 5305-5314.

[248] Gupta, A., Vidyarthi, S. R., & Sankararamakrishnan, N. (2015). Concurrent removal of As (III) and As (V) using green low cost functionalized biosorbent–*Saccharum officinarum* bagasse. *Journal of Environmental Chemical Engineering*, 3(1), 113-121.

[249] Sari, N. H., Arif, R., & Edi, S. (2019). Characterization of *musaceae* and *saccharum officinarum* cellulose fibers for composite application. *International Journal of Nanoelectronics and Materials*, 12(2)193-204

[250] Paulkumar, K., Gnanajobitha, G., Vanaja, M., Pavunraj, M., & Annadurai, G. (2017). Green synthesis of silver nanoparticle and silver based chitosan bionanocomposite using stem extract of *Saccharum officinarum* and assessment of



its antibacterial activity. *Advances in Natural Sciences: Nanoscience and Nanotechnology*, 8(3), 035019.

[251] Weber, B., Heitkam, T., Holtgräwe, D., Weisshaar, B., Minoche, A. E., Dohm, J. C. Schmidt, T. (2013). Highly diverse chromoviruses of *B. vulgaris* are classified by chromodomains and chromosomal integration. *Mobile DNA*, 4(1), 1-16.

[252] Baião, D. D. S., da Silva, D. V., & Paschoalin, V. M. (2020). Beetroot, a remarkable vegetable: Its nitrate and phytochemical contents can be adjusted in novel formulations to benefit health and support cardiovascular disease therapies. *Antioxidants*, 9(10).

[253] Parameshwaran, R., Kalaiselvam, S., & Jayavel, R. (2013). Green synthesis of silver nanoparticles using *Beta vulgaris*: role of process conditions on size distribution and surface structure. *Materials Chemistry and Physics*, 140(1), 135-147.

[254] Molina, G. A., Hernández-Martínez, A. R., Cortez-Valadez, M., García-Hernández, F., & Estevez, M. (2014). Effects of tetraethyl orthosilicate (TEOS) on the light and temperature stability of a pigment from *B. vulgaris* and its potential food industry applications. *Molecules*, 19(11), 17985-18002.

[255] Chhikara, N., Kushwaha, K., Jaglan, S., Sharma, P., & Panghal, A. (2019). Nutritional, physicochemical, and functional quality of beetroot (*B. vulgaris L.*) incorporated Asian noodles. *Cereal Chemistry*, 96(1), 154-161.

[256] Supahan, N., Kunpradid, T., Joradol, A., & Leelahakriengkrai, P. (2017). Diversity of some organisms in Chiang Mai Rajabhat University, Mae Rim Campus, Chiang Mai Province. *Progress in Applied Science and Technology*, 7(2), 1-14.

[257] Zhang, Y., Zhao, L., Guo, X., Li, C., Li, H., Lou, H., & Ren, D. (2016). Chemical constituents from *P. emblica* and the cytoprotective effects on H<sub>2</sub>O<sub>2</sub>-induced PC12 cell injuries. *Archives of Pharmacal Research*, 39(9), 1202-1211

[258] Sriwatcharakul, S. (2020). Evaluation of bioactivities of *P. emblica* seed. *Energy Reports*, 6, 442-447

- [259] Renuka, R., Devi, K. R., Sivakami, M., Thilagavathi, T., Uthrakumar, R., & Kaviyarasu, K. (2020). Biosynthesis of silver nanoparticles using *P. emblica* fruit extract for antimicrobial application. *Biocatalysis and Agricultural Biotechnology*, 24, 101567.
- [260] Sathishkumar, M., Saroja, M., Venkatachalam, M., & Rajamanickam, A. (2017). Biosynthesis of zinc sulphide nanoparticles using *Phyllanthus emblica* and their antimicrobial activities. *Elixir Elec. Eng*, 102, 44411-44415.
- [261] Nayagam, V., Gabriel, M., & Palanisamy, K. (2018). Green synthesis of silver nanoparticles mediated by *Coccinia grandis* and *Phyllanthus emblica*: a comparative comprehension. *Applied Nanoscience*, 8(3), 205-219.
- [262] Singh, M., Sharma, N., Paras, H. S., Hans, N. S., Singh, N. P., & Sarin, A. (2019). Antioxidative potential of *P. emblica* for oxidation stability of biodiesels. *Environmental Progress & Sustainable Energy*, 38(2), 721-726.

